

2013

A Novel Approach to Carbon Dioxide Capture and Storage

Brett P. Spigarelli
Michigan Technological University

Copyright 2013 Brett P. Spigarelli

Recommended Citation

Spigarelli, Brett P., "A Novel Approach to Carbon Dioxide Capture and Storage", Dissertation, Michigan Technological University, 2013.
<http://digitalcommons.mtu.edu/etds/633>

Follow this and additional works at: <http://digitalcommons.mtu.edu/etds>



Part of the [Chemical Engineering Commons](#), and the [Environmental Engineering Commons](#)

A NOVEL APPROACH TO CARBON DIOXIDE CAPTURE AND STORAGE

By

Brett P. Spigarelli

A DISSERTATION

Submitted in partial fulfillment of the requirements for the degree of

DOCTOR OF PHILOSOPHY

In Chemical Engineering

MICHIGAN TECHNOLOGICAL UNIVERSITY

2013

© 2013 Brett P. Spigarelli

This dissertation has been approved in partial fulfillment of the requirements for the Degree of DOCTOR OF PHILOSOPHY in Chemical Engineering.

Department of Chemical Engineering

Dissertation Advisor: *Dr. S. Komar Kawatra*

Committee Member: *Dr. Timothy Eisele*

Committee Member: *Dr. Wenzhen Li*

Committee Member: *Dr. Jeffrey Naber*

Department Chair: *Dr. S. Komar Kawatra*

Table of Contents

| | |
|---|-----|
| PREFACE..... | IV |
| ACKNOWLEDGEMENTS | V |
| ABSTRACT | VI |
| CHAPTER 1: INTRODUCTION..... | 1 |
| CHAPTER 2: OPPORTUNITIES AND CHALLENGES IN CARBON DIOXIDE CAPTURE..... | 7 |
| CHAPTER 3: AN EQUILIBRIUM ANALYSIS OF CARBON DIOXIDE ABSORPTION IN CARBONATE SOLUTIONS | 74 |
| CHAPTER 4: THE EFFECTS OF ABSORBENT TEMPERATURE AND FLUE GAS IMPURITIES ON CARBON DIOXIDE ABSORPTION IN CARBONATE SOLUTIONS | 82 |
| CHAPTER 5: INCREASED CARBON DIOXIDE ABSORPTION RATES IN CARBONATE SOLUTIONS BY SURFACTANT ADDITION | 98 |
| CHAPTER 6: THE EFFECT OF SURFACTANT ADDITION ON CARBON DIOXIDE ABSORPTION IN CARBONATE SOLUTIONS | 112 |
| CHAPTER 7: CARBON DIOXIDE SEQUESTRATION BY CHEMICALLY ENHANCED AQUEOUS MINERAL CARBONATION OF COAL FLY ASH . | 136 |
| CHAPTER 8: A NOVEL APPROACH TO CARBON CAPTURE AND STORAGE | 154 |
| CHAPTER 9: REFERENCE LIST | 180 |

Preface

Chapter 2, “Opportunities and Challenges in Carbon Dioxide Capture,” was previously published in the *Journal of CO₂ Utilization* in 2013, volume 1, pages 69-87. Brett Spigarelli was the first author and Dr. S. Komar Kawatra was the second author on the article. The first author was responsible for researching the subject matter and writing the article. The second author was responsible for proofreading and editing the article before publication.

Chapter 3, “Equilibrium Analysis of Carbon Dioxide Absorption in Carbonate Solutions,” was previously published in *Minerals & Metallurgical Processing* in 2012, volume 29, issue 2, pages 131-132. The sole author on this paper, Brett Spigarelli, conducted the experimental work, analyzed the data, performed the theoretical calculations, and wrote the paper.

Chapter 5, “Increased Carbon Dioxide Absorption Rates in Carbonate Solutions by Surfactant Addition,” was previously published in *Minerals & Metallurgical Processing* in 2013, volume 30, issue 2, pages 95-99. The first author, Brett Spigarelli, analyzed the data, researched the topic, and wrote the paper. The second author, Paul Hagadone II, conducted all the experimental work. The third author, Dr. S. Komar Kawatra, proofread the article and edited it before publication.

Acknowledgements

I would like to acknowledge my advisor, Dr. Kawatra, for his guidance and support throughout my time in graduate school.

I would like to thank Dr. Timothy Eisele for his advice and guidance during graduate school. I would like to thank my family for being there for me throughout this whole process. Without them things would have been much different. I would also like to thank the undergraduates who put in countless hours to help to complete my experimental work: Mark Preston, Jacqueline Walitalo, Paul Hagadone II, and Courtney David.

Abstract

The novel approach to carbon capture and storage (CCS) described in this dissertation is a significant departure from the conventional approach to CCS. The novel approach uses a sodium carbonate solution to first capture CO₂ from post combustion flue gas streams. The captured CO₂ is then reacted with an alkaline industrial waste material, at ambient conditions, to regenerate the carbonate solution and permanently store the CO₂ in the form of an added value carbonate mineral. Conventional CCS makes use of a hazardous amine solution for CO₂ capture, a costly thermal regeneration stage, and the underground storage of *supercritical* CO₂. The objective of the present dissertation was to examine each individual stage (capture and storage) of the proposed approach to CCS.

Study of the capture stage found that a 2% w/w sodium carbonate solution was optimal for CO₂ absorption in the present system. The 2% solution yielded the best tradeoff between the CO₂ absorption rate and the CO₂ absorption capacity of the solutions tested. Examination of CO₂ absorption in the presence of flue gas impurities (NO_x and SO_x) found that carbonate solutions possess a significant advantage over amine solutions, that they could be used for multi-pollutant capture. All the NO_x and SO_x fed to the carbonate solution was able to be captured. Optimization studies found that it was possible to increase the absorption rate of CO₂ into the carbonate solution by adding a surfactant to the solution to chemically alter the gas bubble size. The absorption rate of CO₂ was increased by as much as 14%.

Three coal combustion fly ash materials were chosen as the alkaline industrial waste materials to study the storage CO₂ and regeneration the absorbent. X-ray diffraction analysis on reacted fly ash samples confirmed that the captured CO₂ reacts with the fly ash materials to form a carbonate mineral, specifically calcite. Studies found that after a five day reaction time, 75% utilization of the waste material for CO₂

storage could be achieved, while regenerating the absorbent. The regenerated absorbent exhibited a nearly identical CO₂ absorption capacity and CO₂ absorption rate as a fresh Na₂CO₃ solution.

Chapter 1: Introduction

Introduction

Carbon dioxide capture and storage (CCS) technologies are widely considered to possess the most potential as a near term option for reducing anthropogenic CO₂ emissions from sources such as fossil fuel burning power plants [1, 2]. The implementation of CCS would mitigate environmental risks associated with emitting CO₂ to the atmosphere while allowing for the continued use of fossil fuels until alternative energy technologies mature. However, CCS is sometimes thought of as just an “insurance” policy for reducing CO₂ emissions because of the high operating cost [3]. At the current state of technological development, one cost estimate predicts a carbon price/tax of \$60-65 per metric ton of CO₂ before installation of a CCS system would be economical [4]. To add perspective to that value, on average, a 500 MW fossil fuel burning power plant emits 8,000 metric tons of CO₂ per day [5, 6].

Herein, the authors propose a novel approach to CCS using carbonate solutions as the absorbent for post combustion capture of CO₂ and alkaline industrial waste materials for the permanent storage of CO₂ and regeneration of the absorbent. The novel aspect of the proposed approach is that thermal regeneration is not used to regenerate the absorbent, as is the case with the commercially available technology, amine absorption systems [7-9]. In the current approach, the CO₂ loaded solution will be reacted with an industrial waste material, at ambient conditions, to permanently store the captured CO₂ in the form of a carbonate mineral while simultaneously regenerating the carbonate solution.

In commercially available CCS technology, the CO₂ contaminated gas stream is fed to an absorption column where the CO₂ is absorbed from the gas stream by an amine solution. A CO₂ depleted exhaust gas stream leaves out the top of the absorption column and a CO₂ loaded solution exits out the bottom. The CO₂ loaded solution is then sent to a stripping column where the solution is heated (between

100-200 °C) to desorb high purity CO₂ and regenerate the amine solution [2, 10-12]. The high purity CO₂ is then compressed to a supercritical state (11-14 MPa [13]) and transported, typically via pipeline, for storage in an underground reservoir.

This process has several disadvantages associated with it. The most common amine used for absorption is monoethanolamine (MEA). MEA is highly hazardous, highly volatile, corrosive, degrades in the presence of oxygen and other flue gas impurities (NO_x and SO_x), and it is costly (\$1.25/kg [14]). The regeneration stage requires heating large volumes of absorbent anywhere from 100-200 °C and compression of the high purity CO₂ to a supercritical state for transportation. [10-12]

The proposed approach to CCS is different from the conventional approach to CCS described above. A block diagram of the proposed approach to CCS can be seen in Figure 1.

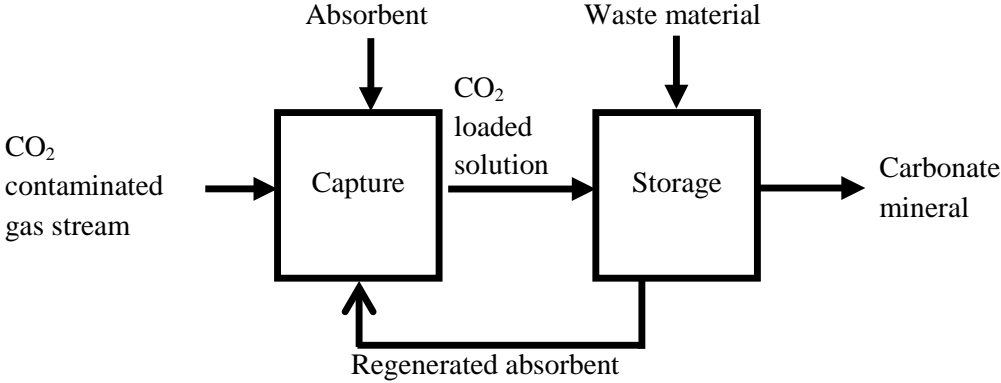


Figure 1: Flow diagram for the proposed carbon dioxide capture and storage process. The proposed process aims to eliminate the need for thermal regeneration of the absorbent

In the proposed approach to CCS, the capture stage is similar to the aforementioned amine capture stage except a Na_2CO_3 solution is used instead of an amine solution. After CO_2 capture, the CO_2 loaded solution is fed to a stirred tank reactor where it is reacted with an alkaline industrial waste material, at ambient conditions, to regenerate the absorbent and to permanently store the CO_2 as an added value carbonate mineral. After reaction, the carbonate mineral is filtered from the solution forming a regenerated absorbent that can be reused to capture more CO_2 .

The proposed CCS system has many advantages over the commercially available technology. The carbonate based solution is considered non-hazardous, has a low volatility, is non-fouling, has a low equipment corrosion rate, low raw material costs (\$0.11/kg [15]), and could be used as a multi pollutant capture system (NO_x , SO_x , and CO_2 removal) [16]. Operating costs of the system are likely to be lower than that of the amine system due to operation at ambient conditions and no need for gas compression.

The goal of the present dissertation was to study the feasibility of the proposed CCS system. First, a review was written examining the various approaches to CO_2 capture that are either currently available, or being studied, to get a better understanding of the current state of technological development. The review is Chapter 2 in the dissertation. Next, a series of experiments (Chapters 3-8) were conducted to examine the behavior of Na_2CO_3 solutions as an absorbent for CO_2 capture and storage.

In Chapter 3, experiments were conducted to determine the optimal amount of Na_2CO_3 in solution for CO_2 absorption in the current system. The optimal % Na_2CO_3 in solution was chosen based upon the CO_2 absorption capacity and CO_2 absorption rate of the solution. A theoretical equilibrium analysis was also

performed to help interpret the experimental results. It was initially hypothesized that more Na_2CO_3 in solution would lead to better CO_2 absorption.

Chapter 4 examined CO_2 absorption in the carbonate solution in the presence of flue gas impurities (NO_x and SO_x) and at elevated absorbent temperatures (25 °C to 60 °C). In an industrial setting it is common for the flue gas to contain the gaseous impurities such as NO_x and SO_x and be at elevated temperatures (around 100 °C). It is important to understand if/how the presence of these impurities will impact the absorption of CO_2 in the carbonate solution. It is likely that the elevated flue gas temperature will cause the absorbent temperature to increase during absorbent. Thus, it is important to understand the effect of absorbent temperature on CO_2 absorption. It was hypothesized that the presence of flue gas impurities will lead to a reduction in the CO_2 absorption capacity of the carbonate solution and increased absorbent temperatures will lead to a reduction in the CO_2 absorption rate.

Chapter 5 studied enhancing the absorption of rate of CO_2 into the carbonate solution. It is perceived in literature that CO_2 has a slower absorption rate in carbonate solutions than in amine solutions. For this reason it was important to study ways to increase the absorption rate of CO_2 into carbonate solutions. In Chapter 5, a polypropylene glycol methyl ether (PPGME) surfactant was used to reduce the gas bubble size in solution. Varying concentrations of surfactant were tested to examine the effect of the surfactant on bubble size and the corresponding CO_2 absorption rate in the carbonate solution. It was hypothesized that reducing the bubble size would result in increased CO_2 absorption rates in the carbonate solution.

In Chapter 6, the effect of surfactant on the rate of mass transfer of CO_2 from the gas bubble to the carbonate solution was examined. The mass transfer of CO_2 is important in determining the absorption rate. Theoretical calculations of the liquid-side mass transfer coefficient, using the Higbie and Frossling models, were

compared to experimental values to determine if the surfactant was impacting the mass transfer of CO₂ from the gas bubble. It was hypothesized that the addition of surfactant to solution would create a film around the gas bubble, limiting the extent to which the absorption rate could be increased.

Chapter 7 examined the feasibility of permanently storing the captured CO₂ as a carbonate mineral using an industrial waste material. In the study, a calcium rich coal combustion fly ash was mixed in with the carbonate solution and contacted with gaseous CO₂. It was hypothesized that the captured CO₂ would react with the fly ash material forming a calcium carbonate precipitate in solution.

Chapter 8 studied the carbonation kinetics and absorbent regeneration potential of three different fly ash materials. The ultimate goal of this study was to determine if the fly ash materials could be used to store the captured CO₂ while simultaneously regenerating the absorbent. It was hypothesized that given a sufficiently long reaction time, the fly ash materials would be able to store a significant amount of the captured CO₂ while regenerating the absorbent.

Chapter 2: Opportunities and Challenges in Carbon Dioxide Capture¹

¹ Spigarelli, B. P. and S. K. Kawatra (2013). "Opportunities and Challenges in Carbon Dioxide Capture." Journal of CO₂ Utilization **1**: 69-87.

Abstract

Various technologies for the capture of CO₂ from fossil fuel fired power plants are available. Each technology has its own advantages and disadvantages and are at different stages of development. This review provides a critical analysis of the major technologies for CO₂ capture from fossil fuel fired power plants so that the appropriate technology can be selected for a particular process. The different capture methods described in this review are: post-combustion, pre-combustion, oxy-combustion, and chemical looping combustion.

1 Introduction

The growing concern over global climate change has sparked a desire for reductions in greenhouse gas emissions, such as CO₂. Currently, fossil fuel fired power plants account for 80% of total energy production worldwide and are the largest point source of CO₂ emissions, accounting for roughly 40% of total CO₂ emissions. This makes fossil fuel burning power plants the most logical targets for immediate CO₂ reductions [1, 5, 17]. Several options do exist for reducing CO₂ emissions, such as demand-side conservation, supply side efficiency improvement, increasing reliance on nuclear and renewable energy, and carbon capture and storage (CCS) systems. Of the options mentioned above it is believed that CCS presents the most practical approach for long term CO₂ emission reductions as fossil fuels will continue to be a major source of energy in the foreseeable future [2, 10, 18].

Carbon dioxide capture and storage is generally a three step process: 1) capture and compression from combustion exhaust (i.e. flue gas), 2) transportation, usually via pipeline, and 3) utilization (e.g. urea production, underground storage, food and beverage industry, enhanced oil recovery, dry ice production, etc.) [19, 20]. It is estimated that the capture stage could account for 70 – 90% of the total operating costs of a CCS system [11]. Due to this high cost percentage much research has been conducted in the area of CO₂ capture. Currently, CO₂ capture technology for fossil fuel fired power plants can be divided into four categories, each of which requires a distinctly different approach to CO₂ capture. The four categories are:

1. *Post-combustion*: capture of CO₂ from flue gases created during fuel combustion with air
2. *Pre-combustion*: capture of CO₂ from a synthesis gas before fuel combustion
3. *Oxy-combustion*: capture of CO₂ from flue gases created during fuel combustion with oxygen
4. *Chemical looping combustion*: capture of CO₂ from flue gases created during combustion with oxygen transported via a metal oxide

This review provides a critical analysis of the major technologies for CO₂ capture from fossil fuel fired power plants within each of the four aforementioned categories. The CO₂ capture technology applicable to each category varies distinctly depending upon the combustion approach taken. Although the review focuses on CO₂ capture from fossil fuel fired power plants, the CO₂ capture technologies within post-combustion are directly applicable to CO₂ capture from industrial operations (e.g. cement and steel industry) because of similar CO₂ concentrations and partial pressures in the gas stream [21]. This review provides advantages and disadvantages to each technology so the most appropriate technology can be chosen for a particular process.

2 Background

Roughly 40% of all CO₂ emissions come from fossil fuel burning power plants; these plants are an obvious target for CO₂ capture. However, CO₂ capture from fossil fuel burning power plants presents several design challenges. The two most notable being 1) how to handle impurities, other than CO₂, in the flue gas stream and 2) how to handle the large quantities of CO₂ formed during fossil fuel combustion.

Common impurities encountered in flue gases may include nitrogen oxides (NO_x), sulfur oxides (SO_x), water vapor (H₂O), and particulate matter (PM). Particulate matter is a combination of un-burned coal and ash formed during coal combustion. The amount of impurities produced will vary depending upon the fuel source combusted. To address the challenge of impurities it is important to know the fundamental mechanisms behind CO₂ and impurity formation during fossil fuel combustion. The general combustion reactions which apply to any fuel for CO₂ formation can be seen in equations 1-4 [22]. Equations 1-3 apply to a coal fuel source (assuming coal consists predominantly of carbon) whereas equation 4 applies to a hydrocarbon fuel source, such as natural gas. In equation 1, the carbon (C)

present in coal reacts with oxygen (O₂) to form carbon monoxide (CO) at temperatures above 1000 °C.



The carbon monoxide will then react with excess O₂ to form CO₂, equation 2. The overall reaction mechanism for CO₂ formation from coal combustion can be seen in equation 3.



During hydrocarbon combustion, the fuel reacts with O₂ at temperatures ranging from 200 – 600 °C to form CO₂ and water vapor [22].



Equations 5-8 are the general combustion equations which apply to the formation of impurities seen in flue gases [22, 23]. During water vapor formation, equation 5, excess hydrogen from the fuel source reacts with excess O₂ during the combustion process. A typical flue gas stream will contain roughly 6-14 % H₂O by volume.



In equation 6, the sulfur (S) present in the fuel source reacts with excess oxygen during the combustion process to form SO₂. Sulfur in the fuel source may be in the form of pyrite (FeS₂) or organic molecules that contain sulfur (usually about half of the sulfur in coal is “organic sulfur”).



Equations 7 and 8 describe the formation of NO_x. In NO_x formation molecular nitrogen (N₂) first reacts with atomic oxygen (O) to form NO_x and atomic nitrogen (N), equation 7. The atomic nitrogen may then react further with O₂ to form NO_x and O, equation 8. NO_x formation occurs at temperatures above 1200 °C and increases as temperature increases. N₂ can originate from the fuel and the air used for combustion [23]. Coal is typically 1-1.5 % Nitrogen [24].



As previously mentioned, the amount of impurities produced will vary depending upon the fuel source combusted. Table 1 gives the average emissions of CO₂, SO₂ and nitrogen oxides in the U.S. on a pounds (lbs) per megawatt hour (MWh) basis for natural gas and coal [5]. Carbon dioxide emissions can be significantly reduced by switching from coal to natural gas as a fuel source. It should be noted that sulfur dioxide and nitrogen oxides are the major contributors to the formation of acid rain.

| Table 1 | | | |
|--|---|---|---|
| Average emission rates of CO₂, SO₂, and NO_x from coal and natural gas burning power plants in the U.S. | | | |
| Fuel Type | CO₂ emissions (lbs/MWh) | SO₂ emissions (lbs/MWh) | NO_x emissions (lbs/MWh) |
| Coal | 2,249 | 13 | 6 |
| Natural gas | 1,135 | 0.1 | 1.7 |

Combustion impurities would be greatly reduced or eliminated if the precursors (H₂, S, N, N₂) were not present in the fuel or combustion environment. Some CO₂ capture technologies, such as pre-combustion, oxy-combustion, and chemical looping combustion take advantage of this by creating a combustion atmosphere free of some impurity precursors. However, complete impurity elimination is not possible since fuels contain inherent amounts of sulfur and nitrogen; the amounts will vary depending upon the fuel and how well they are “cleaned” prior to burning (Table 1). In most cases a process stage is applied to remove flue gas impurities before CO₂ capture. The cleaning levels will vary depending upon the approach taken to CO₂ capture. This issue will be discussed in more detail as it pertains to each CO₂ capture approach.

The second challenge associated with CO₂ capture from fossil fuel fired power plants is handling the large quantity of gas produced. A quick calculation using Table 1 shows that, on average, roughly 8,000 tons/day CO₂ would be emitted from a 500 MW fossil fuel burning power plant. This presents a very difficult design challenge – scaling up or retrofitting current CO₂ capture technologies to the scale of fossil fuel fired power plants. Current commercial CO₂ capture systems have a max capacity near 800 tons per day CO₂; ten times less than what is emitted from the average fossil fuel fired power plant.

Now that the fundamental questions given earlier have been answered, it is appropriate to begin discussing the various CO₂ capture approaches and their associated technologies:

- Post-combustion
- Pre-combustion
- Oxy-combustion
- Chemical looping combustion

3 Post combustion capture of CO₂

Post combustion capture of CO₂ refers to CO₂ capture from flue gases produced by fuel combustion [12, 19]. It is widely believed that post combustion technologies present the greatest near term potential for reduction of CO₂ emissions because they can be retrofit to existing fossil fueled power plants and may be applied to other industrial emitters of CO₂ as well (e.g. the cement industry and iron and steel production). A simplified block diagram of post combustion CO₂ capture can be seen in Figure 2 [25-27].

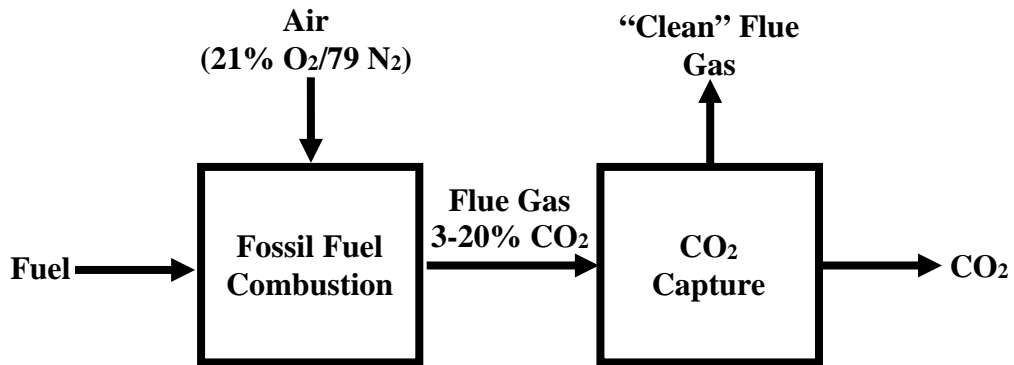


Figure 2: Simplified post-combustion capture block diagram

In post-combustion capture, the CO₂ is captured from a low pressure (1 bar) and low CO₂ content (3-20%) gas stream often at high temperatures (120 – 180 °C) containing the impurities SO_x and NO_x [23]. Cement and iron and steel production also produce gas streams at roughly 1 bar and a CO₂ content in the range of 14-33% [21]. The high temperature and low partial pressure of CO₂ present in post combustion gas streams poses major design challenges, such as large equipment and cooling systems. To date, these problems have been addressed through the use of chemical solvents which chemically react with the CO₂ during capture. Current post combustion technologies employ methods such as chemical absorption, adsorption, gas separation membranes, and cryogenic distillation. The basic operation and pros/cons of these technologies will be discussed further in this section.

In general, when exploring post combustion capture options it is important to take note of:

- Can the technology handle impurities? (NO_x, SO_x, particulate matter must be minimal)
- Can the system handle the large volume of gas produced at fossil fuel burning power plants?
- What is the partial pressure of CO₂ in the flue gas? (best suited for 3-20%)
- What is the temperature of the inlet flue gas stream? (will the gas need to be cooled)
- Required CO₂ removal efficiency. The U.S. DOE has set a target of 90% [18].
- The intended use of the captured CO₂. High purity CO₂ is needed for the food and beverage industry but not geological storage

3.1 Chemical absorption

Chemical absorption is the preferred method for capturing CO₂ from post combustion flue gas streams containing low to moderate partial pressures of CO₂ (3-20%). The term absorption refers to the separation process in which a gaseous component is separated from a gas stream by the use of a liquid. The gaseous component comes into contact with the liquid and is absorbed from the gas phase into the liquid phase. The liquid used for absorption is often referred to as the solvent or absorbent. These terms will be used interchangeably throughout this paper. Factors which need to be considered when choosing an absorbent are: 1) the solubility of the gaseous component in the absorbent and 2) reactive properties of the gaseous component and the absorbent. For example, CO₂ is considered an acid gas. This means that when absorbed by water based absorbent an acidic solution will form. Thus, for acid gas absorption it is desirable if the absorbent is alkaline. Alkaline solutions are basic in pH which enables the neutralization of any acid formed upon absorption of the gas, thereby increasing the amount of gas which can be absorbed for a given volume of liquid. A well-known acid gas absorption process is the removal of SO₂ from combustion gas streams, called flue gas desulphurization (FGD). In FGD SO₂ is removed from flue gas streams by countercurrent contact with a lime slurry in a packed bed absorption column [23]. The lime slurry neutralizes any acid formed when the SO₂ is absorbed into solution. Figure 3 is the basic flow diagram for post combustion capture of CO₂ via chemical absorption.

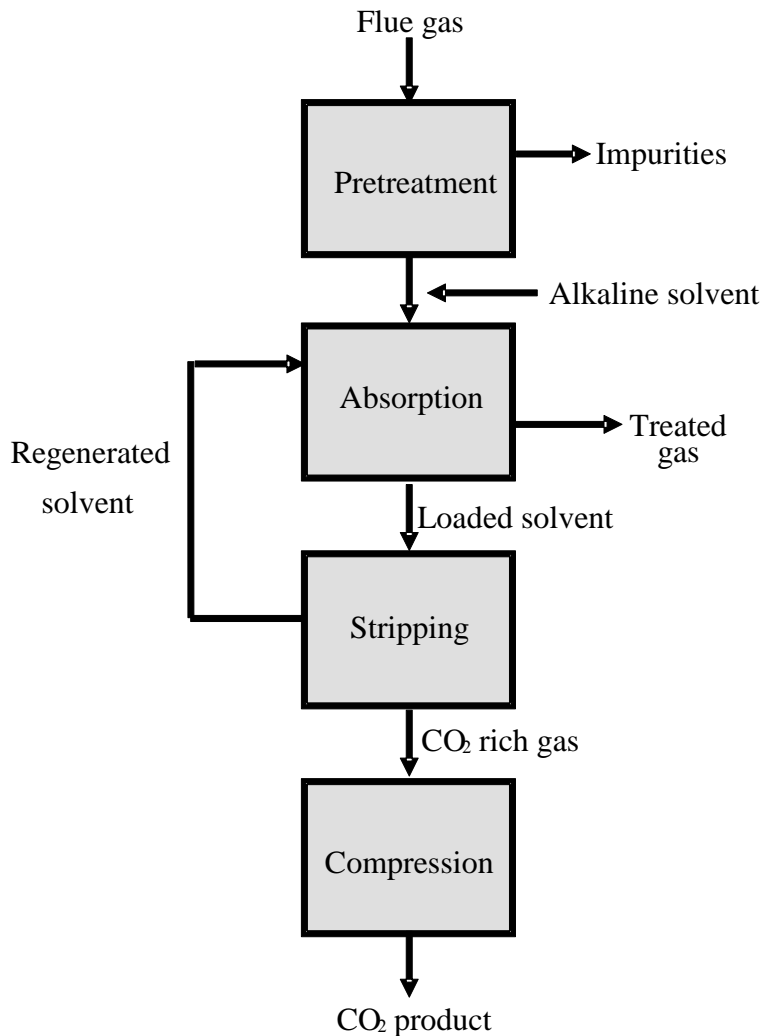


Figure 3: Basic flow diagram for post combustion capture of CO₂ using chemical absorption

In CO₂ absorption processes it is common for the flue gas stream to first go through a pretreatment step to remove impurities such as particulate matter, SO_x, and NO_x. The degree the flue gas needs to be treated will vary depending upon the fuel being combusted, the absorption process/equipment design, and the interactions between the absorbent and impurities. For example, SO₂ will cause some absorbents to degrade, producing unwanted byproducts. In such a case it is required that SO₂

levels in the flue gas be minimal. The minimal amount is defined as the point when it is less expensive to let the SO₂ degrade the absorbent and add makeup than it would be to install additional SO₂ removal measures. After pretreatment, the gas is cooled and then contacted with the solvent in an absorption column forming weak intermediate compounds. Since CO₂ is an acid gas, chemical absorption systems utilize acid-base neutralization principles by employing alkaline solvents to neutralize the absorbed CO₂. After contact with the flue gas, the CO₂ rich solution is then sent to a stripping column where it is heated to break down the intermediate compounds. This regenerates the solvent and emits a concentrated CO₂ stream which is then compressed and transported for use. The CO₂ lean solvent is then recycled back to the absorber. [1, 2, 12, 28]

Several chemical absorption processes do exist, differing in the absorbent used to capture CO₂. The four major processes are: 1) amine absorption, 2) aqua ammonia absorption, 3) dual-alkali absorption, and 4) sodium carbonate (Na₂CO₃) slurry absorption. The operation of these technologies will be reviewed further in this section along with any flue gas considerations critical to operation.

3.1.1 Amine absorption

Amine absorption has been used by the natural gas industry for over 60 years to remove CO₂ from natural gas to produce food and beverage grade CO₂ [2]. Amines are derivatives of ammonia (NH₃), with one or more of the hydrogen groups being substituted with a functional group (e.g. ethanol). Amine absorption closely follows the process flow diagram shown in Figure 3. With amine absorption, the flue gas is cooled to 40-60 °C and contacted with the amine solution in a packed bed absorption column for capture. Some common amines include monoethanol amine (MEA), diethanolamine (DEA), and methyl diethanolamine (MDEA); with the most common being MEA due to its low cost. Basic MEA absorption will be used as an example going forward. The CO₂ is absorbed by, and chemically reacts with, the

MEA solution to form a MEA carbamate and bicarbonate solution. The reaction can be seen in equation 9 [11]. The weight % MEA in solution can vary from 15-35% depending upon the process.



$$\Delta H_{\text{rx}} = -20 \text{ kcal/mol}$$

A 35%, by weight, MEA solution has been reported to have a CO₂ carrying capacity of 0.40 kg CO₂/kg MEA in a clean flue gas stream (i.e. no impurities are present) [29]. If impurities such as NO_x and SO_x are present in the flue gas they will be absorbed by, and react with, the amine to form heat stable salts (HSS) [30]. Heat stable salts can cause plugging in equipment and drastically reduce the CO₂ capacity of the solvent; it is critical impurities are minimized. NO_x reduction is accomplished through selective catalytic reduction or selective noncatalytic reduction and SO_x reduction can be accomplished using any FGD system. After absorption, the loaded CO₂ solution is sent to a stripping column where it is heated between 100-200 °C to produce a gas stream consisting of 99% CO₂ and regenerate the MEA solvent. The CO₂ stream is compressed and transported for geological storage, use in the food and beverage industry, or urea production [1, 2, 10-12]. The regeneration reaction can be seen in equation 10.



$$\Delta H_{\text{rx}} = 20 \text{ kcal/mol}$$

The regenerated solvent is cooled to 40-60 °C and passed through a reclaimer stage to remove any ammonia and HSS that formed before being recycled back to the absorber unit. In the reclaiming unit, the HSS are reacted with a caustic at elevated

temperatures to regenerate additional MEA solvent. The regenerated MEA solvent has a CO₂ carrying capacity of 0.036 kg CO₂/kg regenerated solution [31].

3.1.1.1 Commercially available technologies

There are currently three amine absorption processes which are commercially available: the Kerr-McGee/AGG Lummus Crest (KMALC) process, the Fluor Econamine FG PlusSM (EFG+) process, and the KM-CDR process. The differences between these processes will be discussed briefly.

The KMALC technology uses a 15-20%, by weight (wt%), MEA solution for CO₂ absorption. The main advantage to the KMALC technology is that the low cost of MEA allows for optional flue gas desulphurization below 100 ppm. Below 100 ppm it is less expensive to let the SO_x degrade the MEA and add makeup than to install additional SO_x removal measures. The KMALC technology has demonstrated a max CO₂ absorption capacity of 800 tons/day CO₂ utilizing two absorption columns in parallel. This value is considerably less than the 8,000 tons/day CO₂ emitted from fossil fuel burning power plants. [9, 32]

The EFG+ technology employs a 35 wt% MEA solution mixed with a proprietary inhibitor for CO₂ absorption. The increase in MEA concentration, as opposed to the KMALC technology, reduces the degradation of the solvent from O₂ contact. The EFG+ technology is tailored to handle 1-15% O₂ containing gas streams. The proprietary inhibitor reduces the corrosive nature of the MEA solvent. This allows for the majority of equipment to be constructed from black carbon steel, reducing capital costs. However, the addition of the inhibitor increases the cost of the solvent thus requiring SO₂ removal to below 10 ppm to avoid excessive solvent makeup costs. The EFG+ technology has been demonstrated at over 25 locations worldwide with the main purpose being to extract CO₂ for urea production. It is currently the only amine technology to be demonstrated on gas turbine flue gas which contains

3.5% CO₂ and 13% O₂. The max CO₂ absorption capacity to be demonstrated thus far is 320 tons/day CO₂. [7, 30, 32-36]

The KM-CDR technology is licensed by Mitsubishi Heavy Industries. The technology uses a proprietary line of sterically hindered amines for CO₂ absorption. The sterically hindered amines have a bulky substitute group attached to the nitrogen atom, as seen in equation 11 denoted by the term R.



The sterically hindered amines have a low corrosive nature and less degradation from O₂ compared to MEA as a solvent. The KM-CDR technology has demonstrated a max CO₂ absorption capacity of 500 tons/day CO₂ using the KS-1 amine solvent. [8, 37-40]

3.1.1.2 Advantages and disadvantages

The advantages associated with chemical absorption using amines include:

- Since CO₂ chemically reacts with the amine, the process can handle low CO₂ partial pressure gas streams (3-20%)
- The process is mature. Three commercial technologies are currently available.

The disadvantages with amine absorption include:

- Low CO₂ loading capacity of the solvent (0.40 kg CO₂/kg MEA) [11]
- Solvent cannot be fully regenerated
- Scale up is an issue. Current technologies have a capacity of 320-800 tons/day CO₂. A 500MW power plant will emit roughly 8,000 tons/day CO₂ [6]. This means equipment will need to be much larger than is currently constructed.

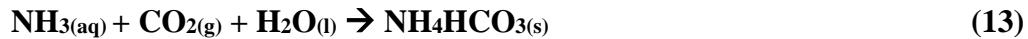
- Equipment corrosion – the amine will cause components in the absorption column and stripper to degrade over time.
- Amine degradation from NO_x, SO_x, O₂, and particulate matter
- High energy consumption during stripping/regeneration
 - Estimated 1/4 to 1/3 of a power plants output [27]
- Reclaimer stage is energy intensive and the waste stream can be hazardous
- Increase in plant footprint
 - Two parallel absorption column system or 12-18 meter diameter columns [9, 33]

To address some of the disadvantages associated with MEA absorption, other amines such as diethanol amine (DEA) and methyldiethanol amine (MDEA) have been used. In many cases mixed amine solvents offer reduced solvent circulation rates and lower heat duties in the stripping stage. Idem and colleagues (2006), compared MEA to a blend of MEA/MDEA. Their results found that with the MEA/MDEA blend a modest decrease in circulation rate could be achieved along with a large decrease in the heat duty needed for stripping compared to the MEA system.

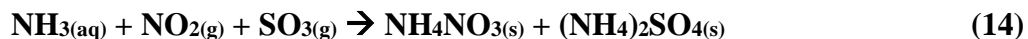
3.1.2 Aqua ammonia absorption

The aqua ammonia (NH₃) process has gained interest because of speculation that it could simultaneously remove NO_x and SO_x along with CO₂ from flue gases [41]. For absorption with ammonia, the flue gas is cooled to 15-27 °C (due to the volatility of ammonia) then contacted with the ammonia solution in a packed bed absorption column to capture CO₂, and possibly NO₂ and SO₃. The reaction mechanisms for CO₂ capture in an ammonia solution are seen in equations 12-13 [12, 42-44].





Possible products formed during CO₂ capture using aqueous ammonia include solid ammonium carbonate and bicarbonate. Bai and Yeh reported the formation of solid NH₄HCO₃ upon sparging CO₂ through an ammonia solution [45]. Yeh and Bai also found that a 35 wt% ammonia solution has a carrying capacity of 1.20 kg CO₂/kg NH₃ in a clean gas stream (CO₂/N₂) [29]. If the impurities NO_x and SO_x are present in the flue gas it may be advantageous to simultaneously capture them along with CO₂ using the ammonia solution. For simultaneous capture of NO_x and SO_x, pretreatment entails an oxidation stage in which the NO_x and SO_x are oxidized to NO₂ and SO₃. Ammonia solutions can only absorb the NO₂ and SO₃ forms of NO_x and SO_x gases. For information regarding oxidation techniques see [46-48]. Equation 14 shows the reaction between the ammonia solution, NO₂, and SO₃.

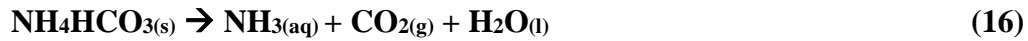


From equation 14 it can be seen that solid ammonium nitrate and sulfate will form upon reaction with the ammonia solution. This is advantageous because both are well known fertilizers which could possibly be sold to generate revenue.

After capture, the CO₂ loaded solution is sent to a stripping column where it is heated between 27-92 °C. The ammonium bicarbonate and carbonate thermally decompose at these temperatures, releasing CO₂ and regenerating the original ammonia solvent. The CO₂ stream is compressed and transported for geological storage, use in the food and beverage industry, or urea production. The regeneration mechanisms can be seen in equations 15 and 16 [31, 43, 49].



$$\Delta H_{\text{rx}} = 24.1 \text{ kcal/mol}$$



$$\Delta H_{\text{rx}} = 15.3 \text{ kcal/mol}$$

As can be seen from the enthalpies of reaction, it takes more energy to decompose the carbonate product as compared to the bicarbonate product. In this sense, it is desirable to form the bicarbonate solid as opposed to the carbonate. The formation of either solid can be controlled by careful monitoring of the solution pH. A high pH favors carbonate formation, whereas a low pH favors bicarbonate formation. After stripping the regenerated ammonia solution has a carrying capacity of 0.07 kg CO₂/kg solution. The loss in carrying capacity is believed to be due to heavy NH₃ losses in the vapor stream during stripping [31].

3.1.2.1 Advantages and disadvantages

Advantages to aqueous ammonia absorption include:

- High CO₂ loading capacity compared to other absorption processes (1.20 kg CO₂/kg ammonia)
- Possible multi pollutant control system
- No equipment corrosion issues
- No absorbent degradation from oxygen
- Ammonium nitrate and sulfate could be sold as fertilizer

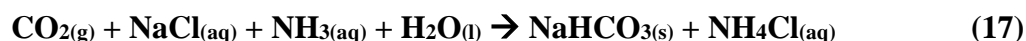
Disadvantages associated with ammonia absorption include:

- Flue gas must be cooled to 15-27 °C due to volatility of ammonia
- Equipment plugging due to solids formation upon CO₂ capture
- High ammonia vapor losses during stripping

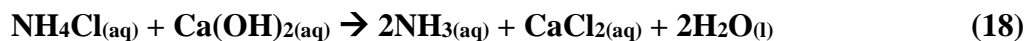
[29, 31, 41, 45]

3.1.3 Dual alkali absorption

The dual alkali absorption approach is a modification of the Solvay process. To understand what the dual alkali approach is proposing, it is necessary to first have an understanding of the Solvay process. The Solvay process is a two step process which converts CO₂ into Na₂CO₃ for commercial use. In the first step of the Solvay CO₂ is reacted with sodium chloride (NaCl), ammonia, and water to produce sodium bicarbonate (NaHCO₃) and ammonium chloride (NH₄Cl), as seen in equation 17 [2, 12].



Ammonia represents the primary alkali and is used to catalyze the absorption of CO₂. The NaCl is added to increase the concentration of Na in solution. This helps increase the precipitation of NaHCO₃. In the second step of the Solvay process the solid NaHCO₃ is filtered out of solution and heated to produce commercial grade Na₂CO₃. The leftover NH₄Cl solution is reacted with the secondary alkali, calcium hydroxide (Ca(OH)₂), to regenerate the NH₃; as seen in equation 18.



The main reason the Solvay process is not applicable to post combustion capture of CO₂ is that Ca(OH)₂ is used for regeneration. Calcium hydroxide is produced from lime which is formed by calcination of CaCO₃. The high energy demand of the calciner and CO₂ production from calcination make this process undesirable for large scale CO₂ capture.

The dual alkali approach, termed so by Huang and coworkers, aims to replace both alkali chemicals to make the Solvay process feasible for large scale CO₂ capture by eliminating the need for Ca(OH)₂ [50]. In the dual alkali process the primary alkali

is replaced with methylaminoethanol (MAE). With MAE as the solvent the flue gas must still be pretreated to remove impurities. The gas stream must be cooled to 25 °C and go through a De-NO_x-SO_x step. Salts formed from NO_x and SO_x reacting with the MAE degrade the performance of the system. Once the gas stream has been treated it is reacted with the MAE (HOCH₂CH₂(CH₃)NH) as seen in equation 19.

(19)



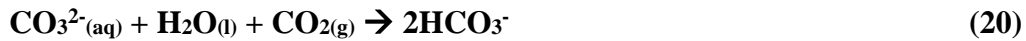
Huang and coworkers found that a 30 wt% MAE solution mixed with the 1.2 molar NaCl yielded the best results. The solution has a carrying capacity of 0.54 kg CO₂/kg MAE. Although a primary alkali has been identified, an alkali to regenerate the original MAE solvent has not been identified. If a secondary alkali were to be determined, this process would be advantageous owing to the fact that CO₂ can be captured to produce commercial grade Na₂CO₃. The obvious disadvantage to this process is that a secondary alkali has yet to be identified for regeneration of the MAE solvent. [50]

3.1.4 Absorption with sodium carbonate slurry

Using Na₂CO₃ solutions CO₂ was captured in the early 1900's for the production of dry ice [51, 52]. Knuutila and coworkers have since conducted a computer simulation to examine using a Na₂CO₃ slurry to capture CO₂. All data that will be discussed in this section was obtained by computer simulations using CHEMCAD 5.6. The simulations varied the Na₂CO₃ wt% (10-30%), the inlet liquid temperature (45-70 °C), inlet flue gas temperature (45-70 °C), liquid to gas (L/G) ratio (2.1-5.5), and the stripper pressure (1-2 bar) to determine the optimal CO₂ capture efficiency and amount of energy required to operate the stripper. Optimal conditions determined by the simulation were: 30 wt% Na₂CO₃ slurry, inlet liquid temperature of 60 °C, inlet flue gas temperature of 70 °C, L/G ratio of 2.3, and a stripper

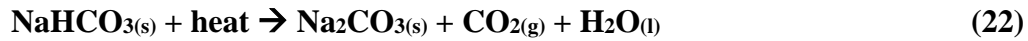
pressure of 2 bar. At these conditions, the simulation predicted a 90% CO₂ capture efficiency and an energy requirement of 3.2 MJ/kg CO₂ in the stripper. A sulphur free flue gas was assumed for the simulations. The simulated gas stream consisted of CO₂/N₂/H₂O vapor. [16]

As previously mentioned, for the capture of CO₂ the simulations found that a 30 wt% Na₂CO₃ slurry and an inlet flue gas temperature of 70 °C was optimal. This creates an environment in which NaHCO₃ precipitates out of solution allowing for more Na₂CO₃ to dissolve in solution; thereby increasing the CO₂ capacity of the solution. The capture of CO₂ and precipitation of NaHCO₃ via the carbonate slurry can be seen in equations 20 and 21 [53].



There was no mention made to the CO₂ carrying capacity of the slurry in the study performed by Knuutila and coworkers. However, a quick calculation based off equation 20 gives a theoretical carrying capacity of *0.73 kg CO₂/kg CO₃²⁻*, higher than that of MEA (0.40 kg CO₂/kg MEA). If impurities are present it is likely that this carrying capacity will decrease. For example, if SO₂ is present in the flue gas it may be absorbed by the solution, most likely creating sodium sulfite (Na₂SO₃) and sodium bisulfate (NaHSO₃) in solution [54]. This would lower the carrying capacity of the Na₂CO₃ slurry but provide a multi pollutant control system. Pretreatment of the flue gas would be optional when using a Na₂CO₃ slurry.

The CO₂ loaded slurry is sent to a stripping column where it is heated to 121 °C at a pressure of 2 bar to drive off CO₂ and produce solid Na₂CO₃. This mechanism can be seen in equation 22 [16].



3.1.4.1 Advantages and disadvantages

The system has many advantages associated with it, such as:

- Possible multi pollutant capture system
- Na_2CO_3 solvent is non-hazardous and non-volatile
- Low equipment corrosion rate
- Solvent will not cause the piping system to foul

The main drawback associated with the Na_2CO_3 system is the perceived slower absorption rate of CO_2 in comparison to amine solutions, leading to tall absorption columns. It is believed that rate increasing additives will need to be indentified for CO_2 capture with Na_2CO_3 solutions/slurries to be feasible. Studies have been conducted studying rate increasing additives such as arsenous acid, formaldehyde, hypochloride, phenols, sucrose, dextrose, piperazine, DEA, and MEA [16, 55-58]. Most of the rate increasing additives have been shown to increase the rate of absorption but also increase the energy needed for regeneration in the stripping column.

Table 2 is a comparison of the aforementioned absorption processes.

| Table 2 Chemical absorption technology comparison for post combustion capture of CO₂ | | | |
|--|---|---|---|
| Chemical Absorption Process Stage | | | |
| Technology | Pretreatment | Capture | Regeneration |
| Amine | Gas cooled (4-60°C) De-NO _x -SO _x required | CO ₂ content 3-20% Carrying capacity: 0.40 kg CO ₂ /kg MEA | Stripping at 100-200 °C Regeneration carrying capacity: 0.036 kg CO ₂ /kg solution |
| Ammonia | Gas cooled (15-27 °C) | CO ₂ content 3-20% | Stripping at 27-92 °C |
| Dual Alkali | NO _x -SO _x must be oxidized Gas cooled (25 °C) | Carrying capacity: 1.20 kg CO ₂ /kg NH ₃ | Regeneration carrying capacity: No regeneration has been accomplished |
| Carbonate | De-NO _x -SO _x required Gas cooled (45-70 °C) De-NO _x -SO _x not required | CO ₂ content 3-20% 0.54 kg CO ₂ /kg MAE Carrying capacity: 0.73 kg CO ₂ /kg CO ₃ ²⁻ | Stripping at 104-121 °C No mention to regeneration carrying capacity |

The carbonate technology is based off of computer simulations using CHEMCAD 5.6. Compression is similar in all cases.

3.2 Adsorption

Carbon dioxide capture using solid adsorbents is considered one of the most promising technologies for CCS [42]. Gas adsorption is a separation process in which a gaseous component is separated from a gas stream by the use of a solid material. The gaseous component comes into contact with the solid and is adsorbed from the gas phase onto the solid surface. The solid material used for adsorption is often referred to as the adsorbent and the gas species being adsorbed, the adsorbate (in this case the adsorbate is CO₂). When considering adsorption for CO₂ capture, it is important that the adsorbent possess certain qualities, such as [59]:

1. High CO₂ adsorption capacity: as a rule of thumb, an adsorbent should possess an adsorption capacity of 0.088 – 0.176 g CO₂/g adsorbent [60]
2. High surface area: a high surface area suggests more surface sites for CO₂ adsorption, possibly leading to a high adsorption capacity.
3. Fast kinetics: the faster the kinetics, the faster CO₂ will adsorb
4. High CO₂ selectivity: CO₂ should preferentially adsorb to the adsorbent. Selectivity also determines the purity of the CO₂ produced during desorption
5. Mild regeneration conditions: the milder the regeneration conditions (i.e. temperature and pressure) the less costly the regeneration stage will be
6. Stability during the adsorption/desorption cycle: the lifetime of the adsorbent has a significant impact on the operating cost of the system
7. Tolerance to impurities: the adsorbent must be tolerant to common flue gas impurities such as NO_x, SO_x, and water vapor. Impurities can significantly reduce the adsorption capacity with respect to CO₂ and even degrade the adsorbent crystal structure
8. A wide range of tunable properties: allows the adsorbent to be tailored to various operating environments
9. Low cost: adsorbents degrade over time, the cost to replace them should be minimal

Adsorbents are unique in that they can be tailored to capture CO₂ from either post or pre-combustion gas streams, depending upon several factors. For the sake of organization within this review, adsorbents will be discussed as a post-combustion technology because of the similarities in the process flow diagram to absorption. Figure 4 is a general flow diagram for CO₂ capture via adsorption.

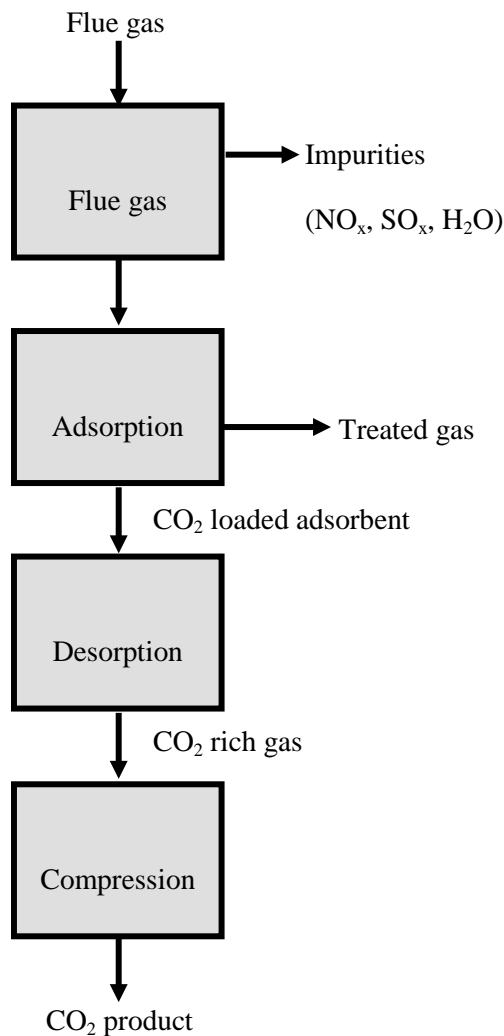


Figure 4: Basic flow diagram for the capture of CO₂ via adsorption

In CO₂ adsorption processes the flue gas stream must go through a pretreatment stage to reduce the concentration of impurities such as NO_x, SO_x, and H₂O in the gas stream. These impurities compete with CO₂ molecules for adsorption sites, drastically reducing the CO₂ adsorption capacity of the adsorbent. It is particularly important that the flue gas be dried prior to adsorption. Water has been shown to not only compete for adsorption sites, but to degrade the crystal structure of some adsorbents. After pretreatment, the gas should be cooled to around room temperature before the adsorption stage. Most adsorbents exhibit a drastic decrease in adsorption capacity at elevated temperatures (100 °C). Depending upon the adsorbent, CO₂ will adsorb either by weak physical interactions (physisorption) or strong chemical interactions (chemisorption). Physisorption is usually accompanied by a lower heat of reaction than chemisorption, making the desorption stage less energy intensive. After adsorption, the solid adsorbents go through a desorption stage. During desorption, gaseous CO₂ is driven off the adsorbent and the adsorbent is consequently regenerated in the process. The two most common approaches to desorption are pressure swing and temperature swing processes. In pressure swing systems the adsorption stage is carried out at an elevated pressure so when the pressure within the system is reduced, the CO₂ is desorbed from the solid. In a temperature swing system, the temperature of the system is increased to drive CO₂ from the adsorbent. The advantage to a temperature swing system is that the adsorbent can be regenerated while maintaining a high CO₂ partial pressure. This avoids the heavy energy penalty associated with having to recompress the CO₂, as is the case in pressure swing systems [61]. However, regeneration with pressure swing systems can be accomplished in matter of seconds, as opposed to hours with temperature swing systems [28].

Adsorbents discussed within this review include: 1) zeolites, 2) activate carbon, 3) amine functionalized adsorbents and, 4) metal organic frameworks (MOFs). For a more comprehensive review of adsorption/adsorbents please see [62, 63].

3.2.1 Zeolites

Zeolites are highly ordered porous crystalline aluminosilicates. Early CO₂ adsorption studies using zeolites have shown the primary mechanism of adsorption to be physisorption [64, 65]. Zeolites are able to adsorb CO₂ largely due to the presence of aluminum in the silicate structure. The presence of aluminum (Al) induces a negative framework charge that is compensated for with exchangeable cations (often alkali) in the pore space. These alkali cations enable zeolites to adsorb acid gases such as CO₂ [62]. Ideally, a low silicon (Si) to Al ratio is desired to promote the presence of more cations [66].

Before adsorption with zeolites, the flue gas must be cooled to around 0-100 °C and scrubbed to remove impurities such as SO_x, NO_x, and H₂O. Zeolites tend to be more sensitive to H₂O than acid gases due to their hydrophilic nature [66]. The polar H₂O molecules will preferentially adsorb to the exchangeable cations, effectively eliminating adsorption sites for CO₂ molecules [67].

After pretreatment, the flue gas is contacted with the zeolite adsorbent to remove CO₂. Zeolite adsorption kinetics are extremely favorable for CO₂ adsorption. In most cases, capacity is reached within minutes. Zeolites have relatively high adsorption capacities at mild operating conditions (0-100 °C, 0.1-1 bar CO₂) but show significant decreases in capacity at elevated temperatures and humid conditions. Adsorption capacities for zeolites at mild operating conditions range from 0.004 – 0.216 g CO₂ / g zeolite [62]. Although adsorption using zeolites is classified as physisorption, studies have found that some CO₂ does irreversibly chemisorb on the zeolite surface in the form of carbonates and carboxylates. If desorption is performed using a pressure swing process these chemisorbed CO₂ molecules cannot be liberated from the surface. This results in a reduction in capacity ranging from 0.007-0.022 g CO₂ / g zeolite [64, 68]. However, using a

temperature swing system it has been shown that complete regeneration can be accomplished at temperatures around 350 °C [62].

Adsorption of CO₂ via zeolites is well suited for post-combustion gas streams due to their favorable kinetics and capacities at mild operating conditions. For optimal adsorption performance using zeolites the flue gas stream needs to be thoroughly cleaned of impurities (NO_x, SO_x, and H₂O) prior to adsorption. To fully recover the adsorption capacity of the zeolite a temperature swing process is recommended for the desorption stage. The temperature swing process will remove any CO₂ that has chemisorbed to adsorption sites.

3.2.1.1 Advantages and disadvantages

Zeolites possess several advantageous for CO₂ adsorption:

- Favorable adsorption kinetics
- High adsorption capacity at mild operating conditions(0-100 °C, 0.1-1 bar CO₂)
 - Suitable for CO₂ capture from post combustion gas streams

Zeolites also possess serious disadvantages which need to be addressed:

- Presence of impurities (NO_x, SO_x, and H₂O) significantly impact performance
- Carbon dioxide has been shown to chemisorb to the zeolite surface. For complete regeneration, desorption must occur via the energy and time intensive temperature swing approach.

3.2.2 Activated Carbon

Activated carbons have an advantage over other adsorbents because of their high thermal stability and low raw material costs [66]. Activated carbons can be formed

from a variety of materials, including coals, industrial byproducts, and wood or other biomass sources [69, 70]. Although advantageous, the large variation in starting materials also contributes to large variations in pore distribution, pore structure, and pore size. This often leads to a wide variation in performance between adsorbents. This section will focus on activated carbons as they are well known adsorbent materials. However, other carbon adsorbents have emerged for CO₂ capture, such as carbon molecular sieves [71, 72] and carbon nanotubes [73]. For information regarding these materials please see the corresponding references.

Before adsorption with activated carbons, the flue gas should be cooled to 25-75 °C and scrubbed of NO_x, SO_x, and H₂O. Impurities such as NO_x, SO_x, and H₂O have been shown to compete with CO₂ for adsorption sites. As is the case with zeolites, activated carbons are extremely sensitive to H₂O (even though they are hydrophobic in nature). A study using bamboo activated carbon at 0 °C and 1 bar CO₂ showed a reduction in capacity of 75% in the presence of H₂O [62].

After pretreatment, the flue gas is contacted with the activated carbon to remove CO₂. Adsorption on activated carbons occurs via physisorption. The adsorption kinetics of CO₂ on activated carbons is similar to that of zeolites; the capacity is reached within minutes. As with zeolites, studies have shown that as the temperature of the system increases, the CO₂ capacity of activated carbon decreases. Activated carbons are most efficient around room temperature. Activated carbons have also been shown to exhibit a lower CO₂ adsorption capacity at mild temperature and pressure compared to zeolites. Adsorption capacities for activated carbon at mild operating conditions (0.1-1 bar CO₂ and 25-75 °C) range from 0.003 – 0.154 g CO₂ / g activated carbon, slightly lower than that of zeolites under similar operating conditions [62]. However, studies have shown that activated carbons are superior to zeolites at elevated pressures. A study comparing activated carbon PX21 to zeolite 5A at ambient temperature and 10 bar CO₂ showed that the

activated carbon had a capacity of 0.44 g CO₂ / g activated carbon, whereas the zeolite had a capacity of 0.22 g CO₂ / g zeolite [69]. Further studies comparing G-32H activated carbon to zeolite 4A and 13X found that the activated carbon had a lower CO₂ adsorption capacity than the zeolites below 1.7 bar CO₂. However, above 1.7 bar CO₂ the activated carbon exhibited a larger CO₂ adsorption capacity than the tested zeolites [74]. The activated carbon, MAXSORB, has been shown to have a CO₂ adsorption capacity as high as 1.13 g CO₂ / g activated carbon at 35 bar CO₂ and room temperature. The increased capacities at elevated pressures suggests that activated carbons would be better for CO₂ capture from pre-combustion gas streams, rather than post-combustion gas streams.

Adsorption studies with activated carbons have also shown that activated carbons exhibit lower heats of adsorption in comparison to zeolites [75]. Because of the lower heats of adsorption, activated carbons can be easily regenerated using a pressure swing system instead of the energy and time intensive temperature swing systems required to regenerate zeolites [66].

Activated carbons will remain competitive with future CO₂ adsorbents because of low raw material and regeneration costs. As with zeolites, extensive pretreatment is required for efficient CO₂ adsorption. Adsorption research on activated carbons show high CO₂ adsorption capacities at elevated pressures and mild temperatures. This suggests they are more applicable for CO₂ capture from the high pressure pre-combustion gas streams.

3.2.2.1 Advantages and disadvantages

Activated carbons possess several advantages:

- High thermal stability
- Favorable adsorption kinetics
- Wide range of starting materials for production of activated carbons

- Leads to lower raw material costs
- Large adsorption capacity at elevated pressures
- Desorption can easily be accomplished by the pressure swing approach

Disadvantages that need to be addressed with activated carbons include:

- Low CO₂ capacity at mild conditions
- Wide variety of starting materials means a wide variety of pore characteristics is often seen between adsorbents
- Negatively impacted by NO_x, SO_x, and H₂O

3.2.3 Amine functionalized adsorbents

Amine functionalized adsorbents consist of an amine immobilized onto solid silica supports (also referred to as impregnating silica supports with amines). Researchers thought to immobilize amines to address some of the major issues with amine absorption, such as: high regeneration costs (due to large volume of liquid associated with absorption), equipment corrosion, and amine loss due to evaporation. Impregnating the silica support with amine is often as simple as mixing the two materials. Sufficient mixing time is needed to allow the amine to diffuse into the silica pore space to create active sites for adsorption. The most common amine used for impregnation is poly(ethyleneimine) (PEI) because of its high amine concentration of roughly 33% nitrogen by weight [62].

Before adsorption with amine adsorbents it is important to cool the flue gas between 50-75 °C and remove impurities such as NO_x and SO_x. At elevated temperatures amine adsorbents have been shown to degrade, significantly limiting their CO₂ adsorption capacity [62]. Impurities such as NO_x and SO_x are harmful to amine adsorption largely because adsorption with amines occurs via chemisorption [66]. This means that adsorption will occur by similar chemical reactions seen in amine absorption. It is well known that NO_x and SO_x will irreversibly react with amines to

form unwanted byproducts, effectively reducing the CO₂ adsorption capacity. Unlike other adsorbents, amine adsorbents do not require that the flue gas stream be dried prior to adsorption. Water has been shown to increase adsorption efficiency by providing a pathway for bicarbonate formation. Studies examining the silica structure SBA-15 impregnated with TEPA and DEA showed a 20% increase in adsorption efficiency under humid conditions [76]. A 1:1 molar ratio of CO₂ to H₂O is believed to be optimal for adsorption [62].

Adsorption is also significantly impacted by the silica support. Amorphous silica frameworks typically have a random array of pore sizes and shapes. This often leads to poor distribution of the amine into the pore structure. For this reason, ordered mesoporous silica supports are preferred for their uniform pore size distribution. Interestingly enough, the CO₂ partial pressure was shown to have a minimal impact on adsorption capacity, unlike zeolites and activated carbons. Studies found that when the CO₂ partial pressure was reduced from 100 – 5 % a minimal decrease in the adsorption capacity was seen [77]. This suggests that amine adsorbents would work well for CO₂ capture from low pressure gas streams, i.e. post-combustion gas streams. Adsorption capacities for amine adsorbents at mild operating conditions (0.05-1 bar CO₂ and 25-75 °C) range from 0.089 – 0.22 g CO₂ / g adsorbent [62].

Since amine adsorption occurs via chemisorption, a temperature swing process is needed for desorption. Studies examining TEPA loaded MCM-41 and SBA-15 silica supports showed a 4-9% loss in the CO₂ adsorption capacity of the regenerated material due to evaporation of the amine [77, 78].

Amine adsorbents are advantageous in that their adsorption capacity is not greatly affected by CO₂ partial pressure. This makes them extremely well suited for capture from post-combustion gas streams. However, the need for a temperature swing

desorption stage and the loss in capacity is a concern that needs to be addressed in the future.

3.2.3.1 Advantages and disadvantages

Amine functionalized adsorbents present some interesting advantages:

- Adsorption capacity minimally impacted by CO₂ partial pressure
- Humid environments improve adsorption efficiency
- Favorable adsorption kinetics

Disadvantages to be addressed with amine functionalized adsorbents include:

- Degrade at temperatures around 100 °C
- Irreversible reactions with NO_x and SO_x produce unwanted byproducts
- A temperature swing approach is needed for desorption
 - 4-9 % loss in adsorption capacity after desorption

3.2.4 Metal organic frameworks (MOFs)

Metal organic frameworks are an emerging class of microporous crystalline structures composed of central cation molecules linked together by organic linkers (ligands) to form a 3-D structure. MOFs have recently seen an increase in popularity due to their applications in separation, catalysis, nonlinear optics, and gas storage [79-84]. MOFs are especially interesting as a CO₂ adsorbent because of the ability to easily tune parameters such as pore size and topography.

With adsorption using MOFs, the flue gas needs to be cooled to around 25 °C and treated to remove impurities such as NO_x, SO_x, and H₂O. Studies have shown that the adsorption capacity of MOFs decreases as temperature increases [62]. If impurities are present they will compete with CO₂ for adsorption sites, drastically reducing the capacity of the MOF. Water vapor has been shown to pose a particularly large problem during adsorption. If not removed, water molecules will

displace the ligands and create structural defects in the crystal lattice of the MOF. Studies have also shown that MOFs exhibit poor adsorption characteristics at low CO₂ partial pressures compared to zeolites and activated carbon [85]. However, studies performed at elevated CO₂ partial pressures showed superior adsorption characteristics to zeolites and activated carbons. Adsorption studies performed with MOF-177 at room temperature and 35 bar CO₂ produced a CO₂ capacity of 1.47 g CO₂ / g MOF [86]. In comparison, the activated carbon MAXSORB has a capacity of 1.13 g CO₂ / g adsorbent at identical conditions [87] and zeolite-13X has a capacity of 0.326 g CO₂ / g adsorbent at 32 bar CO₂ [88]. This suggests that MOFs have enormous potential for CO₂ capture from elevated pressure gas streams, i.e. pre-combustion gas streams. The desorption stage has not been adequately studied to allow for comment on which approach, pressure or temperature swing, would be the most efficient for regeneration.

Although MOFs possess enormous potential for CO₂ capture, some major challenges inhibit their use. Such as, costly starting materials, lack of experimental data examining the impact of multiple adsorption/desorption cycles on performance, and the lack of experimental data describing the effects of pressure or temperature swing on regeneration of the MOF.

3.2.4.1 Advantages and disadvantages

MOFs possess several advantages as an adsorbent for CO₂ capture, such as:

- High thermal stability [89]
- Adjustable chemical functionality [83]
- Extra high porosity [90]
- High adsorption capacity at elevated pressures (35 bar CO₂)
- Easily tunable pore characteristics

Disadvantages to MOFs include:

- Negatively impacted by NO_x , SO_x , and H_2O
- Low CO_2 selectivity in CO_2/N_2 gas streams
- Lack of experimental data on performance after multiple adsorption/desorption cycles
- Pressure and temperature swing desorption approaches have not been adequately researched

3.3 Membrane separation

Membrane separation processes are currently used commercially for CO_2 removal from natural gas; in these streams, the overall pressure and CO_2 concentration are high and the stream consists mainly of CO_2 and CH_4 [1]. This stream is far different from the stream which would be encountered in post combustion flue gas streams which contain impurities such as NO_x and SO_x and are at atmospheric pressure.

Figure 5 is a general schematic of a gas separation membrane. [12, 28, 91, 92]

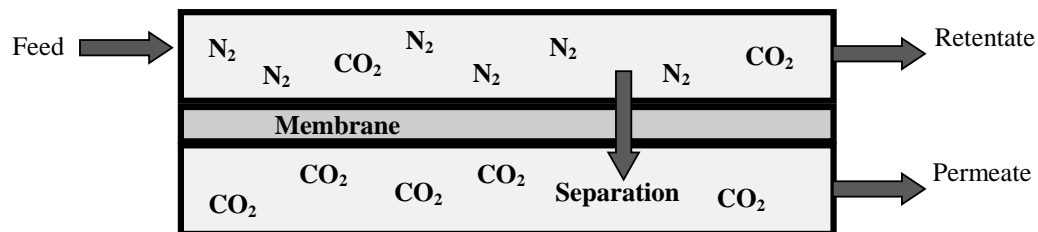


Figure 5: Schematic of a gas separation membrane. Membrane selectively separates the carbon dioxide (CO_2) molecules from the nitrogen (N_2) molecules. Kinetic diameters: CO_2 – 3.30 angstroms; N_2 – 3.64 angstroms.

The membrane acts as a filter to remove one or more gas components from a mixture and generate a component rich permeate. The driving force behind the performance of membranes is the pressure differential between the feed side and the permeate side of the membrane, as seen by Fick's Law in equation 23.

$$J_i = \frac{P_i^*}{\delta} A_m \Delta p \quad (23)$$

Where J_i is the flux of component i across the membrane (cm^3/s), P_i^* is the permeability of the membrane in terms of component i ($10^{-10} \text{ cm}^3 (\text{STP}) \cdot \text{cm}/\text{sec} \cdot \text{cm}^2 \cdot \text{cm Hg}$), δ is the membrane thickness (cm), A_m is the membrane area (cm^2), and Δp is the pressure difference (cm Hg) across the membrane. Fick's Law shows the importance of the pressure differential and permeability in membrane separation; as the pressure differential and permeability increase the flux of a specific component across the membrane will also increase.

There are two characteristics that describe the performance of a membrane, permeability (commonly expressed in units of barrer) and selectivity. Permeability is defined as the volume of a gas species passing through the membrane per unit time and area. Selectivity is determined by the difference in permeability of the gas species: selectivity quantifies a membranes preference to pass one gas species over another [93]. For example, using Figure 5, if the permeability of CO_2 through the membrane is seven times greater than that for N_2 , the permeate stream will contain seven times more CO_2 molecules than N_2 molecules at any given time. The selectivity then, taking the permeability of CO_2 over N_2 , is seven. Ideally, a membrane would possess a high CO_2 permeability and selectivity.

The permeability and selectivity of membranes are strongly dependent upon gas stream characteristics (i.e. velocity and gas component molecular weight and kinetic diameter), the membrane material, and how the membrane is synthesized.

Polymeric membranes generally exhibit high CO₂ permeability but low selectivities. Some control over permeability and selectivity can be obtained by altering the temperature, pressure, and polymer concentration during membrane synthesis. Polymeric membranes are susceptible to aging, plasticization, and degradation in the presence of high temperatures. Inorganic membranes, on the other hand, tend to be highly selective but have a lower CO₂ permeability than most polymeric membranes, which limits their application for CO₂ capture. However, most inorganic membranes exhibit excellent thermal and chemical stabilities. [2, 12, 94]

A simplified flow diagram of post combustion membrane based CO₂ capture can be seen in Figure 6.

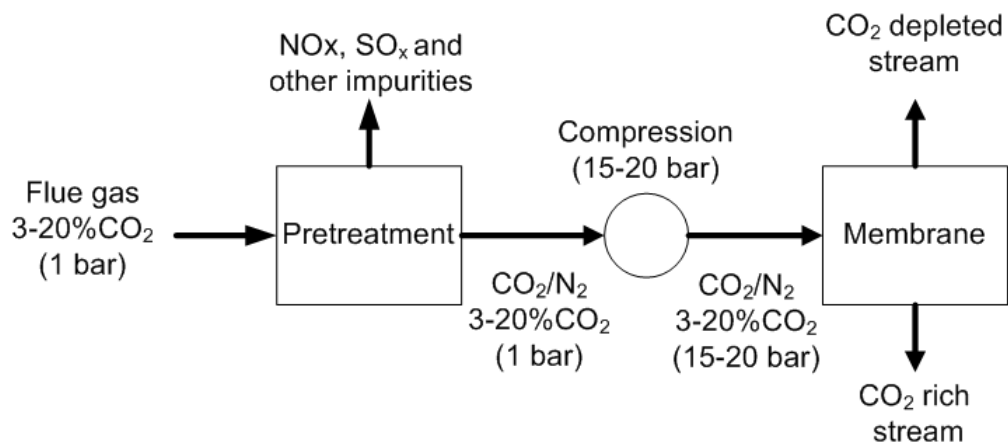


Figure 6: simplified process flow diagram for membrane based CO₂ capture

Membrane separation based CO₂ capture systems use permeable or semi-permeable materials which selectively transport and separate CO₂ from other gas stream constituents. Post combustion membrane separation is based on the separation of CO₂ from CO₂/N₂ gas streams. Thus for membranes to be effective it is believed that the flue gas must first be pretreated to remove impurities such as NO_x and SO_x. A study conducted by Scholes and coworkers examining the effects of minor components on CO₂ separation using polymeric gas membranes, suggests that impurities may have adverse effects on membrane separation [95]. However, a limited number of membranes were tested so the authors could not draw any concrete conclusions about the impact of impurities on membrane performance. Thus, NO_x and SO_x cleaning levels are unknown. After impurities are removed the gas stream must be cooled to below 100 °C to avoid heat degradation of the membrane (in most cases). Once cooled the gas stream is compressed to 15-20 bars to create a large driving force for separation within the membrane. Once within the membrane unit the CO₂ is separated from the N₂. There are innumerable types of membranes which can be used for CO₂ capture. For this reason, it is important to have a basic understanding of how membranes work and how performance is judged.

A brief discussion follows about organic and inorganic membranes with regards to CO₂ removal from CO₂/N₂ gas streams. Also discussed are mixed matrix membrane systems and hybrid membrane/absorption systems.

3.3.1 Organic Membranes (polymeric)

A large variety of polymeric membranes provide good permeability and selectivity towards CO₂ in CO₂/N₂ gas streams [94]. These include polyimides [96], polycarbonates [94], polyethylene oxides (PEO) [97], polyacetylenes [98], polyaniline [99], poly(arylene ether)s [100], polyarylates [101], polyphenylene ethers [102] and polysulfones. Table 3 is a summary of the CO₂ permeability and

CO₂/N₂ selectivity of the more popular polymeric membranes. For further information regarding the other polymeric membranes see the detailed review assembled by Powell and Qiao (2006) or the references given above.

| Material | CO₂ Permeability (Barrer) | CO₂/N₂ selectivity |
|-----------------|---|---|
| Polyarylate | 5 – 85 | 10 – 30 |
| Polycarbonate | 5 – 110 | 15 – 26 |
| Polyimide | 5 – 450 | 5 – 55 |
| Polysulfone | 5 – 110 | 10 – 33 |

3.3.2 Inorganic Membranes

Inorganic membranes will not be discussed in much detail because, as mentioned previously, low CO₂ permeability limits their application for CO₂ capture. Inorganic membranes can be divided into two categories: porous and non-porous. In general, the non-porous membranes are used for highly selective separation of small molecule gases. The porous membrane systems consists of a porous thin top membrane layer which is cast on a porous support, usually metallic or ceramic, to provide mechanical strength. The support must offer minimal mass transfer resistance with respect to the component being removed. Porous inorganic membranes are cheaper than the non-porous membranes, but are less selective with respect to CO₂. Inorganic membranes also suffer from the disadvantage of difficult scale up to large surface areas. Common porous inorganic materials include alumina, silica, and zeolites.

3.3.3 Mixed Matrix Membranes

Mixed matrix membranes are designed to enhance the properties of polymeric membranes. They consist of micro or nano sized inorganic particles incorporated into a polymeric matrix. The addition of inorganic particles enhances the physical, thermal, and mechanical properties of a polymeric membrane thus better suiting them for CO₂ removal from flue gases. Challenges associated with mixed matrix membranes include their high cost, brittleness, and difficult commercial scale manufacture. [2]

3.3.4 Membrane Contactor Systems

Membrane contactor systems combine a membrane with an absorption liquid, such as an amine, into one unit. The absorption liquid could be any liquid used for absorbing CO₂. The target of these systems is to reduce the size of the absorption unit associated with traditional CO₂ absorption systems [103]. A diagram of a hybrid system can be seen in Figure 7 [18, 104, 105].

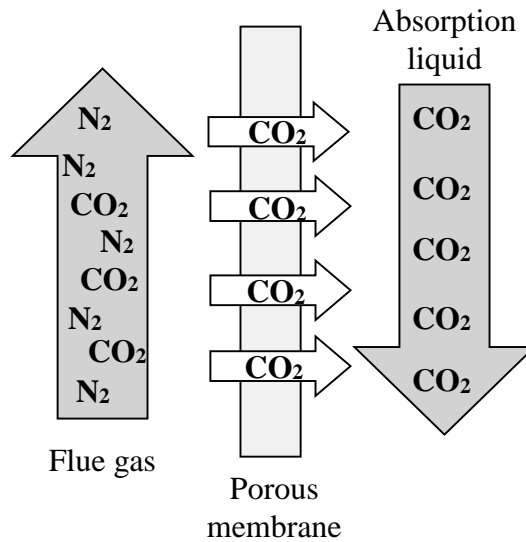


Figure 7: Membrane contactor principle. The CO₂ diffuses through the membrane where it contacts, and is absorbed by, the absorption liquid.

With membrane contactors the gas phase is isolated from the liquid phase via a porous, water repellent polymeric membrane. It is crucial that the gas and liquid phase do not mix, thus the membrane should be hydrophobic. The flue gas stream is fed along one edge of the membrane while the absorption liquid is fed along the other edge. The CO₂ will diffuse through the membrane where it contacts, and is absorbed by, the absorption liquid. The remainder of the flue gas is vented to the atmosphere. Using a membrane to separate the CO₂ from the flue gas before absorption reduces the overall volume of gas that is fed to the absorption column. A reduction in flue gas volume means the absorption equipment may be reduced in size. Advantages to this system include:

- The gas and liquid flows are independent of one another. This alleviates common problems associated with packed columns and can drastically reduce the circulating rate of absorption liquid.

- Possible size reduction of the absorption unit due to a reduced volume of gas
- Easy scale up, high gas-liquid interfacial area, and increased mass transfer rates [104]

For membranes to be practical for post combustion capture of CO₂ it is believed that any membrane used must possess the following properties:

- High CO₂ permeability
- High CO₂/N₂ selectivity
- Thermally and chemically stable
- Plasticization and aging resistant
- Ability to be cheaply manufactured for commercial use

It should be noted that membranes operate best when the CO₂ content in the *feed* stream is 20% or greater [106-108]. However, recent studies point out that a multistage membrane system could be used to sufficiently capture CO₂ on streams less than 20% CO₂ [109, 110].

3.3.4.1 Advantages and disadvantages to membranes

Advantages to membrane separation include:

- Simplicity: no need to add chemicals or regenerate a solvent with membranes
- Low capital costs
- Compact design
- Avoidance of operational problems associated with absorption. Such as, foaming, flooding, entrainment, and channeling.

Issues associated with membrane separation which limit their use include:

- The initial flue gas stream pressure is small (1bar). This means a low driving force for separation in the membrane. Gas stream must be compressed to 15-20 bars for efficient separation.
- Low CO₂ content in the feed stream which requires high selectivity membranes. Bounaceur and Favre (2006) performed a studies comparing membrane separation to basic amine absorption. Studies found that for CO₂ streams containing 10% or less CO₂, energy consumption for membrane separation is much larger than for basic amine absorption. However, at streams of 20% or greater CO₂ content the energy consumption is comparable to that of absorption. [106, 107, 110]
- High temperature of flue gas will degrade organic membranes. Gas must be cooled to below 100 °C.
- Membranes must be resistant to flue gas impurities, aging, and plasticization (hardening).
- Single stage membrane systems are not capable of high CO₂ capture efficiency; a second stage is needed. [2]

3.4 Cryogenic distillation

Cryogenic distillation has been utilized for years to separate atmospheric air into its primary components, but it is a relatively novel idea for post combustion capture of CO₂. In a cryogenic separation system, CO₂ is physically separated from other gas stream constituents on the basis of dew and sublimation points [91, 111, 112]. The main advantage to cryogenic separation is that no chemical reagents are needed. Two cryogenic separation technologies for post combustion capture of CO₂ have been proposed: 1) Clodic and Younes have proposed a process in which gaseous CO₂ is de-sublimated onto the surface of heat exchanger fins and then recovered as liquid CO₂ at elevated pressures [112]; 2) Tuinier and coworkers have proposed a process using packed beds where the CO₂ is de-sublimated onto the packing

material then released to produced gaseous CO₂ [111]. Each process will be discussed in more detail to better understand the differences between the two.

The process proposed by Clodic and Younes has been studied on pretreated gas streams of CO₂/H₂O/N₂ and has 93% CO₂ removal efficiency from a 15% CO₂ containing gas stream. A simplified process flow diagram can be seen in Figure 8.

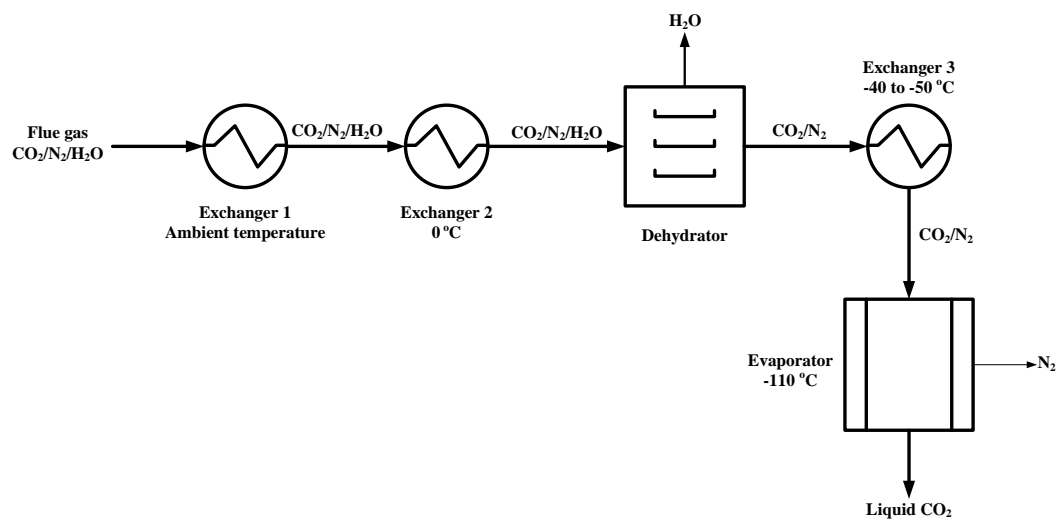


Figure 8: Process flow diagram for cryogenic distillation of CO₂ as proposed by Clodic and Younes

First, the entering flue gas stream (60-100 °C) is cooled to near ambient conditions using ambient air and water. The water helps to remove any residual particulates in the gas stream. The flue gas then enters a second heat exchanger where the temperature is reduced to just above 0 °C to remove water vapor. The flue gas is then passed through a dehydrator to remove any trace elements of water. (Since the operating temperature of the system is well below the freezing point of water, it is critical that all traces of water be removed from the system to prevent unwanted plugging and system efficiency degradation from ice formation. The water levels in the dry flue gas must be reduced to 1.1×10^{-4} grams H₂O/gram dry flue gas.) After the remaining water is removed from the flue gas a third exchanger is used to bring the flue gas temperature down to -40 to -50 °C. This stage is primarily used to condense trace gases or any unburned hydro carbons still present. The flue gas stream, now composed of CO₂/N₂, is sent to an evaporator operated at an average temperature of -110 °C. The CO₂ de-sublimates onto the cold surface in the evaporator while the N₂ exits unaffected. The solid CO₂ is then recovered as a liquid by “heating” the system to -56 °C under 520 kPa (roughly 5 atm) of pressure [28, 112, 113]. Drawbacks to this process include:

- water content of the feed stream must be removed to prevent equipment plugging from the formation of ice
- buildup of solid CO₂ reduces the efficiency of the evaporator over time
- high capital cost of equipment
- high cost of refrigerant used to cool the system

The process proposed by Tuinier and coworkers looks to circumvent the drawbacks associated with Clodic’s process, such as the need for complete H₂O removal and costly high pressure vessels. Tuinier’s technology utilizes three packed beds to continuously capture CO₂. Each bed operates a different cycle: capture, recovery, and cooling.

During the capture cycle CO₂ is separated from the CO₂/H₂O/N₂ gas stream in a packed bed at -150 °C. In the capture stage the H₂O first condenses out of the gas stream onto the packing material. As the H₂O in the gas stream becomes depleted the CO₂ will then start to de-sublimate onto the cold packing material. As the fresh flue gas is fed to the bed it heats up the packing material causing the de-sublimated CO₂ to transition to the gas phase producing a gaseous CO₂ stream. The CO₂ stream is then fed to the recovery bed at roughly -70 °C. Due to the increased partial pressure of CO₂ in this stream some CO₂ will, again, de-sublimate onto the cold packing material. As the fresh CO₂ stream continues to be fed to the recovery bed the packing material is heated up. This causes the de-sublimated CO₂ to transition to the gas phase again, creating a concentrated CO₂ stream which is compressed for various uses. During the cooling cycle the H₂O remaining in the beds is removed and vented to the atmosphere. The main advantage to Tuinier's technology is that water can be tolerated in the inlet gas stream. Other advantages to this process over Clodic's include: the use of low pressure vessels and inexpensive packing material for CO₂ to de-sublimate onto [111, 114]. The main drawbacks to this technology are the scale up of the equipment and the continuous operation of the three packed beds.

For cryogenic distillation processes, the flue gas still needs to go through a pretreatment step to remove impurities such as NO_x and SO_x to increase the concentration of CO₂ in the gas stream. As the concentration of CO₂ in the gas stream increases, the temperature that the gas stream must be cooled to for CO₂ de-sublimation becomes less negative. For example, at 2% CO₂ in the gas stream the temperature required for de-sublimation is -116 °C, while at 15% CO₂ the temperature required is -99 °C. For operation it is recommended the flue gas stream contain greater than 10% CO₂, as lower concentrations of CO₂ will lead to higher cooling requirements per mass of CO₂ captured.

3.5 Conclusions to post combustion capture of CO₂

Of all the approaches that can be taken for post combustion capture of CO₂, amine absorption is currently the most mature technology on the market; three commercial technologies are available. However, no technology mentioned above is yet suited for the scale of CO₂ capture from fossil fuel burning power plants. Every post combustion capture approach suffers from the same design challenge: *how to scale up a system to handle the enormous volume of flue gas produced from fossil fuel combustion.*

As a reminder, when exploring post combustion capture options it is important to take note of:

- The level of impurities present in the flue gas (NO_x, SO_x, particulate matter must be minimal)
- Total volumetric flow of the flue gas. This is the **main** factor in sizing all equipment needed.
- The partial pressure of CO₂ in the flue gas (suited for 3-20%)
- The temperature of the inlet flue gas stream (gas will need to be cooled)
- Required CO₂ removal efficiency
- The intended use of the captured CO₂. High purity CO₂ is needed for the food and beverage industry but not geological storage

4 **Pre-combustion capture of CO₂**

Pre-combustion capture of CO₂ refers to CO₂ capture from a synthesis gas (syngas) stream before combustion and power production occurs. It applies to integrated gasification combined cycle (IGCC) power plants. At IGCC power plants the primary fuel (coal, natural gas, crude oil, etc.) is first “gasified” to produce a syngas consisting primarily of carbon monoxide (CO) and hydrogen (H₂). The CO in the gas stream is then converted to CO₂, to create a gas stream consisting of CO₂/H₂

from which the CO₂ is separated. The remaining H₂ gas stream is then used as the fuel source for energy production. Pre-combustion gas streams contain 15-40% CO₂ at elevated pressures (200-600 psi). A simplified block diagram for pre-combustion capture of CO₂ can be seen in Figure 9. [25]

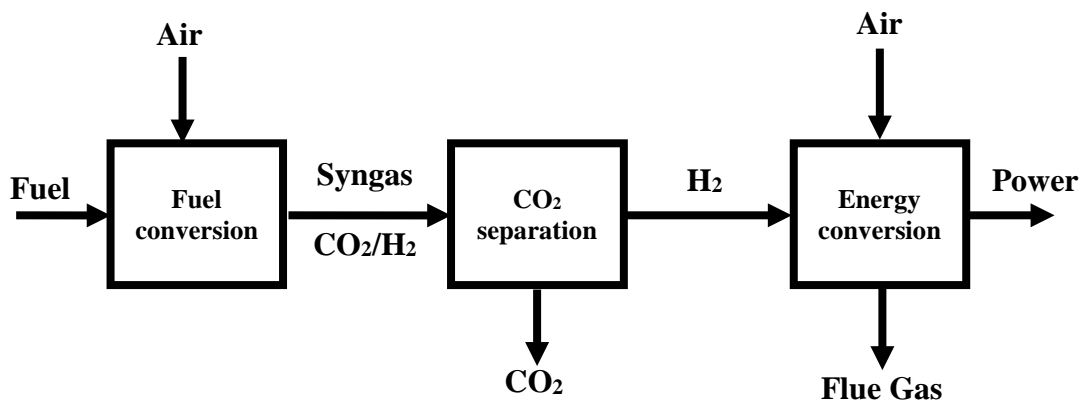
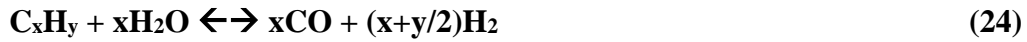


Figure 9: Simplified block diagram for pre-combustion capture of CO₂

The syngas is created by reacting the primary fuel with either steam or oxygen (steam if the fuel is solid, oxygen if fuel is liquid or gaseous) at elevated temperature (1,400 °C) and pressure (500-800 psi), as seen in equations 24 and 25 [1, 115, 116].



The syngas is then reacted with steam in a water-gas-shift (WGS) reaction to convert the CO to CO₂, producing a gas stream consisting of CO₂/H₂, seen in equation 26 [1, 117].



The WGS reaction increases the partial pressure of CO₂ in the gas stream, thereby increasing the driving force for capture. Due to the increase in the partial pressure of the CO₂ it can be captured by contact with physical solvents in an absorption column or by the use of membranes. Physical solvents will be discussed going forward as membranes were previously discussed in detail for post combustion capture of CO₂. The same basic principles and technology apply for membrane technologies for pre-combustion capture of CO₂.

Physical solvents selectively capture CO₂ without the use of a chemical reaction. They rely on the solubility of CO₂ into solution; thus they obey Henry's Law which states that the solubility of a gas is proportional to its partial pressure. According to Henry's Law, this means that high partial pressures of CO₂, and low temperatures, are desirable for capture using physical solvents [42, 118]. Once the CO₂ is removed, the H₂-rich syngas is combusted to ultimately produce electricity and the

CO₂ loaded solvent is regenerated. The CO₂ loaded solvent can be regenerated by two methods: 1) flash desorption and 2) stripping. In flash desorption the CO₂ loaded solvent, still at elevated pressure, is degassed through a series of pressure reduction stages. When the pressure is reduced the gaseous CO₂ will be released from the physical solvent, thus regenerating the capacity of the original solvent. In stripping, the CO₂ loaded solvent is first degassed in a similar manner as with flash desorption. After degassing, the solvent is stripped with an inert gas (such as N₂) to drive out the remaining CO₂. Currently, four pre-combustion capture technologies exist which use physical absorption to capture CO₂: Selexol, Rectisol, Fluor, and Purisol. A comparison between the technologies can be seen in Table 4 and they will be discussed in more detail to illustrate the differences between them.

4.1 Selexol

The Selexol technology has been in use since the 1960's for natural gas sweetening. The process is for high partial pressure CO₂ gas streams (450 psi) and is capable of simultaneously removing CO₂ and sulfur compounds without degrading the solvent. The technology uses Union Carbide Selexol solvent; a mixture of dimethyl ethers and polyethylene glycol (CH₃O(C₂H₄O)_nCH₃), with "n" ranging from 3-9 [12, 119]. In the Selexol process the flue gas must first be dehydrated before contact with the solvent. Once dehydrated, the flue gas contacts the solvent in an absorption column at roughly 450 psi and 0-5 °C producing a loaded CO₂ solvent. Regeneration of the original solvent is then accomplished by flash desorption or stripping of the CO₂ loaded solvent. The CO₂ gas stream obtained is then compressed and stored while the regenerated solvent is recycled back to the column [12, 120, 121]. Advantages to the Selexol process include:

- No chemical reaction means the heat rise within the absorption column will be minimal
- Non-thermal solvent regeneration
- Non corrosive - equipment can be constructed out of carbon black steel

- Gas from the absorber leaves dry due to the high affinity of the Selexol solvent to capture water vapor

Disadvantages to the Selexol process include:

- Process is most efficient at elevated pressures

4.2 Rectisol

The Rectisol process is for low to moderate partial pressure (250 psi) CO₂ gas streams. The technology makes use of chilled methanol as the solvent for CO₂ capture. Due to the high vapor pressure of methanol, the absorption stage must take place at low temperatures (-30 to -100 °C) [120, 122]. The gas stream entering the absorber contacts the chilled methanol solvent at 700 psi with a CO₂ content of 35% (250 psi CO₂). After CO₂ has been captured the original solvent is regenerated by flash desorption of the CO₂-loaded methanol solvent. The CO₂ gas released is then compressed and stored while the regenerated solvent is recycled back to the absorber. The Rectisol process produces a gas stream that is 98.5% CO₂. This means the CO₂ is not suitable for the food and beverage industry but can be used for urea production [116]. Advantages to the Rectisol process include:

- The solvent does not foam in the absorber and is completely miscible in water [12]
- Solvent has a high chemical and thermal stability
- Non-corrosive → carbon black steel can be used for construction
- Non-thermal solvent regeneration

Drawbacks to the Rectisol process are:

- The solvent is capable of absorbing trace metal compounds, such as mercury, to form amalgams at the low operating temperatures
- Refrigeration of the solvent results in high operating costs
- Complex operating scheme results in high capital costs

4.3 Fluor

The Fluor process is one of the most attractive processes for treating high CO₂ partial pressure flue gas streams [12]. The process utilizes a solvent composed of propylene carbonate (C₄H₆O₃). In the Fluor process, the flue gas must first be dehydrated before contact with the solvent to prevent water buildup within the solvent. Once dehydrated, the flue gas contacts the Fluor solvent in an absorption column at roughly 400-1200 psi with the CO₂ content varying from 30-70% (Max range of 280-850 psi CO₂) at ambient temperature, producing a loaded CO₂ solvent. Regeneration of the original solvent is then accomplished by flash desorption of the CO₂ loaded Fluor solvent. The CO₂ gas stream obtained is then compressed and stored while the regenerated solvent is recycled back to the column [12, 120].

Advantages to the Fluor system are:

- CO₂ is highly soluble in the Fluor solvent
- Simple operating scheme
- Regeneration does not require heating of the solvent
- Solvent freezes at low temperatures (-57 °C) so winterization is minimal

Disadvantages to the Fluor process include:

- High solvent circulation rates (increased operating cost)
- Solvent is costly

4.4 Purisol

The Purisol process uses N-methyl-pyrrolidone as a solvent to capture CO₂. The solvent is advantageous for treating high pressure gas streams due to its high boiling point. Capture of CO₂ in the Purisol process occurs at roughly -15 °C with a total flue gas pressure of 1000 containing 35% CO₂ (350 psi CO₂). Regeneration of the original solvent is then accomplished by stripping the CO₂ loaded Purisol solvent with an inert gas. The CO₂ gas stream obtained is then compressed and stored while

the regenerated solvent is recycled back to the column [116, 121]. Advantages to the Purisol process include:

- The solvent does not foam in the absorber and is completely miscible in water
- High thermal and chemical stability
- Non corrosive → equipment may be constructed from carbon black steel
- Purisol solvent has a low volatility

Disadvantages to the Purisol process are:

- Additional compression is needed after the WGS reaction

| Technology | Process Stage | | |
|-------------------|---|---|-------------------------------|
| | Pretreatment | Capture | Regeneration |
| Selexol | Removal of sulfur compounds Dehydrate gas stream | Dimethyl ether + polyethylene glycol 0-5 °C 450 psi CO ₂ | Flash desorption or stripping |
| Rectisol | Removal of sulfur compounds | Chilled methanol -30 to -100 °C 250 psi CO ₂ | Flash desorption |
| Fluor | Removal of sulfur compounds Dehydrate gas stream | Propylene carbonate Ambient temperature 280-850 psi CO ₂ | Flash desorption |
| Purisol | Removal of sulfur compounds | N-methyl-pyrrolidone 0 to -15 °C 350 psi CO ₂ | Stripping |

4.4.1.1 Advantages and disadvantages to pre-combustion capture

General advantages to pre-combustion capture of CO₂ include:

- It is a proven industrial scale technology [115]
- Increased CO₂ partial pressure allows for efficient separation techniques [11]
- CO₂ is generated under pressure thus less compression is needed for transport or storage [115]
- Solvent regeneration by pressure reduction is much more energy efficient than heating the solvent [32]

General disadvantages with pre-combustion capture of CO₂ include:

- Syngas must be dried prior to CO₂ capture
- For non-gaseous feed stocks (i.e. coal or crude oil) the syngas stream must be cleaned due to impurities present in the material being gasified [115]
- IGCC system have high investment and operational costs [123]
- Retrofit to existing plants is costly and difficult

Note that many of the physical solvents used in pre-combustion capture of CO₂ could be used in post-combustion capture of CO₂ if the gas stream were properly scrubbed and pressurized.

5 Oxy-combustion technology

Oxy-combustion technology is a relatively new approach to reducing CO₂ emissions. It was originally developed in 1982 to produce high purity CO₂ (>99%) for enhanced oil recovery (EOR). A renewed interest in the technology has recently taken place due to the concerns over global climate change and CO₂ emissions [124]. A basic process flow diagram of the oxy-combustion technology can be seen in Figure 10 [25]. In oxy-combustion the fuel is combusted in an oxygen (O₂)/CO₂ atmosphere as opposed to air. This produces a gas stream containing CO₂, H₂O, and other trace impurities. The CO₂ is then captured, *post oxy-combustion*, from a

“cleaned” flue gas stream consisting of 75-80% CO₂ and water vapor [123, 125]. After the CO₂ is captured it is compressed for transportation and storage. The main advantage to this technology is that much more efficient capture techniques compared to those used in traditional post combustion capture of CO₂ can be applied. Oxy-combustion technology also eliminates NO_x formation during combustion. A more in depth examination of the basics to the technology (air separation, combustion and CO₂ recycle, and cleaning and CO₂ capture) is to follow along with a look pilot scale demonstrations of oxy-combustion systems.

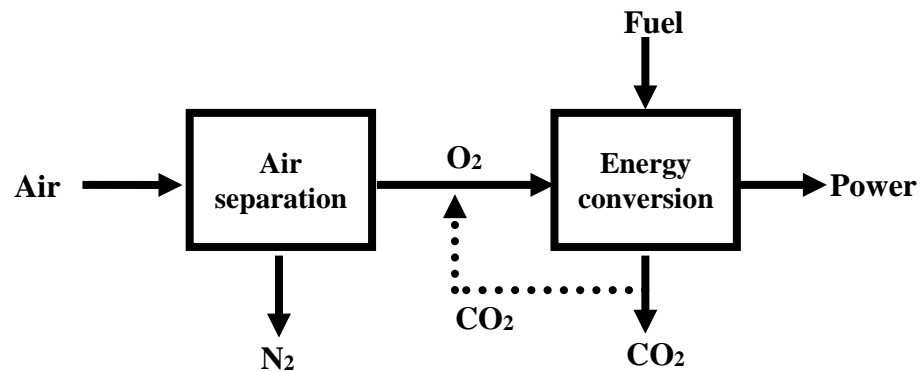


Figure 10: Simplified block diagram of an oxy fuel combustion system

Air separation

The pure O₂ for combustion is obtained by separating the oxygen from nitrogen in air using an air separation unit (ASU). In an ASU the air is separated into liquid oxygen, gaseous nitrogen, argon and other trace components of air. The purity of the oxygen stream can vary from 95-99% pure. Several methods exist for obtaining the high purity oxygen needed for combustion: cryogenic distillation, adsorption using multi-bed pressure swing units, and polymeric membranes. Studies have shown that only cryogenic distillation is economic for the large volumes of oxygen needed for power production at fossil fuel burning power plants [1, 32, 125]. The use of an ASU reduces NO_x emissions by as much as 50% in comparison to combustion in an air atmosphere [126]. However, it has been estimated that the ASU may consume up to 15% of a power plant's electrical output [11]. The remaining nitrogen and other trace components of air are vented to the atmosphere.

Combustion and CO₂ recycle

After the pure oxygen stream is obtained it is mixed with recycled "clean" CO₂ and fed to the combustion chamber for energy conversion. Recycled CO₂ is added to the oxygen stream to control the flame temperature in the furnace; carbon burning in pure oxygen has a combustion temperature of about 3500 °C. This is far too hot for traditional furnace materials used in fossil fuel burning power plants. For a retrofit to a traditional fossil fuel burning power plant, the flame temperature must be reduced to 1300-1400 °C. Even with construction of new oxy-combustion equipment the flame temperature still must be reduced to around 1900 °C [1]. Studies have shown that to mimic the flame temperature exhibited with combustion in an air atmosphere the gas composition needs to be 30-35% O₂ and 65-70% recycled CO₂ [1, 124].

Cleaning and CO₂ capture

Combustion in the O₂/CO₂ atmosphere produces a flue gas that is predominantly CO₂ (75-80%), H₂O vapor and other trace impurities (NO_x, SO_x, and particulate matter). A major advantage to the oxy-combustion technology is that the high concentration of CO₂ in the flue gas stream allows for efficient capture of the CO₂. However, before the CO₂ can be captured the flue gas stream must go through a “cleaning” stage to remove any trace impurities and water vapor. An electrostatic precipitator (ESP) is used to remove any particulate matter and any conventional FGD technology will do to remove sulfur compounds. Once all sulfur compounds are removed the CO₂ is captured by simply cooling the gas stream to condense out the water vapor until levels reach 50-100 ppm. It is estimated that the cost of cleaning the gas stream before CO₂ capture is the highest for oxy-combustion out of all available CO₂ capture technologies [124]. After cleaning the gas stream contains 80-90% CO₂. This stream is then dried, compressed, and further purified for transport. [1, 124, 127]

5.1 Current oxy-combustion demonstrations

Several pilot scale demonstrations have taken place to address some unknowns with oxy-combustion, such as: heat transfer, environmental issues, ash issues, ignition stability, and flame stability. This paper will briefly discuss the major demonstrations and their findings; for a more detailed summary please see the review assembled by Buhre and colleagues [124]. When talking about oxy-combustion demonstrations it is important to understand what the term “full chain” means. A “full chain” oxy-combustion system consists of the following equipment [126]:

- Air separation unit → for oxygen production

- An oxy boiler → designed for fuel combustion in an oxygen atmosphere
- Conventional air quality control systems
 - Electrostatic precipitator → particulate matter removal
 - Flue gas desulphurization unit → sulfur compound removal
- Gas processing unit (GPU) → used to further process the CO₂ stream depending upon its intended application, i.e. geological storage or food and beverage grade CO₂. The GPU itself consists of many components.

There are currently five major oxy-combustion demonstration plants in operation [128, 129]:

1. Schwarze Pumpe (operation started in 2008): A 30 MW lignite coal plant operated by Vattenfall and located in Brandenburg, Germany. First full chain oxy-combustion pilot demonstration. Produced a gas stream greater than 99.7% CO₂. Major findings included:
 - Air leakage into the system greatly degrades performance
 - No new environmental issues were encountered
2. Lacq, France (operation started in 2009): A retrofit demonstration to a 30 MW natural gas plant developed by Total. Transported captured CO₂ over 30 km of pipe for storage in a depleted oil reservoir. First integrated and industrial natural gas fired oxy-combustion plant.
3. Alstom Power Plant Laboratory: A retrofit demonstration to a 15 MW lignite and bituminous coal plant. Major finding was that the NO_x emissions created during oxy-combustion were 50% lower than with standard air combustion.
4. Callide Oxy Fuel Project (operation started in 2011): First full chain retrofit demonstration performed on a coal fired power plant. First demonstration to also have power generation, carbon capture, and carbon storage.

5. Endesa/CIUDEN CFB (operation started in 2011): Largest pilot scale demonstration of the oxy-combustion technology on a coal fired boiler (320 MW).

5.1.1 Advantages and disadvantage to oxy-combustion

Advantages to oxy-combustion include:

- CO₂ capture efficiency close to 100% [1].
- Elevated CO₂ concentrations lead to simple, efficient methods for CO₂ capture.
- Suppressed NO_x formation. At least 50% less than with traditional air combustion [126].

Drawbacks associated with oxy-combustion technology include:

- Large volume of O₂ is required. Increases the capital and operating costs due to the need for an ASU
- Retro fit is an issue due to the high combustion temperatures
- Air leaks into the system significantly degrade performance [128]
- Water vapor must be reduced to 50-100 ppm to prevent corrosion
- Large plant footprint associated with necessary oxy-combustion equipment

6 Chemical looping combustion

Chemical looping combustion (CLC) was first proposed in 1983 as an alternative approach to traditional fuel combustion but was later found to possess benefits related to CO₂ capture [130, 131]. In CLC, the oxygen needed for combustion is transferred from the combustion air to the fuel by use of an oxygen carrier; most commonly an oxidized metal is used as the oxygen carrier. In a typical CLC system the oxygen carrier (the metal oxide) is transported between two fluidized bed reactors – an air and a fuel reactor, seen in Figure 11. Thus a system is created in

which the fuel and combustion air never come into contact with one another, creating a CO₂ exhaust gas stream not diluted with N₂. This makes for relatively easy CO₂ capture. [132-134]

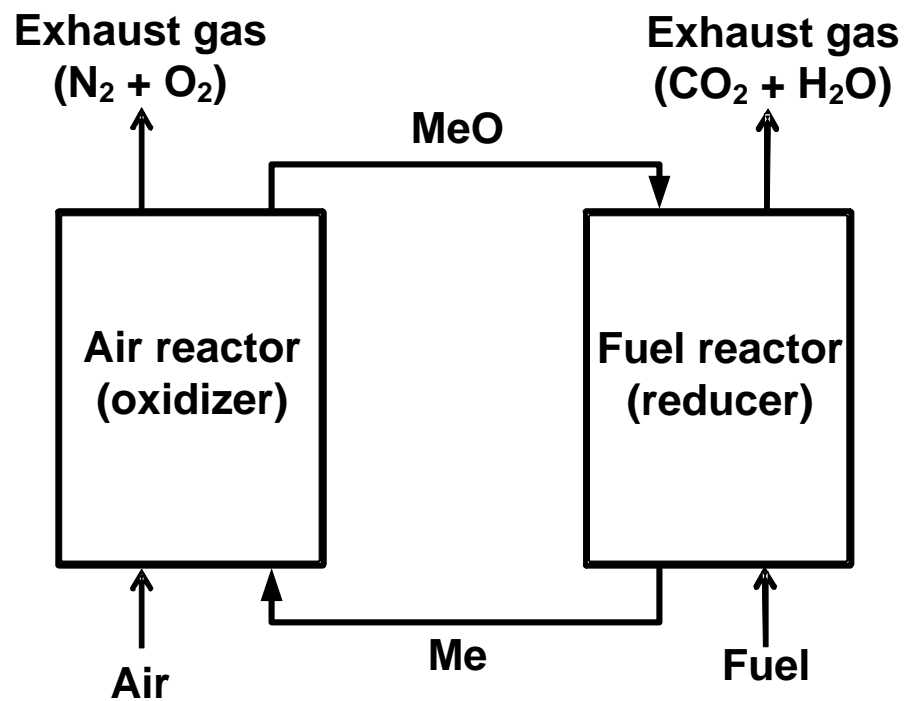
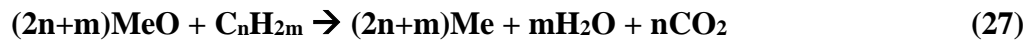


Figure 11: Chemical looping flow diagram. Me denotes the metal material and MeO represents the corresponding metal oxide.

In the fuel reactor, or reducer, the metal oxide (MeO) reacts with the fuel producing an exhaust gas stream consisting of gaseous CO₂ and H₂O along with the reduced metal oxide component. The fuel and the metal oxide react according to equation 27 [135].



The CO₂ can be recovered from the fuel reactor exhaust gas stream by simply condensing out the water vapor [136]. The CO₂ is then sent through a series of compressors to obtain liquid CO₂. It is possible to obtain a gas stream greater than 99% CO₂ using CLC [137]. The reduced metal oxide, Me, is then transported to the air reactor (or oxidizer) to be re-oxidized. In the air reactor, oxygen is transferred from the combustion air to the Me, creating a MeO via equation 28 [133].



The exhaust gas stream leaving the air reactor, containing N₂ and any excess O₂, is vented to the atmosphere. The MeO is then cycled back to the fuel reactor for combustion. This cycle is repeated for the lifetime of the oxygen carrier.

The operating temperature and pressure of the reactors may range from 800 – 1200 °C and 1 – 69 atm, depending heavily upon the type and size of oxygen carrier used [1, 138]. Some common metals used as oxygen carriers include iron, nickel, cobalt, copper, manganese, and cadmium which can range from 70 μm to 2 mm in size. For more specifics regarding oxygen carriers please see [132, 136, 137, 139].

Chemical looping has several advantages that make it an attractive technology, such as:

- No energy loss during the separation of CO₂ [133]
- CO₂ stream is not diluted with N₂. Makes for easier CO₂ separation [133]

- Inherent reduction of NO_x emissions since air and fuel never contact one another [132]
- Process can be applied to any form of fuel (i.e. solid, liquid or gas) [138]

The drawbacks associated with CLC include:

- Difficult operation of the fluidized bed reactors. Pressure of the two reactors must be the same to prevent air leakage to the fuel reactor. [133]
- Sustained contact between the MeO and fuel [133]
- Reduced reduction rate of the MeO after the first cycle [132]
- Deactivation of the MeO due to unburned carbon deposition on the surface of the particles [138]
- Technology is in the R&D phase, with no demonstrations or commercial plants in operation [138]
- Sulfur compounds will react to form metal sulfides. Fuel must be desulphurized before entering the fuel reactor. [139, 140]

Compared to previously discussed technologies, CLC is the furthest behind in terms of commercial development. For CLC to be a viable option for reducing CO₂ emissions several areas must still be addressed, such as large scale chemical looping operation and conversion/retrofitting of existing facilities [138].

7 Challenges and Opportunities

The capture technologies discussed within this review all show promise as possible CO₂ mitigation technologies. However, each must overcome similar challenges before implementation on the industrial scale can become a reality. Such challenges include how to utilize the concentrated CO₂ stream produced from the capture technologies, reducing the effects of impurities on the operating system, scaling technologies up to the level of 500 MW fossil fuel burning power plants, and retrofitting technologies to existing facilities. This section will discuss these

challenges and some research opportunities that exist to address the challenges. For specific challenges regarding each technology see the advantages and disadvantages section for the technology of interest.

How will technologies scale up to the level of 500 MW fossil fuel burning power plants or be retrofit to existing facilities? A 500 MW fossil fuel burning power plant emits, on average, 8000 tons/day CO₂. Handling this volume of gas presents unique challenges in the design of capture equipment. Retrofitting will, at the least, involve modification of existing equipment. Innovative design of equipment could solve many of the challenges associated with scaling up and retrofitting technologies. Innovative design could include methods for reducing the size of equipment required for scale up (such as with absorption column diameter and height), new techniques to obtain high purity O₂ (for oxy-combustion), improved operation/control of the dual fluidized beds in chemical looping, how to pelletize adsorbents for use on an industrial scale, etc. These are all aspects not specifically related to actually capturing CO₂ which could lead to significant advances in the application of each technology.

How do impurities (mainly NO_x and SO_x) in the flue gas affect the capture system? In almost all cases, the presence of impurities reduces the CO₂ capture efficiency of the system. Pretreatment stages to remove impurities require additional equipment and lead to increased operating costs. Development of a system that efficiently and simultaneously removes NO_x, SO_x, and CO₂ would significantly reduce the costs associated the pretreatment stage of CO₂ capture systems. Innovative design of absorbents or adsorbents could possible address this issue.

How will the concentrated CO₂ stream produced from capture technologies be utilized? The major uses include underground storage, enhanced oil recovering, sale to the food and beverage industry, or fertilizer production. These uses will not be able to consume all of the CO₂ captured on a daily basis from fossil fuel burning

power plants. Discovery of novel approaches to CO₂ utilization to produce a value added product. If capture technologies are implemented at fossil fuel burning power plants there will be a sudden abundance of high purity gaseous CO₂. Discovery of a novel, yet high demand, use for high purity CO₂ would help to offset the costs associated with operating a carbon capture system.

8 Conclusions

- Post combustion capture of CO₂ involves capturing CO₂ after fuel combustion has occurred. Post combustion capture technologies possess the greatest potential for near term implementation at fossil fuel fired power plants because they can be retrofit to existing facilities with the least difficulty. Of the current post combustion capture technologies, chemical absorption with amines is the most mature technology. However, every post combustion capture approach still suffers from the same design challenge: how to design a system to handle the enormous volume of flue gas produced from fossil fuel combustion. Large volumes of gas mean large quantities of liquid will be needed for capture along with large equipment. This equates to high operational costs overall and safety hazards associated with storing such large volumes of liquid. For example, current amine capture systems can handle around 800 tons per day CO₂. A 500 MW fossil fuel burning power plant emits roughly 8,000 tons per day CO₂. For use on the scale of a 500 MW power plant, scale up would be substantial. At the current state of development, post combustion capture technologies present a costly solution to CO₂ capture.
- Pre-combustion methods capture CO₂ before fuel combustion by first gasifying the fuel to create a high pressure CO₂/H₂ gas stream. This allows for efficient capture of the CO₂ via physical absorption or even membranes. However, retrofit of an existing plant to incorporate precombustion

technology is very difficult and costly. Thus, precombustion capture applies only to IGCC plants, which in themselves have high investment and operational costs. At the current state of development pre-combustion technology should only be applied if a new IGCC facility is being constructed.

- Oxy-combustion refers to CO₂ capture after combusting fuel in an oxygen rich atmosphere. Fuel combustion in an oxygen rich atmosphere reduces the formation of NO_x and creates a flue gas stream consisting primarily of CO₂/H₂O. The advantage to this is that NO_x formation is suppressed and CO₂ can easily be separated by cooling the flue gas stream to condense out the H₂O. However, disadvantages associated with oxy-combustion include: 1) the equipment needed to obtain the large volume of oxygen needed is costly to operate and 2) retrofitting to existing facilities is difficult. Current facilities are not designed to handle the elevated temperatures seen with combustion in oxygen rich atmospheres. At the current state of development, oxy-combustion would be a costly approach to CO₂ capture.
- Chemical looping combustion uses oxygen carriers, typically metal oxides, to transport the oxygen needed for fuel combustion. In turn this creates an exhaust gas stream free of NO_x emissions with the primary constituents being CO₂/H₂O. The CO₂ can be easily separated by the same means as with oxy-combustion. However, CLC is behind in development compared to the other technologies. Until CLC is demonstrated on a larger scale it will remain an unviable option for CO₂ emission reductions.
- Table 5 is a summary of the typical flue gas characteristics encountered with the four aforementioned CO₂ capture technologies.

| Table 5 Flue gas characteristics for the aforementioned CO₂ capture approaches | | | |
|--|-------------------------|-----------------------|--|
| Capture Approach | % CO₂ | Pressure (atm) | Possible Impurities |
| Post combustion | 3 – 20 | 1 | NO _x , SO _x , particulate matter |
| Pre-combustion | 15 – 40 | 15 – 40 | NO _x and SO _x |
| Oxy-combustion | 75 – 80 | 1 | NO _x and SO _x |
| Chemical looping | Unknown | Unknown | NO _x , SO _x , particulate matter |

9 Acknowledgements

The authors would like to acknowledge the Department of Education, the National Science Foundation, and ASISC for support of this work. The authors are grateful to Joseph Halt for all his hard work and important feedback he provided.

Chapter 3: An Equilibrium Analysis of Carbon Dioxide Absorption in Carbonate Solutions²

² Spigarelli, B. P. (2012). "Equilibrium Analysis of Carbon Dioxide Absorption in Carbonate Solutions." Minerals & Metallurgical Processing **29**(2): 131-132.

Abstract

To meet the growing need for CO₂ capture and storage technology, Michigan Technological University is researching CO₂ capture and storage using carbonate solutions. Without implementing emission controls, world energy emissions will rise from 29.7 billion metric tons in 2007 to 42.4 billion metric tons in 2035. The first objective of the project was to determine the optimal amount of Na₂CO₃ in solution for CO₂ absorption. This was accomplished using theoretical equilibrium calculations and experimental absorption rate data for Na₂CO₃ solutions of 1, 2, 3, 4, and 5 weight % (wt%). As the wt% Na₂CO₃ in solution increased so too did the ionic strength of the solution. Theoretical calculations took into account the effect increasing ionic strength will have on the solubility of gaseous CO₂. The calculations assumed negligible formation of H₂CO₃, constant temperature, and constant pressure. In the experimental set-up, a 16% CO₂/balance air gas mixture was bubbled through an Erlenmeyer flask filled with a carbonate solution. The gas exiting the flask was fed to a gas analyzer to record the % CO₂ in the exhaust gas stream. The % CO₂ absorbed was taken as the % CO₂ in the exhaust gas minus the % CO₂ in the feed. Theoretical calculations found that as the wt% Na₂CO₃ in solution increased, the solubility of CO₂ decreased. This was verified by experimental absorption rate data which found that the absorption rate of CO₂ decreased as the wt% Na₂CO₃ increased. Examination of the theoretical and experimental data concluded that a 2 wt% Na₂CO₃ solution was the ideal solution for CO₂ absorption in the present system. The 2 wt% Na₂CO₃ solution yielded the best trade-off between absorption rate and absorption capacity.

Introduction

Currently, the most mature CO₂ capture and storage (CCS) technologies use amine solvents to capture the CO₂ and then pipelines to transport the CO₂ to underground reservoirs for storage. The amine solvent CCS process is problematic and costly due to waste generated by amine degradation, equipment corrosion, and that the capture stage consists of CO₂ absorption, stripping, and compression which accounts for 70-90% of the total CCS system operating cost [1, 141]. Our simple system uses a carbonate absorbent to capture CO₂ from the gas stream. The captured CO₂ is then reacted with an industrial waste, such as fly ash, for permanent storage in the form of a carbonate mineral. The advantages to this system are that the process can be retrofit to pre-existing SO₂ scrubbing technology, cost reduction by complete elimination of the stripping and compression stages, and on-site storage using an industrial waste to create an added value product. Our end goal is that our CCS technology transplants the amine solvent CCS technology.

Materials and Methods

Materials used in the present study include:

- **Sodium Carbonate (Na₂CO₃):** Na₂CO₃ was used in the studies as the source for carbonate ions. The Na₂CO₃ was granular, anhydrous, ACS reagent grade purchased from Sigma Aldrich with a purity of greater than or equal to 99.5% Na₂CO₃.
- **Distilled H₂O:** Distilled H₂O was mixed with the Na₂CO₃ to create the carbonate solvent.

- **Gases:** Industrial grade CO₂ and compressed air were used to create the contaminated gas mixture. The gas mixture was roughly 16% CO₂ and 84% air (21% O₂ and 79% N₂) for all trials.
- **Gas Diffuser:** A medium porosity, ASTM standard gas diffuser was purchased for bubbling the gas mixture through the absorbent. The pore diameter of the gas diffuser ranges from 10 – 15 microns

Absorption Rate Measurements

The experimental set-up used for CO₂ absorption rate measurements can be seen in Figure 12.

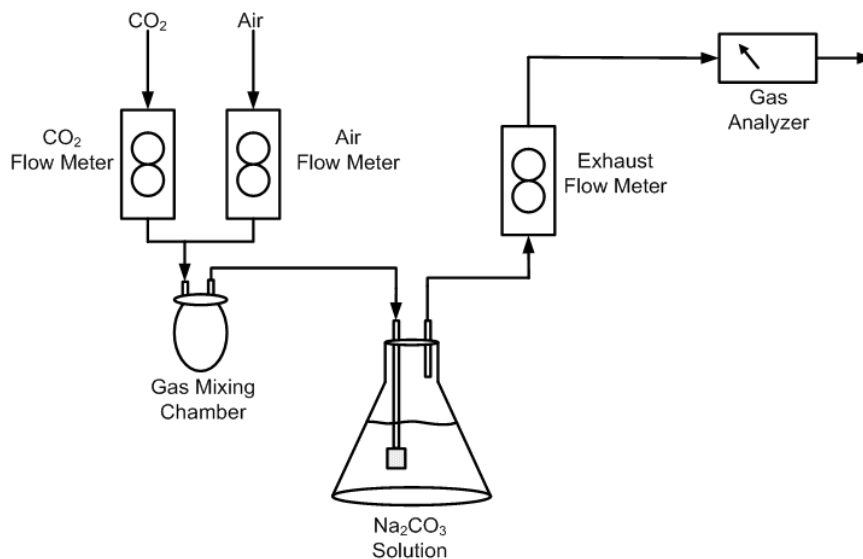


Figure 12: Experimental set-up for measuring CO₂ absorption rates. All experiments carried out at ambient temperature and pressure. Sodium carbonate solutions of 1, 2, 3, 4, and 5 wt% were tested.

The %CO₂ in the gas stream was controlled by using separate CO₂ and air flow meters to monitor the volumetric flow rates of each gas. The CO₂ flow rate was set at 2.57 ml/sec and the air set at 14.57 ml/sec; this amounted to a roughly 16% CO₂ gas mixture. The gases were then sent to a gas mixing chamber to assure uniform composition of the gas entering the absorption flask. Once mixed, the gas was bubbled into a 1000 ml Erlenmeyer flask containing the desired wt% Na₂CO₃ solution. The gas not absorbed by the solution was emitted out of the flask to an exhaust gas flow meter to record the volumetric flow rate of the gas leaving the flask. After the flow meter, the gas was passed through a CAI 600 series infrared gas analyzer to obtain the %CO₂ in the exhaust gas stream. The CO₂ absorption rate was taken as the difference between the CO₂ fed and CO₂ exhausted during this process. CO₂ absorption rate measurements were repeated in triplicate to ensure the accuracy of the data.

Results and Discussion

The theoretical analysis was performed by first establishing a chemical equilibrium model for CO₂ absorption in water [142]. The model was then adjusted to represent the carbonate system by using activity coefficients to account for ionic strength and ion pairing. The model was used to determine the theoretical solubility of CO₂ at varying weight percentages of Na₂CO₃ in solution. The CO₂ solubility is a good indicator for predicting the relative affinity of a solution to absorb CO₂.

The ionic strength for the 1, 2, 3, 4, and 5 wt% Na₂CO₃ solutions are as follows: 0.28, 0.58, 0.87, 1.16, and 1.44 mol/L. Results of the theoretical CO₂ solubility calculations at varying Na₂CO₃ weight percentages can be seen in Figure 13.

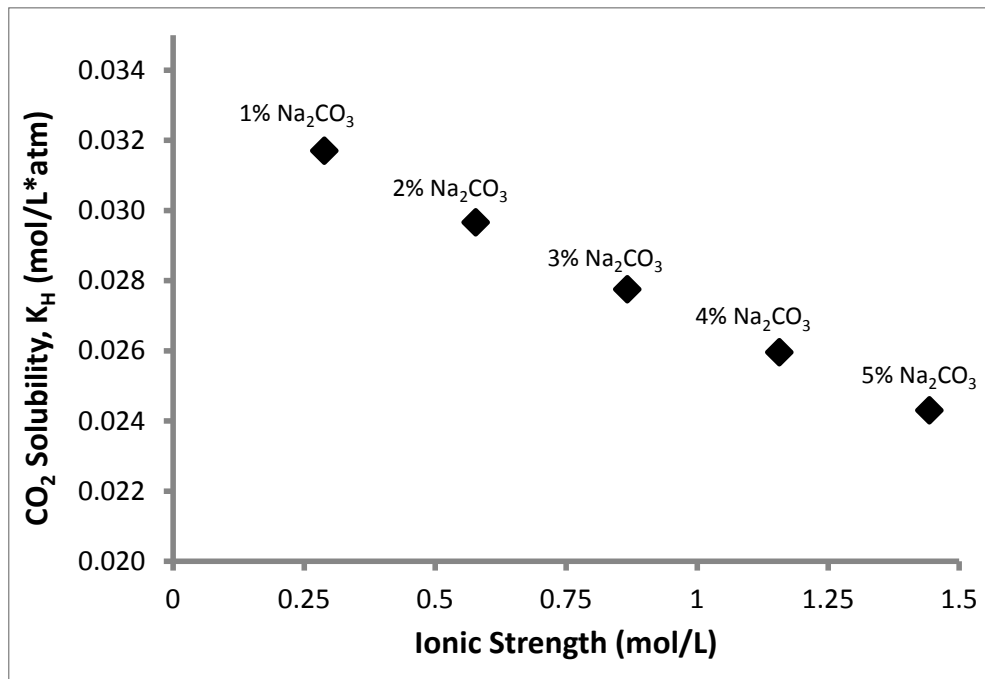


Figure 13: Carbon dioxide solubility with respect to ionic strength. As the ionic strength increases, or as the wt% Na₂CO₃ increases in solution, the solubility of CO₂ decreases in solution.

Figure 13 shows that as the ionic strength in solution increased (or as the wt% Na₂CO₃ in solution increased) the solubility of CO₂ in the Na₂CO₃ solution decreased; with 5 wt% Na₂CO₃ in solution showing the lowest CO₂ solubility and 1wt% Na₂CO₃ in solution showing the highest CO₂ solubility of the tested concentrations. This suggests that the 5 wt% Na₂CO₃ solution will yield the slowest CO₂ absorption rate and the 1 wt% Na₂CO₃ solution will yield the fastest CO₂ absorption rate. Experimental absorption rate data can be seen in Figure 14.

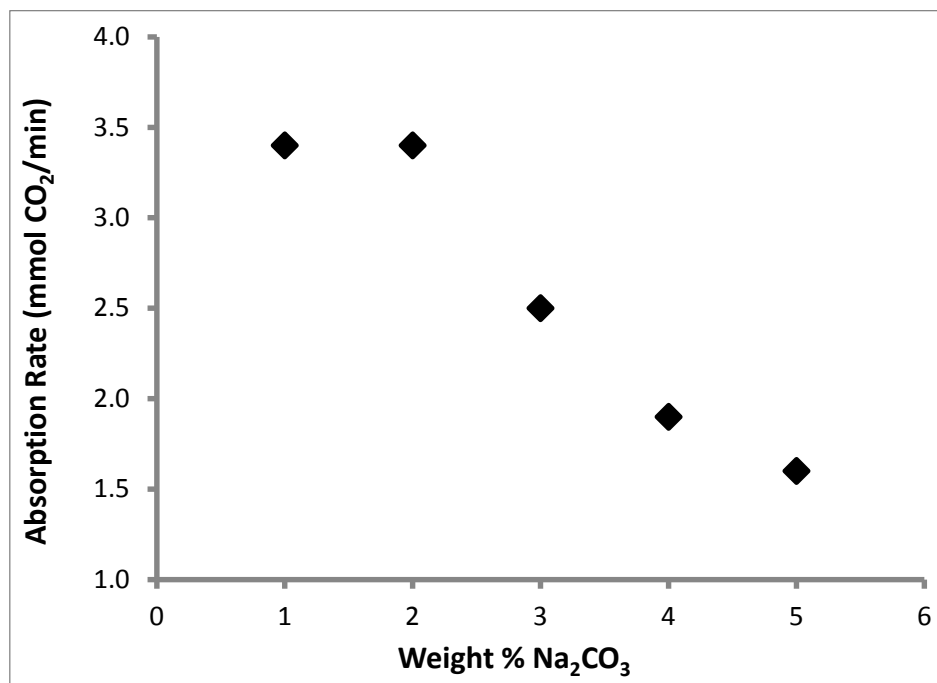


Figure 14: Experimental CO₂ absorption data. As the wt% Na₂CO₃ increased, the CO₂ absorption rate decreased. A 2 wt% Na₂CO₃ solution was chosen as the optimal solution for absorption. Constant CO₂ feed rate of 7.42 mmol CO₂/min. Experimental run time of 22 minutes.

From the Figure 14 it can be seen that as the wt% Na₂CO₃ in solution increased, the absorption rate of CO₂ decreased. This implies that the decrease in the CO₂ absorption rate is largely due to the decrease in the solubility of the CO₂ as the ionic strength increased, as seen in Figure 13. The 1 wt% and 2 wt% Na₂CO₃ solutions have nearly identical absorption rates. This leads to the conclusion that the 2 wt% Na₂CO₃ solution is optimal for the current system. The 2 wt% solution has the capacity to absorb a larger total volume of CO₂, due to the increase in carbonate ions in solution, at roughly the same rate as a 1 wt% solution.

Conclusions

Theoretical calculations were performed to determine the solubility of CO₂ at varying weight percentages of Na₂CO₃ in solution. The theoretical solubility calculations were examined with experimental absorption rate data to determine an optimal wt% Na₂CO₃ in solution. Examination of the experimental results and the theoretical calculations concluded that a 2 wt% Na₂CO₃ solution was optimal for the present system. The 2 wt% Na₂CO₃ solution yielded the best trade-off between absorption rate and absorption capacity.

Chapter 4: The Effects of Absorbent Temperature and Flue Gas Impurities on Carbon Dioxide Absorption in Carbonate Solutions

Abstract

Capture of carbon dioxide (CO₂) from fossil fuel burning power plants is considered a logical target for mitigation of anthropogenic CO₂ emissions. Chemical absorption via carbonate solutions has been proposed as a possible CO₂ mitigation technology. Fossil fuel burning power plants present unique challenges to CO₂ capture, such as elevated flue gas temperatures (may lead to heating of the solution) and the presence of impurities (NO_x and SO_x) in the flue gas which may degrade the solution. Unlike the commercially available amine absorption technology, carbonate solutions may be able to act as a multi pollutant capture system. Carbonate solutions could serve as a cheap outlet for other impurities such as NO_x and SO_x which have their own dedicated, and costly, removal systems. In the present work, the absorption of CO₂ into a 2% (w/w) sodium carbonate solution was studied at solution temperatures from 25 °C to 60 °C and with gas streams containing a mixture of CO₂, NO_x, SO_x, and N₂. The goal of the study was to assess the potential/performance of carbonate solutions as a multi pollutant control technology at fossil fuel burning power plants. Studies found that when the solution temperature was increased from 25 °C to 60 °C, roughly a 50% decrease in the CO₂ absorption rate was seen. This implies that the solution should be kept as cool as possible for absorption. Absorption of carbon dioxide in the presence of NO_x and SO_x revealed a slight decrease in both the CO₂ absorption capacity of the solution and the rate of CO₂ absorption into the solution. However, these negatives were offset by the complete capture of all the NO_x and SO_x that was fed to the solution. Current studies suggest sodium carbonate solutions possess the potential to serve as a multi pollutant capture technology at fossil fuel burning power plants.

Introduction

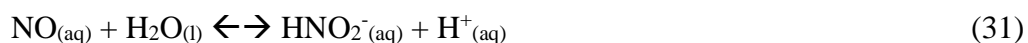
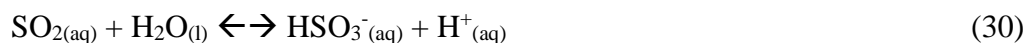
Chemical absorption via carbonate (CO_3^{2-}) solvents has been proposed as a possible technology to reduce CO_2 emissions from fossil fuel fired power plants [16, 143]. During chemical absorption, the contaminated gas stream comes into contact, and reacts, with the liquid solvent. The solvent captures the CO_2 and then acts as a carrier to transport the CO_2 for further processing.

Chemical absorption of CO_2 using carbonate solvents was first used commercially in the early 1900's. The process was used to capture CO_2 from the combustion of low sulphur metallurgical coke to obtain relatively pure gaseous CO_2 for dry ice production [51, 52]. In carbonate solvents, the CO_3^{2-} ions in solution buffer the carbonic acid formed when CO_2 hydrolyzes. Initially, the carbonate solution will be at an elevated pH (>10.5) containing largely carbonate ions. Over time, as CO_2 is absorbed and the carbonate ions are consumed, the pH of the solution decreases until it becomes neutral and can no longer buffer the formation of H^+ ions: at this point the solution can no longer capture CO_2 . The overall reaction of CO_2 with a sodium carbonate (Na_2CO_3) solution can be seen in Eq. 29 [118].



Studies that have examined CO_2 absorption using sodium carbonate based solvents suggest an absorbent temperature of 50-60 °C is optimal for absorption [16, 51, 52] and assume absorption in a “cleaned” flue gas stream (a gas stream with minimal SO_x , NO_x , and particulate matter). This study looks to experimentally verify that the 50-60 °C temperature range is optimal by varying the absorbent temperature from ambient to 60 °C. The temperature that corresponds to the highest CO_2 absorption rate will be considered optimal. This study will also examine CO_2 absorption in carbonate solutions from gas streams that have not been “cleaned”.

A “cleaned” flue gas stream consists of CO₂, nitrogen (N₂), and oxygen (O₂) [16, 143]. However, actual flue gas contains other gaseous impurities (most notably, sulfur dioxide (SO₂) and nitrogen oxides (NO_x)) which may interact with the solvent. During combustion, 90-95% of NO_x emissions in flue gas are comprised of NO [23]. Dissolved SO₂ and NO_x will undergo hydrolysis when contacted with water producing hydrogen ions according to Eqs. 30 and 31 [144].



The solubility of the impurities will play a significant role in how carbonate based absorption systems perform with respect to CO₂ absorption. The solubility of SO₂, CO₂ and NO in water can be seen in Table 6.

| Table 6 Solubility of common flue gas impurities in water[145] | |
|---|-------------------------------|
| Impurity | Solubility (mol/L*atm) |
| SO ₂ | 1.2 |
| CO ₂ | 3.4x10 ⁻² |
| NO | 1.9x10 ⁻³ |

Sulfur dioxide is by far the most soluble of the gaseous impurities present in flue gas. It is believed that SO₂ will have the largest impact on CO₂ absorption. As the SO₂ hydrolyzes it will produce a free H⁺ ion, as seen in Eq. 30. In alkaline conditions, as is the case in carbonate based absorption systems, the H⁺ ion will react with the carbonate ions (from the Na₂CO₃) in solution to form bicarbonate ions, Eq. 32.



The consumption of CO₃²⁻ ions from the hydrolysis of SO₂ will reduce the capacity of the solution to buffer CO₂. This could be beneficial, or detrimental, to the absorption system depending upon needs. It may be beneficial to sacrifice some of the CO₂ absorption capacity of the absorbent in return for significant SO₂ reductions, thus creating a multi pollutant control system.

Impurity levels vary with fuel source and combustion atmosphere, but a typical flue gas will contain SO₂ (1-5000 ppm) and NO (1-500 ppm) [9, 10, 146, 147] at high temperatures (100 °C). Although SO₂ and NO are present in flue gas, research regarding carbonate solvents has largely ignored the effects that they may have on CO₂ absorption.

To the authors' knowledge, the only study examining the effect of impurities on CO₂ absorption in carbonate solvents was performed by Wappel and colleagues (2009) in a hot potassium carbonate solution at 90 °C and 100 °C [54]. The authors concluded that the SO₂ was preferentially reacting with the carbonate solvent, thereby decreasing the ability of the carbonate solvent to absorb CO₂. Yet, the authors did not quantify what impact the SO₂ actually had on the CO₂ absorption capacity or the absorption rate. Because of this, the present work examines the effects that flue gas impurities, SO₂ and NO_x, have on the CO₂ absorption capacity

and absorption rate in carbonate solvents to better understand how the solution may perform if implemented for CO₂ capture at a fossil fuel burning power plant.

Therefore, this paper examines the effects of flue gas impurities on the absorption of CO₂ in a carbonate solvent. For the current study, CO₂ absorption studies were carried out in 2% (w/w) Na₂CO₃ solution. Objectives of the study include the following:

- Study the effect of absorbent temperature on the CO₂ absorption rate into carbonate solutions,
- Study the affect SO₂ and NO may have on the CO₂ absorption capacity of the solution, and
- Study the affect SO₂ and NO may have on the absorption rate of CO₂ into the carbonate solution.

Materials and Methods

Materials used in the present study included:

- **Sodium carbonate (Na₂CO₃):** Na₂CO₃ was used in the studies as the source for carbonate ions. The Na₂CO₃ was granular, anhydrous, ACS reagent grade purchased from Sigma Aldrich with purity greater than or equal to 99.5% Na₂CO₃.
- **Distilled water:** Distilled water was mixed with the Na₂CO₃ to create the carbonate solution.
- **Gas mixtures:** Four pre-mixed gas cylinders were ordered from Praxair. They were mixed in proportions to mimic high SO₂ and NO concentrations:
 - 84% N₂ – 16% CO₂

- 83.50% N₂ – 16% CO₂ – 0.50% SO₂
 - 83.95% N₂ – 16% CO₂ – 0.05% NO
 - 83.45% N₂ – 16% CO₂ – 0.50% SO₂ – 0.05% NO
-
- ***Gas Diffuser:*** A medium porosity, ASTM standard gas diffuser was used for bubbling the gas through the carbonate solution. The pore diameter of the gas diffuser ranges from 10 – 15 microns

Absorbent Temperature Variation

The experimental set-up used for studying the effects of absorbent temperature on CO₂ absorption can be seen in Figure 15. A fresh carbonate solution was prepared before each trial.

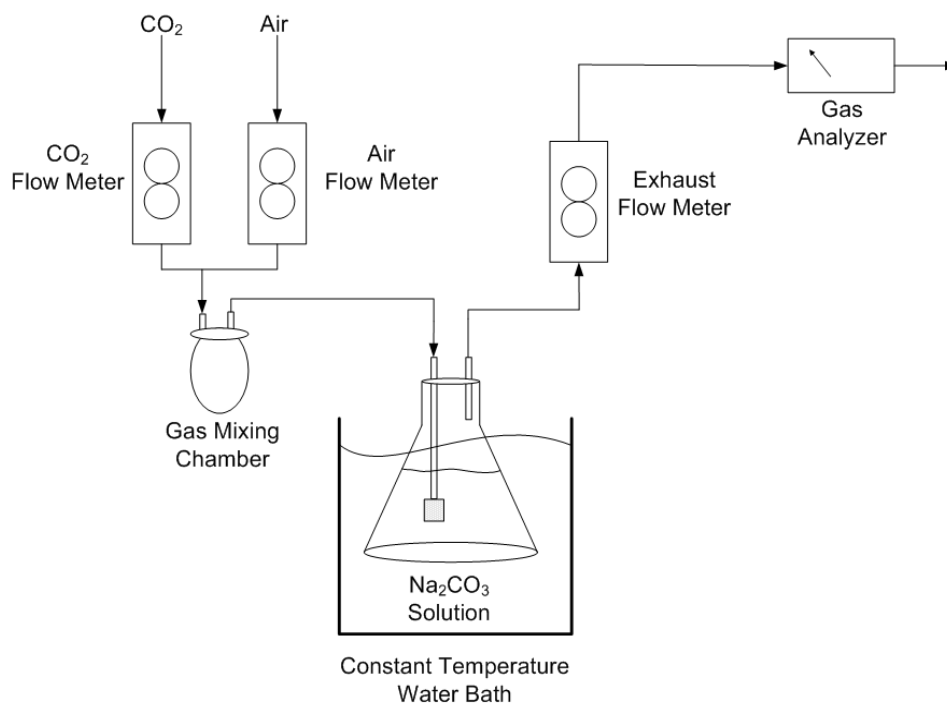


Figure 15: Experimental set-up for measuring CO₂ absorption in carbonate solutions at varying absorbent temperatures

The %CO₂ in the gas stream was controlled by using separate CO₂ and air flow meters to monitor the volumetric flow rates. The CO₂ flow rate was set at 2.57 ml/sec and the air set at 14.57 ml/sec; this amounted to a roughly 16% CO₂ gas mixture. The gases were then sent to a gas mixing chamber to assure uniform composition of the gas entering the absorption flask. Once mixed, the gas was bubbled into a 1000 ml Erlenmeyer flask containing the 2% Na₂CO₃ solution (800 g distilled H₂O and 16.33 g Na₂CO₃) at varying temperatures of 25, 30, 40, 50, and 60 °C. From previous studies the 2% Na₂CO₃ solution was determined to be ideal based on the rate of CO₂ absorption [148]. The gas not absorbed by the solution was emitted out of the flask to an exhaust gas flow meter to record the exit volumetric flow rate of the gas. After the flow meter, the gas was passed through a CAI 600 series infrared gas analyzer to obtain the %CO₂ in the exhaust gas stream.

The CO₂ absorption rate was taken as the difference between the CO₂ fed and CO₂ exhausted during this process. From the experimental set-up it was possible to understand whether the CO₂ absorption capacity and rate were affected by solution temperature. All experiments were repeated in triplicate.

Flue Gas Impurities

The experimental set-up used for studying the effects of flue gas impurities is similar to that seen in Figure 15 with minor operational differences. The constant temperature bath was removed and four pre-mixed gas cylinders, ordered from Praxair, were used to supply the CO₂, SO₂, NO and N₂ gas mixtures. The cylinders were mixed in proportions to mimic the extreme SO₂ and NO concentrations seen in combustion exhaust gases. Gas stream composition can be seen in the materials and methods section. All experiments studying the effects of SO₂ and NO on CO₂ absorption were carried out at ambient temperature and pressure. The gas stream consisting of only N₂ and CO₂ is considered the “clean” flue gas stream. This gas stream was used as a point of comparison to see whether SO₂ and NO impact CO₂ absorption in the carbonate solution.

Results and Discussion

Results quantifying the effects of absorbent temperature and flue gas impurities on CO₂ absorption in a carbonate solution are presented herein.

Effects of Absorbent Temperature

The effect of absorbent temperature on the absorption rate of CO₂ in the carbonate solution can be seen in Figure 16.

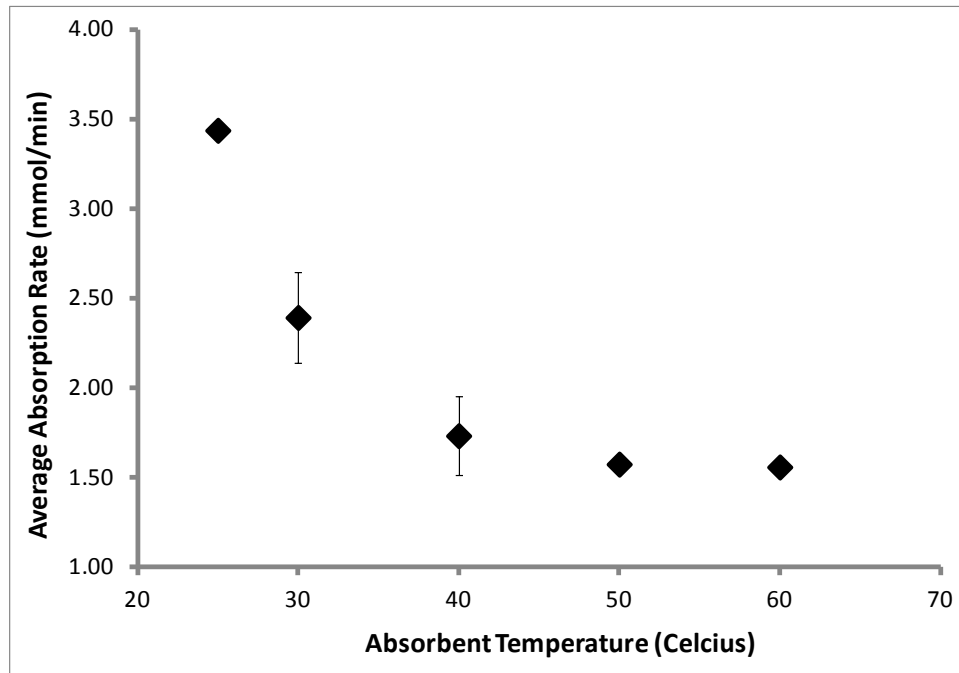


Figure 16: Carbon dioxide absorption rates with respect to absorbent temperature in a 2% (w/w) sodium carbonate solution. Where errors bars do not show up they are smaller than the marker.

As the temperature increased, the CO₂ absorption rate decreased exponentially. The CO₂ absorption rate decreased 55% from 25-60 °C. The decrease in absorption rate can be explained by the decrease in gas solubility at increased temperature. Effects of temperature on gas solubility are shown by the Van't Hoff equation, Eq. 33 [142, 145].

$$k_H = k_H^o * \exp\left[\frac{-\Delta H_{solution}}{R}\left(\frac{1}{T} - \frac{1}{T^o}\right)\right] \quad (33)$$

where k_H^o is the Henry's coefficient at standard state (mol/L*atm), $\Delta H_{solution}$ is the enthalpy of solution (-51,890 Joules/mol [149]), R is the gas constant (8.314 Joules/mol*K), T is the system temperature (K), and T^o is the standard temperature (298 K). In the Van't Hoff equation, the Henry's law coefficient is used to quantify the change in gas solubility as solution temperature changes.

The Van't Hoff equation will predict an exponential decrease in gas solubility, similar to the exponential decrease seen with the absorption rate in Figure 16. Calculations using the Van't Hoff equation predict a 67% decrease in the solubility of CO₂ from 25 °C to 60 °C in the carbonate solution. Given that only absorbent temperature is accounted for, this value is reasonably close to the 55% decrease in absorption rate seen in the experimental trials. This indicates that the decrease in the absorption rate is due largely to the reduction in gas solubility at elevated temperatures. Gas solubility is a controlling factor behind the driving force for CO₂ absorption in carbonate solutions. That is, the concentration gradient between the CO₂ in solution at saturation (i.e. the solubility of CO₂) and the bulk dissolved CO₂. The amount of CO₂ in solution at saturation is governed by Henry's Law, Eq. 34 [145].

$$C_{\text{CO}_2(\text{aq})} = k_{\text{H}} * P_{\text{CO}_2} \quad (34)$$

where $C_{\text{CO}_2(\text{aq})}$ is the concentration of CO₂ in solution at saturation (mol/L), k_{H} is the Henry's Law constant (mol/L*atm), and P_{CO_2} is the partial pressure of CO₂ in the gas stream (atm). The amount of CO₂ in solution at saturation is proportional to the Henry's Law constant. As the temperature increases the Van't Hoff equation predicts that k_{H} will decrease, thus the amount of CO₂ in solution at saturation will decrease. This effectively reduces the driving force for CO₂ absorption, leading to the observed reduction in CO₂ absorption rate at elevated temperature (Figure 16). Given that absorbent temperature has such a drastic impact on the absorption rate it would be beneficial to keep the absorbent as cool as economically possible for optimal CO₂ capture. Amine absorption studies performed by Fluor® have shown that absorber intercooling (to keep the absorbent cool) leads to a significant increase in the CO₂ absorption rate and consequently a reduced absorber size [30, 33].

Effects of Flue Gas Impurities

The effect of SO₂ and NO on the CO₂ absorption capacity of the sodium carbonate solution can be seen in Figure 17. The theoretical maximum absorption capacity of the sodium carbonate solution is 0.415 g CO₂/g Na₂CO₃.

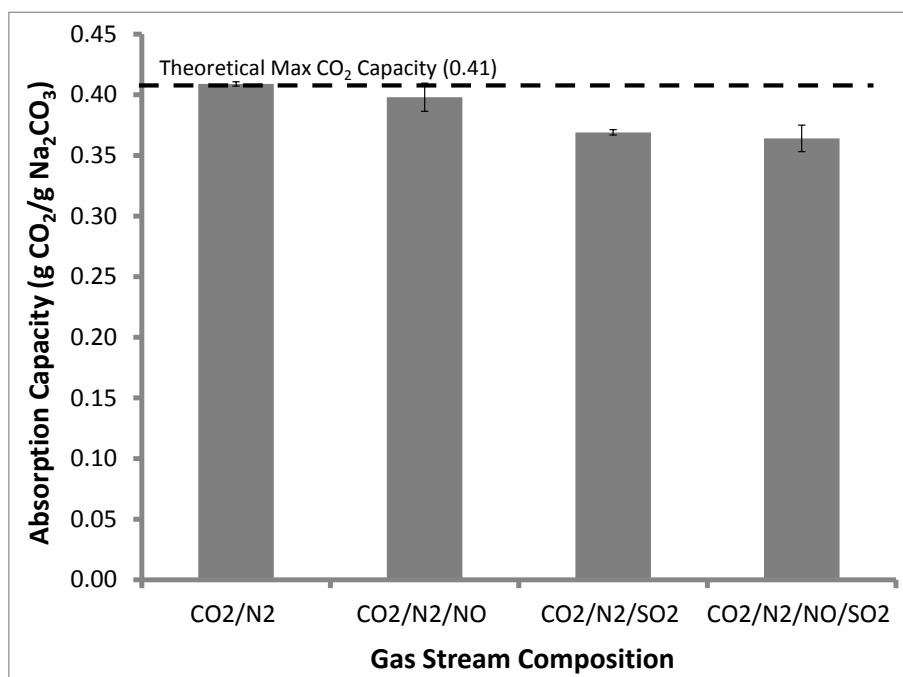


Figure 17: The effect of flue gas impurities on CO₂ absorption in a 2% (w/w) sodium carbonate solution

With the “clean” gas stream (CO₂/N₂) an absorption capacity of 0.409 g CO₂/g Na₂CO₃ was obtained. This is close to the theoretical maximum of 0.415 g CO₂/g Na₂CO₃. A negligible decrease in the absorption capacity was seen with the addition of just NO to the CO₂/N₂ flue gas stream. This is likely because of the low solubility of NO in water based solutions. However, the addition of just of SO₂ caused a noticeable decrease in the CO₂ absorption capacity. The capacity decreased from 0.41 to roughly 0.36 grams of CO₂ absorbed per gram of Na₂CO₃. Roughly the same reduction in capacity was seen in the flue gas stream containing CO₂/N₂/NO/SO₂. The difference in capacity can be attributed to the consumption of the carbonate ions by the free hydrogen ions produced during SO₂ hydrolysis (Eq. 30). In both cases that SO₂ was present, a 12% decrease in the CO₂ absorption capacity of the solution was observed. Theoretically, a 9% decrease in absorption capacity should be seen assuming all the SO₂ fed to the system was absorbed by the solution. The discrepancy between the theoretical and experimental results could be attributed to the gaseous SO₂ reacting with the CO₃²⁻ ions to produce CO₂ and sulfite (SO₃²⁻), Eq. 35 [144].



Thus, SO₂ will affect the CO₂ absorption capacity of carbonate solvents in two ways. First, the extra H⁺ ions produced during SO₂ hydrolysis will consume CO₃²⁻ ions, producing HCO₃⁻ ions. Second, gaseous SO₂ will react with CO₃²⁻ causing some CO₂ to desorb from the solution. This desorbed CO₂ may then be absorbed by the solution consuming CO₃²⁻ ions that would otherwise be consumed by CO₂ from the flue gas stream.

When the carbonate solution was contacted with SO₂ and NO, no solid precipitates were observed. This is a significant advantage over the more popular amine absorption approach. When amines come into contact with SO₂ and NO, heat stable

salts precipitate out of solution. These salts significantly degrade the performance of the amine absorbent and require extra energy to remove them from the system [9, 30]. It is possible that the carbonate solvent could be used as a solvent for a multi pollutant control system to simultaneously capture SO_2 , NO , and CO_2 .

It is also important to understand the effect the SO_2 and NO will have on the CO_2 absorption rate in the carbonate solution. Carbonate solutions already suffer from the perception that the CO_2 absorption rate is slower than in amine solutions [16]. Any decrease in the CO_2 absorption rate would severely hinder the application of using carbonate solutions over amines for CO_2 capture or as a multi-pollutant control system. Figure 18 illustrates the effect SO_2 and NO had on the absorption rate of CO_2 in the carbonate solution.

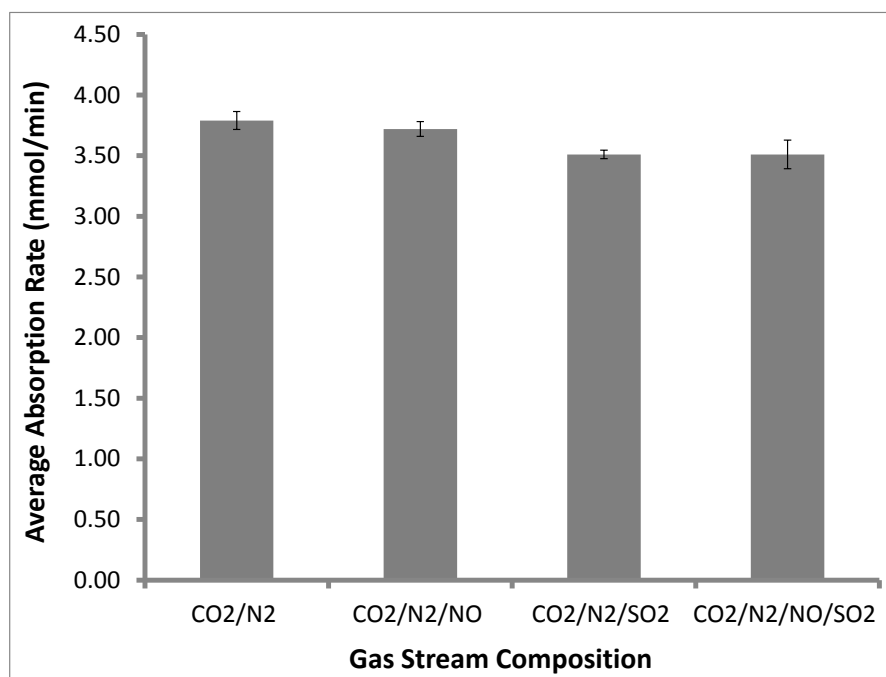


Figure 18: The effect of flue gas impurities on the absorption rate of CO_2 in a 2% (w/w) sodium carbonate solution

Figure 18 shows that NO had a negligible impact on the absorption rate of CO₂. Once again, it is likely that NO had a negligible impact because of its low solubility in water based solutions. In both experiments where SO₂ was present the absorption rate of CO₂ decreased by 7%. As previously stated, when SO₂ goes through hydrolysis two hydrogen ions are produced; one of which produces a bisulfate ion and the other will consume a free carbonate ion to produce a bicarbonate ion. The reduction in free carbonate ions will lead to a more rapid decrease in solution pH. The ability of the solution to buffer the dissolved CO₂ is effectively reduced, leading to a reduced CO₂ absorption rate.

Conclusions

Some important conclusions can be made about absorbent temperature and the effects of flue gas impurities on CO₂ absorption in carbonate solutions. Increasing the absorbent temperature from 25 °C to 60 °C severely hindered the CO₂ absorption rate, reducing it by as much as 55%. A reduction in the absorption rate means larger absorption equipment will be needed, thus adding to capital cost of the absorption system. To limit the impact of temperature, the absorbent should be cooled to at least 25 °C before absorption. Current experimental results do not support literature on carbonate absorption which suggest absorbent temperature should be between 50-60 °C.

The presence of NO in the flue gas stream had little effect on CO₂ absorption capacity in the carbonate system due to its low solubility in comparison to SO₂ and CO₂. When SO₂ was present in the flue gas stream, the CO₂ absorption capacity of the solution was decreased by 12% while the CO₂ absorption rate was decreased by 7%. Current studies suggest sodium carbonate solutions possess the potential to capture both CO₂ and SO₂, serving as a multi pollutant capture technology at fossil fuel burning power plants. The ability to simultaneously capture multiple pollutants

could eliminate the need for costly pretreatment of the flue gas before CO₂ absorption.

Chapter 5: Increased Carbon Dioxide Absorption Rates in Carbonate Solutions by Surfactant Addition³

³ Spigarelli, B., P. Hagadone, et al. (2013). "Increased Carbon Dioxide Absorption Rates in Carbonate Solutions by Surfactant Addition." Minerals and Metallurgical Processing **30**(2): 95-99.

Abstract

To meet the growing need for CO₂ capture and storage technology, Michigan Technological University is researching CO₂ capture and storage using carbonate solutions. The objective of the present study was to increase the absorption rate of CO₂ into the carbonate solution without reducing the absorption capacity of the solution. This approach used a polypropylene glycol methyl ether (PPGME) as a surfactant to chemically alter the gas bubble size. Experiments were conducted to study the absorption rate of CO₂ at varying surfactant concentrations of 0, 0.12, 0.24, 0.36, and 0.48 g/L. Results showed that as the concentration of surfactant increased in solution, the absorption rate also increased. The CO₂ absorption rate increased from 3.45 mmol/min CO₂ at 0g/L PPGME to 3.92 mmol/min CO₂ at 0.48 g/L PPGME. This amounted to a 14% increase in the CO₂ absorption rate with no decrease in absorption capacity of the solution.

Introduction

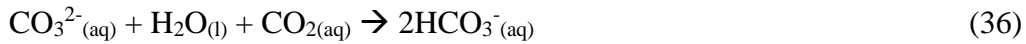
The growing concern over global climate change has sparked a desire for reductions in greenhouse gas emissions. Several options do exist for reducing CO₂ emissions: demand-side conservation, supply side efficiency improvement, increasing reliance on nuclear and renewable energy, and carbon capture and storage (CCS) systems. Of the options mentioned above it is believed that CCS presents the most practical approach for long term CO₂ emission reductions [2, 150]. Currently, fossil fuel fired power plants are one of the largest point sources of CO₂ emissions, making them attractive sites for CO₂ emission reductions [17]. The most mature and attractive CCS technology for application to fossil fuel burning power plants is chemical absorption. During chemical absorption, the contaminated gas stream comes into contact with a liquid solvent in an absorption column. The liquid absorbent captures the CO₂ and then acts as a carrier to transport the CO₂ for further processing [1, 12, 25, 26]

Chemical absorption using an amine solvent is currently the most mature CCS technology available. The natural gas industry has used amine absorption for over 60 years to remove CO₂ from natural gas. Amines are advantageous in that they have a fast CO₂ absorption rate which leads to a high CO₂ removal efficiency. However, amine absorption has some considerable drawbacks, such as: high energy requirements, high equipment corrosion rates, amine degradation in the presence of oxygen, high waste generation, and a large increase in plant footprint if new equipment is constructed [10, 11].

Due to the drawbacks associate with amine solvents, Michigan Technological University (MTU) is studying CO₂ absorption using carbonate based solvents.

Basics to CO₂ absorption in carbonate solvents

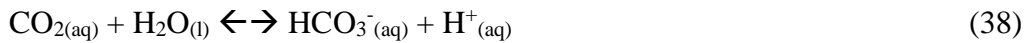
Overall, CO₂ is absorbed by, and reacts with the carbonate (CO₃²⁻) solution to produce bicarbonate ions (HCO₃⁻), as seen in Eq. (36) [16, 53].



The overall reaction seen in Eq. (36) can be divided into two general steps. First, gaseous CO₂ is dissolved into the liquid to form aqueous CO₂, Eq. (37).



Second, the aqueous CO₂ will ionize into HCO₃⁻ and CO₃²⁻ ions, seen in Eqs. (38) and (39). The pH of the solution will determine which species, HCO₃⁻ or CO₃²⁻, dominates in solution.



At a pH below 10 bicarbonate ions are the dominate species in solution; at a pH above 10, carbonate ions dominate in solution [142]. For carbonate systems the solution pH is near 11. This means that CO₃²⁻ ions, needed for CO₂ absorption, will dominate in solution initially, but drop with pH.

Carbon dioxide absorption using carbonate solutions has been around since the early 1900's when it was first used for dry ice production [51, 52]. Carbonate solutions are advantageous for several reasons:

- Non-hazardous, non-volatile, and non-fouling

- Environmentally benign
- No degradation in the presence of oxygen
- Low equipment corrosion rate
- Possible multi pollutant control system (SO_x capture)
- Easy retrofit to current wet flue gas desulphurization units

The main drawback associated with the carbonate system is the slow absorption rate of CO₂ in comparison to amine solutions. The absorption rate is important because it is a controlling factor in the design of equipment. A slower absorption rate requires longer contact times between the gas and liquid, which will lead to larger capital costs for equipment. It is believed that rate increasing additives will need to be identified for CO₂ capture with carbonate solvents to be feasible. Studies have been conducted examining rate increasing additives such as arsenous acid, formaldehyde, hypochloride, phenols, sucrose, dextrose, piperazine, DEA, and MEA [16, 55-58]. The rate increasing additives have been shown to increase the rate of absorption but they are hazardous, produce unwanted by products, or negatively affect the absorption capacity of the solution.

The focus of this paper is to identify a surfactant which can increase the CO₂ absorption rate into a carbonate solution without adversely impacting the absorption capacity of the solution. For the present study, CO₂ was bubbled through a carbonate solution with varying concentrations of a polypropylene glycol methyl ether (PPGME) surfactant called DOWFROTH 200, a non-hazardous chemical. The PPGME surfactant was chosen because it reduces the gas bubble size distribution and average bubble diameter. This would thereby increase the gas-liquid interfacial area, in theory increasing the CO₂ absorption rate. Thus, objectives of the study include the following: 1) quantify the effect of PPGME concentration on gas bubble size and 2) quantify the effect of PPGME concentration on the CO₂ absorption rate and capacity of the solution.

Materials and Methods

Materials used in the present study include:

- **Sodium Carbonate (Na_2CO_3):** Na_2CO_3 was used in the studies as the source for carbonate ions. The Na_2CO_3 was granular, anhydrous, ACS reagent grade purchased from Sigma Aldrich with a purity of greater than or equal to 99.5% Na_2CO_3 .
- **Distilled H_2O :** Distilled H_2O was mixed with the Na_2CO_3 to create the carbonate solvent.
- **Polypropylene glycol methyl ether (PPGME) – DOWFROTH 200:** The surfactant PPGME was used in the studies to chemically alter the gas bubble size. The PPGME is a neutral charge surfactant with a mean molecular weight of 200. It is a combination of polypropylene glycols and monomethyl ethers.
- **Gases:** Industrial grade CO_2 and compressed air were used to create the contaminated gas mixture. The gas mixture was roughly 16% CO_2 and balance air.
- **Gas Diffuser:** A medium porosity, ASTM standard gas diffuser was purchased for bubbling the gas mixture through the absorbent. The pore diameter of the gas diffuser ranges from 10 – 15 microns

Bubble Size Analysis

Bubbles were produced with an ASTM standard medium porosity gas diffuser in a clear plastic, rectangular shaped vessel at the same gas flow rates used in the

absorption rate experiments. Photographs of the bubbles produced in each solution were captured with a Canon 10 D camera with a 100 mm F2.8 macro lens, using the on camera flash. Three images taken of each solution were used for the bubble size analysis. One hundred bubbles were analyzed from each image; in all 300 bubbles produced in each solution were analyzed to obtain a bubble size distribution and average bubble diameter. Image analysis software, ImageJ, was used to determine the bubble distribution and average bubble diameter produced in each solution [151].

Absorption Rate Measurements

The experimental set-up used for CO₂ absorption rate measurements can be seen in Figure 19.

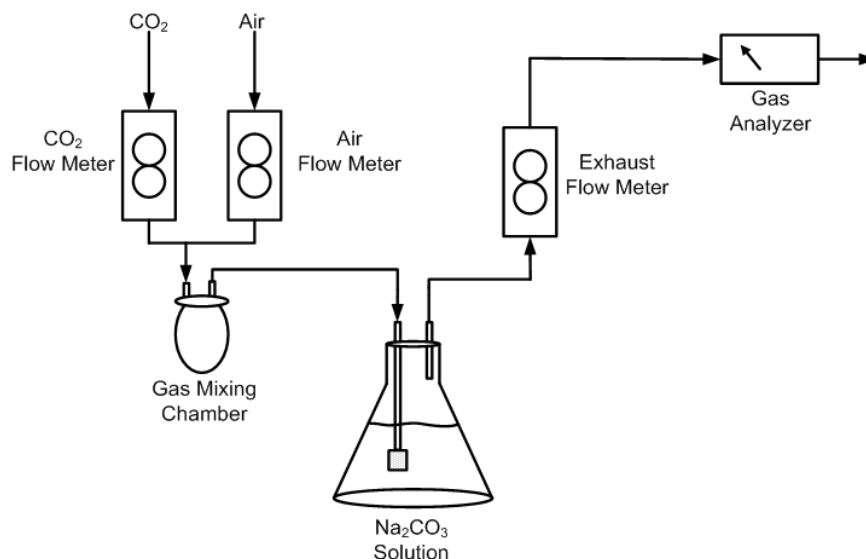


Figure 19: Experimental set-up for measuring CO₂ absorption rates. Experiments were carried out at ambient temperature and pressure.

The %CO₂ in the gas stream was controlled by using separate CO₂ and air flow meters to monitor the volumetric flow rates. The CO₂ flow rate was set at 2.57 ml/sec and the air set at 14.57 ml/sec; this amounted to a roughly 16% CO₂ gas mixture. The gases were then sent to a gas mixing chamber to assure uniform composition of the gas entering the absorption flask. Once mixed, the gas was bubbled into a 1000 ml Erlenmeyer flask containing the 2% Na₂CO₃ solution (800 g distilled H₂O and 16.33 g Na₂CO₃) and varying concentrations of polypropylene glycol methyl ether (PPGME). From previous studies the 2% Na₂CO₃ solution was determined to be ideal for CO₂ absorption [152]. The PPGME was added to the 800 g distilled H₂O before addition of the Na₂CO₃ to solution. The gas not absorbed by the solution was emitted out of the flask to an exhaust gas flow meter to record the exit volumetric flow rate of the gas. After the flow meter, the gas was passed through a CAI 600 series infrared gas analyzer to obtain the %CO₂ in the exhaust gas stream. The CO₂ absorption rate was taken as the difference between the CO₂

fed and CO₂ exhausted during this process. CO₂ absorption rate measurements were repeated in triplicate to ensure the accuracy of the data.

Results and Discussion

As stated previously, the addition of surfactant to the carbonate solution should reduce the size of gas bubbles produced in solution. A reduction in the size of gas bubbles will lead to an increase in the gas-liquid interfacial area between the CO₂ and carbonate solution. An increase in the gas-liquid interfacial area will, theoretically, lead to an increase in the rate of CO₂ absorption. Equation 40 relates the gas-liquid interfacial area to the rate of CO₂ absorption into the carbonate solution [153-155].

$$r = k_L \cdot a \cdot \Delta C \quad (40)$$

where “r” is the rate of absorption, “k_L” is the liquid-side mass transfer coefficient, “a” is the gas-liquid interfacial area, and “ΔC” is the change in CO₂ concentration at the gas-liquid interface and the bulk liquid. Literature has shown that surfactant addition may negatively impact the value of k_L by creating a surfactant barrier around the gas bubble [156, 157].

The results of the bubble size analysis, Figure 20, illustrate that as the surfactant concentration in solution increases, the bubble size distribution narrows and the average bubble diameter decreases.

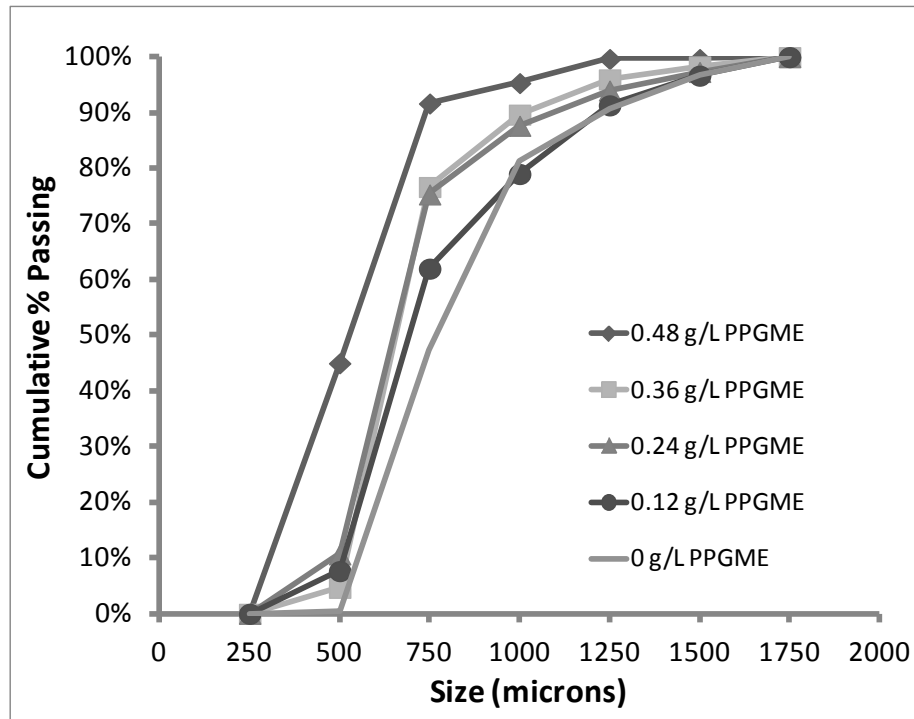


Figure 20: Bubble size distribution at varying Polypropylene glycol methyl ether (PPGME) concentrations. As the concentration of PPGME in solution increased the bubble size distribution narrowed, as evident by the reduction in the 80% passing value.

For example, narrowing of the bubble size distribution is evident by examining the % of total bubbles passing 750 microns. At 0 g/L PPGME in solution, only 47% of the total bubbles analyzed passed 750 microns. This number steadily increases with increasing frother concentration: from 62% at 0.12 g/L PPGME to 92% at 0.48 g/L PPGME in solution.

Using the bubble size distribution, a number average bubble diameter and gas-liquid interfacial area at the varying PPGME concentrations was obtained. The gas liquid interfacial areas were calculated using standard practices, as described in [154, 158-160]. The average bubble diameters and gas-liquid interfacial areas at each PPGME concentration can be seen in Table 7.

| Surfactant in solution (g/L) | Average bubble diameter (um) | Gas-liquid interfacial area (m ² /m ³) |
|------------------------------|------------------------------|---|
| 0 | 585.69 | 208 |
| 0.12 | 537.32 | 313 |
| 0.24 | 461.69 | 397 |
| 0.36 | 450.68 | 430 |
| 0.48 | 288.80 | 823 |

Table 7 shows that as the concentration of PPGME in solution is increased, the average bubble diameter produced decreases. As the bubble diameter decreases, the gas-liquid interfacial surface area increases. At a concentration of 0 g/L PPGME in solution, the gas-liquid interfacial area is 208 m²/m³. At a concentration of 0.48 g/L PPGME, the gas-liquid interfacial area almost quadruples to 823 m²/m³. An increase in gas-liquid interfacial area means an increase in the volume of gas in contact with the solution at any given time.

Theoretically, an increase in gas-liquid interfacial area (Table 1) should lead to an increase in absorption rate. Experimental results seen in Figure 21 show that as the gas-liquid interfacial area increases, or as the PPGME in solution increases, the absorption rate does indeed increase. Carbon dioxide absorption rates were obtained from Figure 21 by calculating the slope of each curve for the entire experimental run time.

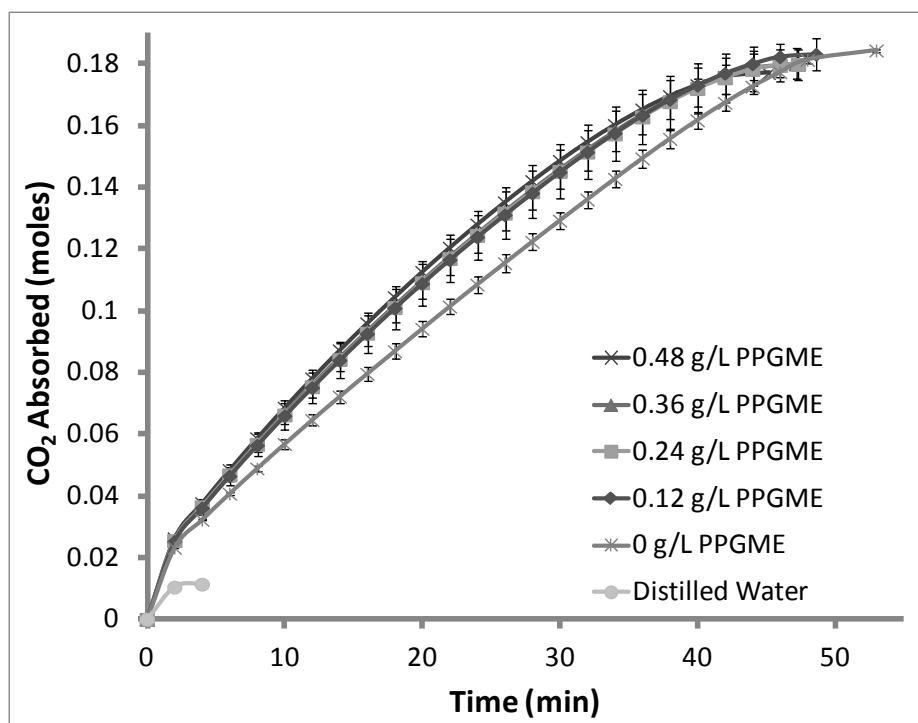


Figure 21: CO₂ absorption in a 2% Na₂CO₃ solution with varying concentration of PPGME in solution. As the concentration of PPGME increases, the absorption rate of CO₂ also increases.

Figure 21 is a plot of the moles of CO₂ absorbed versus time. Carbon dioxide absorption in distilled water is presented in the figure to clearly illustrate the benefit of Na₂CO₃ to solution on CO₂ absorption. The benefit is clearly evident by comparing the distilled water curve to the 0 g/L PPG methyl ether curve. An increase of roughly 92% is seen in the absorption capacity of the solution. Figure 21 shows that the addition of PPGME to solution does in fact increase the absorption rate in solution. To confirm that the absorption rate was increasing as PPGME concentration increased, absorption rates were calculated from the experimental data at each concentration of PPGME. These results, along with the % CO₂ absorbed and saturation time can be seen in Table 8.

| Table 8 CO₂ absorption in a 2% Na₂CO₃ solution with varying concentration of PPGME in solution | | | | |
|--|----------------------------|-----------------------|------------------------------------|-------------------------------|
| Surfactant concentration (g/L) | % CO ₂ absorbed | Saturation time (min) | Average absorption rate (mmol/min) | % Increase in absorption rate |
| 0 | 46.60 (+/- 0.89) | 53 (+/- 1) | 3.45 | NA |
| 0.12 | 49.58 (+/- 0.06) | 48.62 (+/- 1.23) | 3.76 | 8.98 |
| 0.24 | 48.69 (+/- 0.22) | 47.33 (+/- 1.88) | 3.78 | 9.56 |
| 0.36 | 49.69 (+/- 0.71) | 47.16 (+/- 1.04) | 3.82 | 10.72 |
| 0.48 | 52.41 (+/- 0.11) | 45.16 (+/- 0.57) | 3.92 | 13.62 |

% increase in rate is based off the increase in absorption rate with respect to the 0 g/L surfactant solution. The solution pH dropped from 11 to 8 during absorption.

From Table 8 it can be seen that as the concentration of PPGME in solution is increased (or as bubble diameter decreases), the absorption rate of CO₂ into solution increases. At a PPGME concentration of 0.48 g/L, the absorption rate increased by 14% compared to a solution with no PPGME.

Even though the interfacial bubble area increased by 300%, there was only a 14% increase in the CO₂ absorption rate. If the value of the liquid-side mass transfer coefficient (k_L) remained constant, then equation 40 predicts that the CO₂ absorption rate should have also increased by 300%. A possible explanation is that the layer of surfactant on the bubbles reduces the k_L value by producing a low permeability film over the bubbles surface. Higher dosages of surfactant will tend to increase the density of this film, as can be calculated from the Gibbs absorption equation [161]. As a result, the decrease in k_L with increasing surfactant concentration will cancel out part of the increase in absorption rate due to the increased bubble surface area. This suggests that a different surfactant, with better CO₂ permeability, would give greater benefit than the PPGME frother studied in this paper. Use of CO₂

permeable surfactants would give the benefit of reduced bubble size, without an accompanying reduction in the specific mass transfer coefficient.

Table also shows that the percent of CO₂ absorbed by the solution increases as the concentration of PPGME is increased. This shows that the addition of surfactant to solution has no ill effects on the absorption capacity of the solution.

Conclusions

From the results obtained it was concluded that as the concentration of PPGME in solution increased, the gas bubble size distribution narrowed and the average gas bubble diameter decreased. The % of total bubbles passing 750 microns increased from 47% at 0 g/L PPGME to 92% at 0.48 g/L PPGME. The reduced bubble size led an increase in the gas liquid interfacial area, thus leading to an increase in the absorption rate of CO₂ into solution evident by the absorption rate studies. It was determined that the absorption rate could be increased by roughly 14% during the present study with no decrease in absorption capacity of the solution. Future studies will focus on the mass transfer theory behind the results to better understand the impact the PPGME is having on CO₂ absorption.

Acknowledgements

The authors would like to acknowledge the Department of Education, the National Science Foundation, and the Advanced Sustainable Iron and Steel Making Center for support of this work.

Chapter 6: The Effect of Surfactant Addition on Carbon Dioxide Absorption in Carbonate Solutions

Abstract

In the present work, carbon dioxide (CO₂) absorption in carbonate solutions was studied. The objective of the present study was to increase the absorption rate of CO₂ into carbonate solutions by using a surfactant to chemically alter the gas bubble size in solution. A neutral charge polypropylene glycol methyl ether surfactant was used to chemically alter the gas bubble size. Experiments were conducted to study the absorption of CO₂ at surfactant concentrations of 0, 0.12, 0.24, 0.36, and 0.48 g/L in the carbonate solution. Results showed that only a small dosage (0.12 g/L) of surfactant was needed to cause a significant increase in the CO₂ absorption rate. As the dosage of surfactant in solution was increased, the absorption rate of CO₂ into the solution plateaued. Experimental determination of the liquid-side mass transfer coefficient found that even though the CO₂ absorption rate was increasing, the presence of the surfactant was limiting the extent to which the absorption rate could be increased by reducing the mass transfer rate of CO₂ to the bulk liquid. Comparison of the experimental values for liquid side mass transfer coefficient to theoretical values, calculated using the Higbie and Frossling models, found that the surfactant was reducing the mass transfer rate by creating a surfactant film around the bubble.

Introduction

Chemical absorption of carbon dioxide (CO₂) using carbonate solvents has been proposed as a possible CO₂ mitigation technology for fossil fuel fired power plants [16, 143]. Carbonate solvents possess many advantages over the commercially available amine solvents which make them extremely attractive. Such advantages include a lower toxicity, low volatility, non-fouling, low equipment corrosion rate, and the possibility for use as a multi pollutant capture system (NO_x, SO_x, and CO₂ removal) [16]. However, the absorption rate is slow compared to amine solvents limiting its attractiveness [51, 52, 162]. Thus, the main purpose to the present work was to increase the absorption rate of CO₂ into carbonate solutions. Increasing the absorption rate can be accomplished in a variety of ways. Figure 22 will be used to assist in describing CO₂ absorption in carbonate solutions to help better understand the ways in which the absorption rate may be increased.

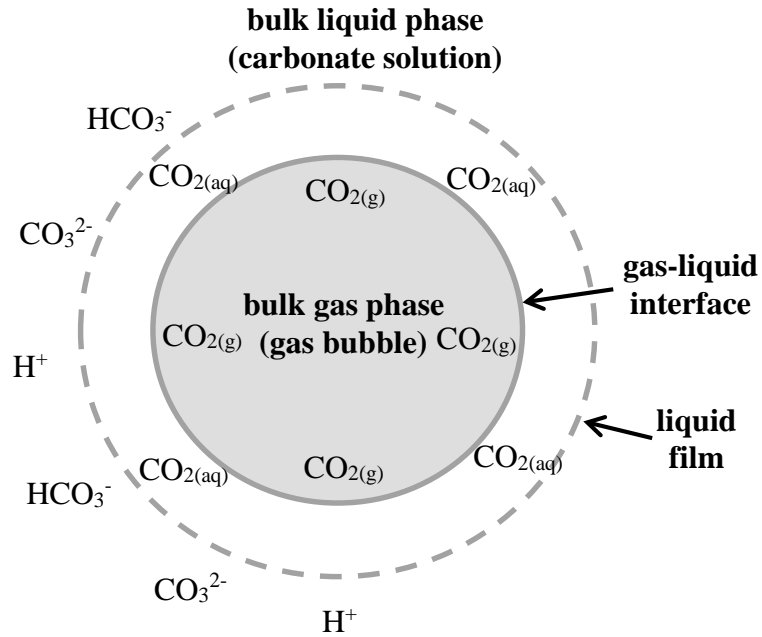
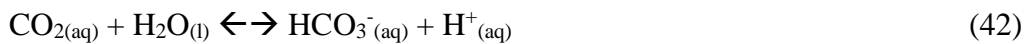


Figure 22: Carbon dioxide absorption from a gas bubble in a carbonate solution

As the CO₂ contaminated gas stream comes into contact with the carbonate solvent CO₂ is transferred from the bulk gas phase (the gas bubble) to the gas-liquid interface, where it is absorbed into bulk liquid phase (the carbonate solution) as aqueous CO₂ (CO_{2(aq)}), Eqn. (41).



Once in the aqueous form CO₂ will ionize to bicarbonate (HCO₃⁻), carbonate (CO₃²⁻), and hydrogen (H⁺) ions, seen in Eqns. (42) and (43). At the elevated pH (>10.5) of the carbonate solution, CO₃²⁻ ions will initially dominate in solution [142], Eqn. (43).





In carbonate absorption, the CO_3^{2-} ions in solution buffer the hydrogen ions formed when CO_2 hydrolyzes. Thus, as CO_2 is absorbed by the solution the CO_3^{2-} ions will be consumed by the H^+ producing bicarbonate ions, the reverse of Eqn. (43). This occurs until the pH of the solution becomes neutral and can no longer buffer the H^+ . At this point CO_2 is no longer being absorbed by the carbonate solution. Studies in literature have examined increasing the rate of Eqns. (42) and (43) by addition of arsenous acid, formaldehyde, hypochlorite, phenols, sucrose, dextrose, diethanol amine, and monoethanol amine [16, 55-58] to solution. These additives were shown to increase the CO_2 absorption rate into carbonate solutions but produced unwanted byproducts, reduced the CO_2 absorption capacity of the solution, or presented significant safety concerns.

An alternative approach to increasing absorption is by altering characteristics of the gas-liquid interface. It is well known that the ionization of CO_2 (Eqns. (42) and (43)) is fast in comparison to the mass transfer of CO_2 to the aqueous phase (Eqn. (41)) [142]. Carbon dioxide is also a relatively insoluble gas in water (3.4×10^{-2} mol/L*atm [145]). Thus, the mass transfer of gaseous CO_2 to the bulk liquid phase phase is considered to be the rate controlling step in the absorption process. Because of this, the absorption of CO_2 into carbonate solvents can be modeled using the bubble dissolution model seen in Eqn. (44) [157, 163-166],

$$\frac{dC}{dt} = k_L \cdot a \cdot (C^* - C) \quad (44)$$

where dC/dt is the absorption rate of CO_2 in the carbonate solution, k_L is the liquid-side mass transfer coefficient (i.e. the resistance from the liquid film seen in Figure 22), “a” is the gas-liquid interfacial area, C^* is the CO_2 concentration at saturation i.e. the solubility of CO_2 ($\text{CO}_{2(\text{aq})}$ in Figure 22), and C is the bulk concentration of

dissolved CO₂. Clearly, the absorption rate can be changed by altering the magnitude of the interfacial area and/or the liquid-side mass transfer coefficient, k_L . A relatively simple way proposed to do this is by adding surface active agents (surfactants) to solution, which significantly alter the gas-liquid interfacial properties of the solution through surface tension, bubble size, gas hold-up, and bubble rise velocity.

The focus of this paper is to examine the affect a polypropylene glycol methyl ether (PPGME) surfactant will have on the gas-liquid interfacial area and liquid-side mass transfer coefficient, and consequently the absorption rate of CO₂ into the carbonate solution. Absorption rate and bubble size data from a previous study [167] will be combined with data on gas hold-up and bubble rise velocity to explain how the surfactant is affecting the gas-liquid interfacial area and liquid side mass transfer coefficient. Experimental liquid-side mass transfer coefficients will be compared to theoretical models to explain the behavior of the surfactant and propose further ways to increase CO₂ absorption in carbonate solutions.

Theory/Background

Mass transfer between a bubble and the surrounding liquid is largely dependent upon properties of the gas-liquid interface, including the liquid-side mass transfer coefficient (k_L) and the gas-liquid interfacial area (a). Therefore it is important to determine the effect of the surfactant on these values. For the present study, the liquid-side mass transfer coefficient, k_L , was determined at each experimental condition from Eqn. (44) using experimentally determined absorption rates and calculated gas-liquid interfacial areas. Theoretical values for k_L were estimated using the Higbie and Frossling models.

The gas-liquid interfacial area quantifies the surface area of gas in contact with the liquid at any given time. The gas-liquid interfacial area was calculated at each

experimental condition as a function of the gas hold-up and mean number bubble diameter, Eqn. (45) [168],

$$a = \frac{6 \cdot \varepsilon_G}{d_b} \quad (45)$$

where ε_G is the gas hold-up and d_b is the mean number bubble diameter. The mean number bubble diameter was determined experimentally using a photographic method and the gas hold-up (ε) was estimated using the Lockett correlation [169], Eqn. (46),

$$V_G(1-\varepsilon_G) + V_L \cdot \varepsilon_G = V_b \cdot \varepsilon_G (1-\varepsilon_G)^{2.39} (1 + 2.55\varepsilon_G^3) \quad (46)$$

where V_G is the superficial gas velocity, V_L is the liquid velocity, and V_b is the bubble rise velocity. The gas hold-up value is defined as the volume fraction of gas phase present in the reactor and is valuable in determining an accurate gas bubble retention time in the solvent [144, 170, 171]. The liquid velocity for the present study was zero since absorption was carried out in a static bed of liquid and the bubble rise velocity was determined experimentally. Further details on how the bubble rise velocity was determined can be seen in the materials and methods section.

Motarjemi and Jameson (1978) have shown that experimental values for k_L will typically fall between two theoretical models: the Higbie and Frossling models. The Higbie model estimates a liquid-side mass transfer coefficient for bubbles with a completely mobile interface [172, 173]. A mobile interface implies that the solution around the gas-liquid interface will be well mixed. This allows fresh solution to be continually contacted with the interface increasing the driving force for CO_2 absorption, resulting in the faster mass transfer rates. The Higbie model will predict

an upper value for the liquid side mass transfer coefficient at each experimental condition. The Higbie model can be seen in Eqn. (47),

$$k_L = 2 \cdot \sqrt{\frac{D_L}{\pi \cdot t_b}} \quad (47)$$

where D_L is the diffusivity of CO_2 in water and t_b is the time it takes a bubble to travel one bubble diameter. For the present study, the diffusivity of CO_2 in water was assumed because experiments were carried out in a dilute sodium carbonate solution. The time it takes a bubble to travel one bubble diameter was calculated using Eqn. (48) [172].

$$t_b = \frac{d_b \cdot \varepsilon_G}{V_G} \quad (48)$$

The time it takes a bubble to travel one bubble diameter is a good indication of bubble retention time in the absorbent. The impact of the time it takes a bubble to travel one bubble diameter on the liquid-side mass transfer coefficient is apparent by examination of Eqn. (47). As t_b decreases the liquid-side mass transfer coefficient increases, and vice versa (as it applies to the Higbie model).

For bubbles with a rigid interface the Frossling model was used to estimate the value of the liquid-side mass transfer coefficient [165]. The Frossling model will predict a lower value for k_L at each experimental condition. With an immobile interface bubbles tend to be surrounded by a laminar boundary layer. This leads to poor mixing of the solution around the gas-liquid interface, i.e. less fresh solution will come into contact with the interface leading to lower predicted mass transfer rates. The Frossling model can be seen in Eqn. (49),

$$k_L = \frac{D_L}{d_b} (2 + 0.6 \text{Re}^{\frac{1}{2}} \cdot \text{Sc}^{\frac{1}{3}}) \quad (49)$$

where Re and Sc are the Reynolds and Schmidt number. It is likely that experimental results will behave similarly to the Frossling model as it is well known that many surfactants build up at the gas-liquid interface creating an immobile surface.

Materials and Methods

Materials used in the present study include:

- **Sodium Carbonate (Na₂CO₃):** Na₂CO₃ was used in the studies as the source for carbonate ions. The Na₂CO₃ was granular, anhydrous, ACS reagent grade purchased from Sigma Aldrich with a purity of greater than or equal to 99.5% Na₂CO₃.
- **Distilled H₂O:** Distilled H₂O was mixed with the Na₂CO₃ to create the carbonate solvent.
- **Polypropylene glycol methyl ether (PPGME) – DOWFROTH 200:** The surfactant PPGME was used in the studies to chemically alter the gas bubble size. The PPGME is a neutral charge surfactant with a mean molecular weight of 200. It is a combination of polypropylene glycols and monomethyl ethers. PPGME 200 is technically considered a frothing agent.
- **Gases:** Industrial grade CO₂ and compressed air were used to create the contaminated gas mixture. The gas mixture was roughly 16% CO₂ and 84% air for all trials.

- **Gas Diffuser:** A medium porosity, ASTM standard gas diffuser was purchased for bubbling the gas mixture through the absorbent. The pore diameter of the gas diffuser ranges from 10 – 15 microns

Bubble Size Analysis

Bubbles were produced with a medium porosity ASTM standard gas diffuser in a clear plastic rectangular shaped vessel. The gas mixture was bubbled in at 17.14 ml/sec. Photographs of the bubbles produced in each solution were captured with a Canon 10 D camera with a 100 mm F2.8 macro lens, using the on camera flash. Three images taken of each solution were used for the bubble size analysis. One hundred bubbles were analyzed from each image; in all 300 bubbles produced in each solution were analyzed to obtain a bubble size distribution and average bubble diameter. Image analysis software, ImageJ, was used to obtain the bubble distribution and average bubble diameter produced in each solution [151].

Interfacial Surface Tension

Interfacial surface tension measurements of the solutions were taken using a Fisher Surface Tensiomat Model 21. The instrument is similar to those currently specified by ASTM standards D-971 (interfacial tension of oil against water) [174] and D-1331 (surface and interfacial tensions of detergents) [175]. The Tensiomat measures the interfacial surface tension using the du Nouy ring method. This, in brief, measures the force necessary to pull a test ring free from the surface film of the liquid and then relates the force to the interfacial surface tension. Surface tension measurements were taken at 25 °C and repeated 10 times on three different solutions for each concentration of surfactant; totaling 30 surface tension measurements at each surfactant concentration.

Bubble Free Rise Velocity

Bubble free rise velocity measurements were carried out in a transparent polyvinyl chloride column (with an inside diameter of 0.10 meters and a height of 0.61 meters) filled to 0.45 meters with a 2% (w/w) Na_2CO_3 solution and the desired concentration of PPGME 200. An ASTM standard medium porosity gas diffuser was used to bubble gas through the solution at a rate of 17.14 ml/sec. With the diffuser used it was not possible to measure the velocity of a single bubble due to the large volume of bubbles produced. Instead, the velocity of a plume of bubbles was measured to obtain the bubble rise velocity. To create a plume of bubbles a valve was placed before the diffuser which allowed for the gas feed to the carbonate solution to be easily opened and closed. The velocity was obtained by timing how long it took the plume to travel a distance of 0.30 meters through the solution. Bubble rise velocity measurements were repeated 30 times at each concentration of PPGME 200.

Absorption Rate Measurements

The experimental set-up used for CO_2 absorption rate measurements can be seen in Figure 23.

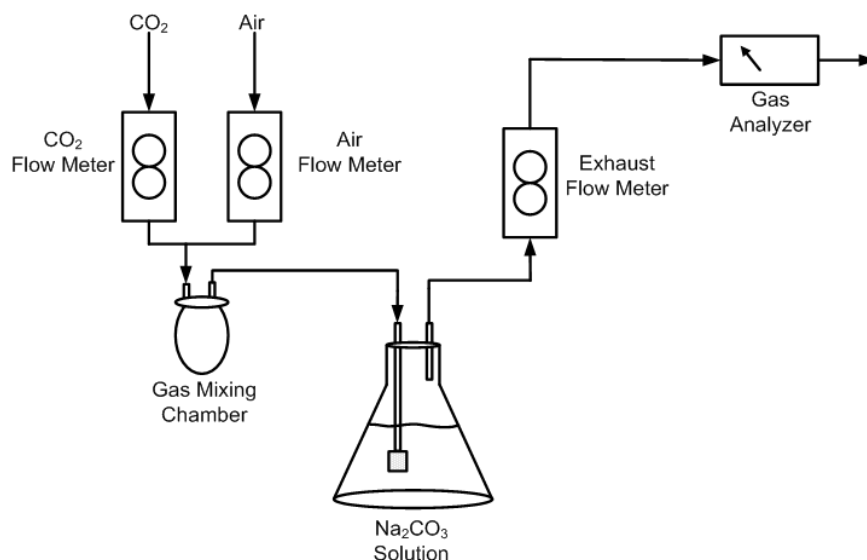


Figure 23: Experimental set-up for measuring CO₂ absorption rates

The %CO₂ in the gas stream was controlled by using separate CO₂ and air flow meters to monitor the volumetric flow rates. The CO₂ flow rate was set at 2.57 ml/sec and the air set at 14.57 ml/sec; this amounted to a roughly 16% CO₂ gas mixture. The gases were then sent to a gas mixing chamber to assure uniform composition of the gas entering the absorption flask. Once mixed, the gas was bubbled into a 1000 ml Erlenmeyer flask containing a 2% (w/w) Na₂CO₃ solution and varying concentrations of PPGME. From previous studies the 2% Na₂CO₃ solution was determined to be ideal for CO₂ absorption [148]. The PPGME was added to the distilled water before addition of the Na₂CO₃ to solution. The gas not absorbed by the solution was emitted out of the flask to an exhaust gas flow meter to record the exit volumetric flow rate of the gas. After the flow meter, the gas was passed through a CAI 600 series infrared gas analyzer to obtain the %CO₂ in the exhaust gas stream. The CO₂ absorption rate was taken as the difference between the CO₂ fed and CO₂ exhausted during this process. CO₂ absorption rate measurements were repeated in triplicate to ensure the accuracy of the data.

Results and Discussion

Surfactants have the ability to reduce bubble size by lowering the solution surface tension and preventing bubble coalescence. All surfactants possess a value known as the critical coalescence concentration (CCC). This is the concentration above which bubble growth does not occur by the mechanism of coalescence. PPGME 200 has a CCC value of 0.0138 g/L [176]. The minimum surfactant concentration used in this study was 0.12 g/L PPGME 200, well above the CCC value. This suggests that bubble size will largely be controlled by the gas diffuser geometry and solution surface tension. Bubble size is important because it is used to determine the gas-liquid interfacial area across which the mass transfer of gaseous CO₂ to the bulk liquid phase takes place. It will also have a significant effect on other variables that may affect mass transfer, such as the bubble rise velocity and gas hold-up. Data obtained from the bubble size analysis and surface tension measurements can be seen in Figure 24.

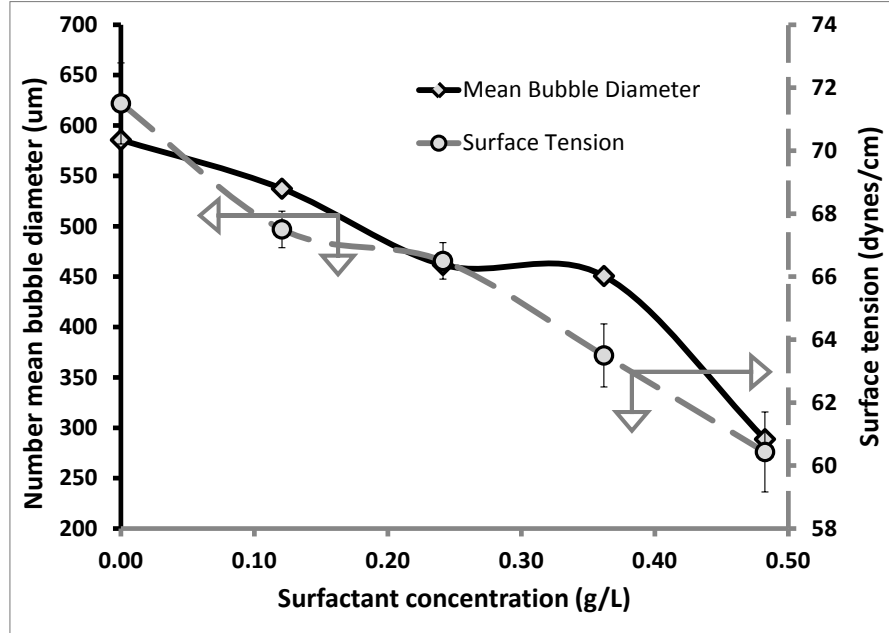


Figure 24: The effect of surfactant concentration on bubble size and surface tension. A decrease in the surface tension of the solution leads to a decrease in the gas bubble size.

As the surfactant concentration increased a noticeable decrease in both the bubble diameter and surface tension was seen. This was expected as it is well known that the surface tension of a solution plays an important role in determining bubble size [176, 177]. The change in bubble size will have a significant effect on the velocity of the bubbles, and consequently the bubble retention time, by altering the buoyancy force of the bubble in solution, Eqn. (50),

$$F_B = \left(\frac{4\pi}{3}\right)(\rho_L - \rho_G)g \cdot r_b^3 \quad (50)$$

where F_B is the buoyancy force, ρ_L and ρ_G are the liquid and gas density, g is the acceleration due to gravity, and r_b is the bubble radius. A decrease in bubble size will cause a decrease in the buoyancy force of the bubble, leading to a reduction in the bubble rise velocity. Surfactant will further slow bubble rise velocity by increasing the drag force acting on the bubbles as they rise through the solution.

When surfactants adsorb to a rising bubble they concentrate towards the rear of the bubble, adding weight to the bubble. This added weight will increase the drag force acting on the bubble as it rises through the solution. A reduction in the bubble rise velocity should increase the gas hold-up within the solution. Figure 25 is a plot comparing the bubble rise velocity and gas hold-up of the system as surfactant concentration changes. The bubble rise velocity was experimentally determined at each surfactant concentration and the gas hold-up (ϵ) was calculated at each concentration using Eqn. (46).

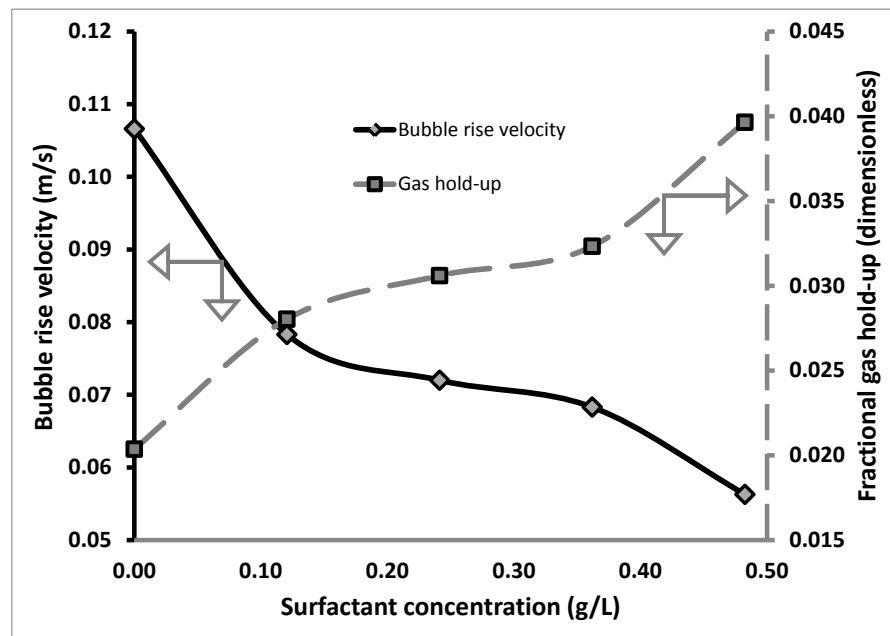


Figure 25: The effect of surfactant concentration on bubble rise velocity and gas hold-up. As the bubble rise velocity decreases, more gas is being “held up” in solution. This exposes the gas to a given volume of solution for a longer period of time.

As the surfactant concentration increased, the bubble rise velocity decreased and the gas hold-up increased. This means that as the surfactant concentration increased the retention time of a gas bubble in the liquid is increased, thus a given volume of gas is being exposed to the solution for a longer period of time. The initial drop in bubble rise velocity can be attributed to the aforementioned effect of bubble size on the buoyancy force and the effect of the surfactant on the drag force as the bubble rises through solution. Since CO₂ is a low solubility gas, the longer it can be exposed to the solution the better the chances of it getting absorbed by the carbonate solution.

According to Eqn. (45), as the gas hold-up increases and the bubble diameter decreases, the gas-liquid interfacial area should increase. Calculated gas-liquid interfacial area values can be seen in Figure 26.

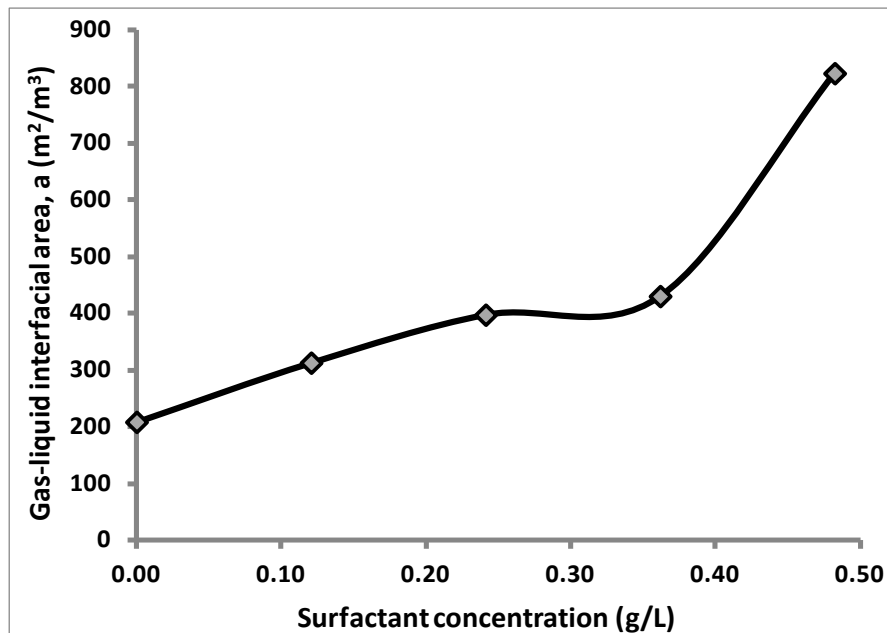


Figure 26: Gas-liquid interfacial area as a function of surfactant concentration. The addition of surfactant to solution reduced the bubble size leading to a larger surface area of gas being exposed to the solution.

Figure 26 shows that as the surfactant concentration increased the gas liquid interfacial area increased. This indicates that roughly 300% more surface area was present for the mass transfer of gaseous CO_2 to the bulk liquid phase to take place. According to Eqn. (44), if the surfactant had no impact on the value of k_L the absorption rate should also increase. Experimental absorption rate data can be seen in Figure 27.

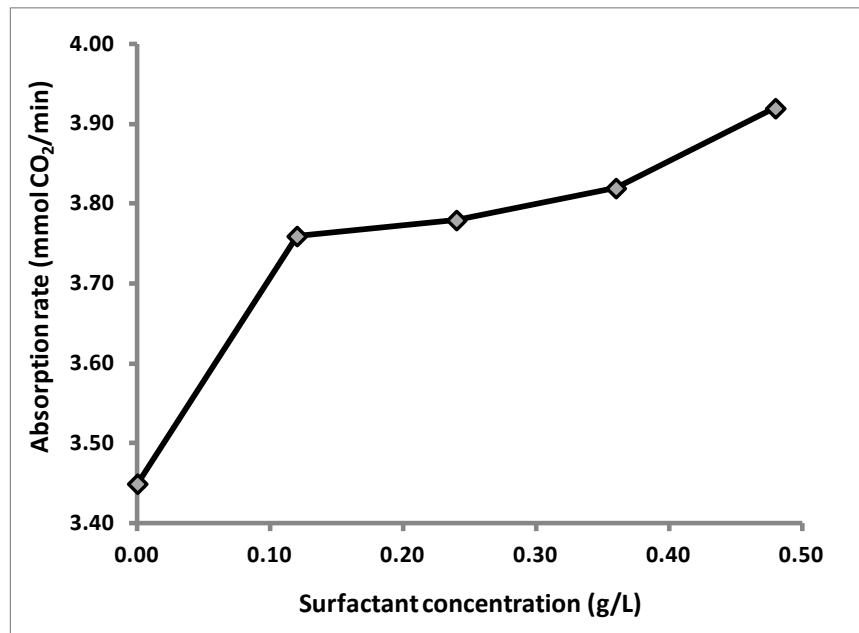


Figure 27: Carbon dioxide absorption rate in a 2% (w/w) sodium carbonate solution at varying surfactant concentration. The absorption rate was increased by as much as 14%.

Results show that the addition of PPGME to the carbonate solution increased the absorption rate of CO₂. Initially, at 0.12 g/L PPGME, a significant increase in absorption rate was seen. However, above 0.12 g/L PPGME diminishing returns were seen with respect to increasing the absorption rate. The diminishing return in absorption rate at elevated surfactant concentration implies that the surfactant is inhibiting the mass transfer of CO₂ to the bulk liquid phase (i.e. impacting the liquid side mass transfer coefficient). This could be caused by the surfactant altering the behavior of the gas-liquid interface by either creating an immobile interface or by creating a surfactant film around the bubble. An immobile interface will cause poor mixing of the solution at the gas-liquid interface. This causes solution already saturated with CO₂ to stay in contact with gas bubble, thus reducing the driving force for CO₂ transport across the interface. A surfactant film around the bubble would create an additional barrier for the CO₂ to diffuse across before reaching the

bulk fluid phase. The affect the surfactant is having on mass transfer will be examined in more detail further in the article.

Since altering the surface tension of the solution was the driving force behind all the changes seen in the present system, it was of interest to see if the change in surface tension was closely related to the change in absorption rate. Figure 28 shows the relationship between the change absorption rate and change solution surface tension.

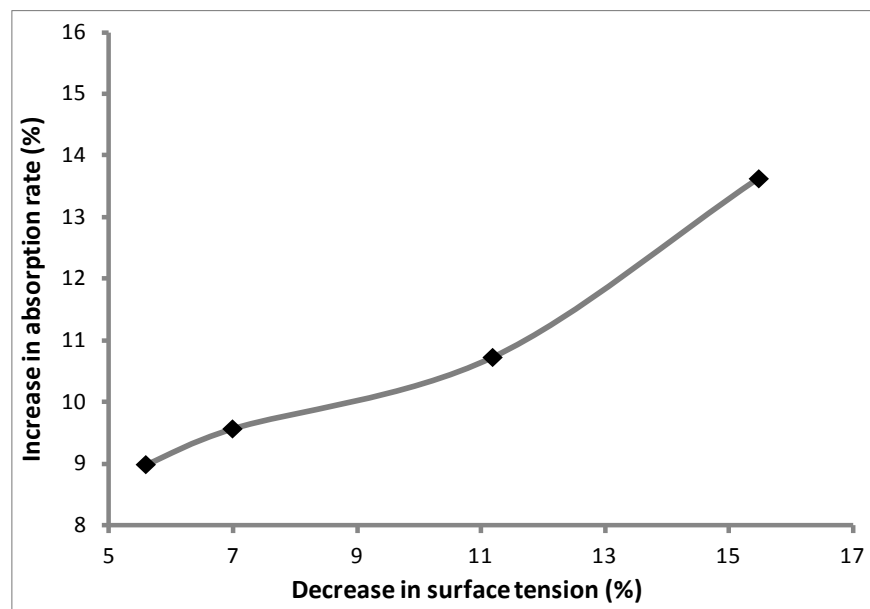


Figure 28: Change in absorption rate with respect to changing surface tension. The CO₂ absorption rate appears to be related to the surface tension of the solution.

Figure 28 shows an almost linear relationship between the % change in absorption rate and % change in solution surface tension for the current system. This suggests that CO₂ absorption in carbonate based solvents is heavily dependent upon the surface tension of the solution. This relationship could have application in predicting the response of the absorption process to a change in the solution surface tension. However, before any concrete conclusions can be drawn from this relationship further research is needed with varying types of surfactants over a wider range of surface tensions.

Liquid-Side Mass Transfer Coefficient Comparison

Using the absorption rate and calculated gas-liquid interfacial area values, Eqn. (44) can be solved to determine the effect the surfactant is having on the liquid side mass transfer coefficient. As aforementioned, surfactant addition can affect the value of k_L in two ways. The surfactant could be creating an immobile gas-liquid interface which would lead to poor mixing of the solvent around the gas-liquid interface; or, the surfactant could be creating a film around the bubble. The film may behave as an additional barrier to the mass transfer of CO₂ from the bulk gas phase to the bulk liquid phase. A plot comparing the experimentally determined k_L values to theoretical values obtained using the Higbie and Frossling models can be seen in Figure 29.

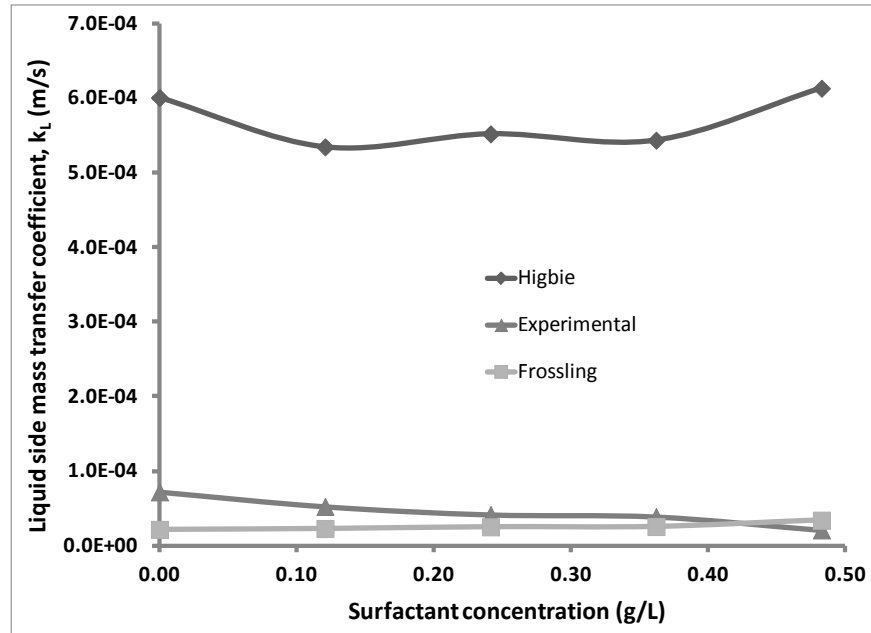


Figure 29: Comparison of experimental k_L values to theoretical values obtained using the Higbie and Frossling models. The Higbie model represents bubbles with a mobile gas-liquid interface. The Frossling model represents bubble with a rigid gas-liquid interface

Experimental results for the liquid side mass transfer coefficient show that even when no surfactant was present in solution the system behaved more closely to the Frossling model than the Higbie model. This could be due largely to the fact that the bubbles in the present system are so small that they are behaving as though having an immobile interface. The bubble size range for the present system is roughly 300 μm to 600 μm . Painmanakul and colleagues (2005), state that bubbles in the size range of 100 μm to 2000 μm behave as though having an immobile gas-liquid interface. As expected then, the experimental values for the liquid-side mass transfer coefficient are more closely related to those calculated using the Frossling model than the Higbie Model.

The experimental k_L values differ from the Frossling model in that the value for k_L continued to decrease as surfactant concentration increased. The Frossling model predicted a slight increase in k_L even as surfactant concentration increased. This is because the Frossling model does not explicitly account for the addition of surfactant. The discrepancy in trends between the experimental and Frossling k_L values suggests that the surfactant is creating a film around the bubble, not an immobile gas-liquid interface. The continued reduction in the experimental k_L value as surfactant concentration increased indicates that as the surfactant concentration was increased the density of the film around the bubble also increased. The formation of a film around the bubble implies that if a more CO_2 permeable surfactant were used, larger gains in the CO_2 absorption rate could possibly be seen.

Conclusions

The addition of the surfactant PPGME 200 to the carbonate solvent increased the gas-liquid interfacial area of the system and increased the absorption rate of CO_2 into the solvent. It was found that initially only a small dosage (0.12 g/L) was needed to significantly increase the gas-liquid interfacial area and absorption rate. As the dosage of surfactant increased the gas liquid interfacial area continued to increase while the absorption rate plateaued. Experimental determination of the liquid-side mass transfer coefficient found that the surfactant was inhibiting the mass transfer of gaseous CO_2 to the bulk liquid phase causing the absorption rate to plateau.

To determine how the surfactant was inhibiting the mass transfer of CO_2 the experimental k_L values were compared to theoretical values calculated from the Higbie and Frossling models. Comparison of the experimental k_L values to those calculated using the Higbie and Frossling models found that the values were more similar to the Frossling model than the Higbie. Although similar the trends in the values were different. The experimental k_L values continued to decrease as

surfactant concentration increased, whereas the values calculated using the Frossling model increased. This suggests that the surfactant was inhibiting the mass transfer of CO₂ by creating a film around the bubble. This film acted as an additional barrier to the mass transfer of the CO₂ from the bulk gas phase to the bulk liquid phase. It is reasonable to believe that this reduction in mass transfer could be overcome by a more CO₂ permeable surfactant.

Acknowledgements

The authors would like to acknowledge ASISC for support of this work.

Notation

| | |
|-----------------|---|
| a | gas-liquid interfacial area (m^{-1}) |
| C | bulk concentration of dissolved CO ₂ (mol/L) |
| C^* | CO ₂ concentration at saturation (mol/L) |
| D_L | diffusivity of CO ₂ in water (m^2/s) |
| d_b | number mean bubble diameter (m) |
| F_B | buoyancy force ($\text{kg}\cdot\text{m}/\text{s}^2$) |
| g | acceleration due to gravity (m/s^2) |
| k_L | liquid side mass transfer coefficient (m/s) |
| Re | bubble Reynolds number (dimensionless) |
| r_b | bubble radius (m) |
| Sc | Schmidt number (dimensionless) |
| t_b | time it takes a bubble to travel one bubble diameter (s) |
| V_G | superficial gas velocity (m/s) |
| V_L | liquid velocity (m/s) |
| V_b | mean bubble rise velocity (m/s) |
| ε_G | fractional gas hold-up (dimensionless) |

ρ_G gas density (kg/m³)
 ρ_L liquid density (kg/m³)

Chapter 7: Carbon Dioxide Sequestration by Chemically Enhanced Aqueous Mineral Carbonation of Coal Fly Ash

Abstract

Carbon dioxide (CO₂) sequestration via ex-situ aqueous mineral carbonation has become a promising option for “permanent” CO₂ storage. The current study is focused on enhancing ex-situ aqueous mineral carbonation of coal combustion fly ash at ambient conditions by the addition of sodium carbonate (Na₂CO₃) to the aqueous environment. The fly ash used in the current study was a lignite fly ash containing 14.94% calcium. In the study, a gaseous mixture of CO₂ and air was bubbled through varying fly ash, Na₂CO₃, and distilled water mixtures. The CO₂ absorption capacity, rate, and sequestration potential of the different mixtures was determined. The addition of Na₂CO₃ to distilled water increased the CO₂ absorption capacity of distilled water by nearly 1,200 %. The addition of Na₂CO₃ to a fly ash/distilled water mixture also increased the CO₂ sequestration capacity of the fly ash from 0.012 kg CO₂ / kg fly ash to 0.099 kg CO₂ / kg fly ash; this is also an improvement upon literature values. Although the storage capacity of the fly ash was improved, the impact for CO₂ sequestration on a large scale is negligible. It was determined that the amount of fly ash produced per day from a fossil fuel burning power plant would have the potential to sequester roughly 0.3% of the total CO₂ emitted per day using the present approach.

Introduction

The growing concern over global climate change has sparked a desire for reductions in greenhouse gas emissions. Carbon dioxide (CO₂) is currently the most abundant greenhouse gas. In 2007, world energy related CO₂ emissions totaled 33.8 billion metric tons. By the year 2035, it is predicted that this number will rise to 42.4 billion metric tons, amounting to a 25% increase in CO₂ emissions globally[17]. A technology that has the potential to mitigate this drastic increase in CO₂ emissions is CO₂ sequestration via mineral carbonation.

Carbon dioxide sequestration via mineral carbonation was first proposed in 1990 by Seifritz[178]. It was not until 1995 that a thermodynamic study on the process was published by Lackner, which outlined the feasibility of the process for use on an industrial scale[179]. The basic concept behind the process of mineral carbonation is natural rock weathering. In weathering, gaseous CO₂ reacts chiefly with solid calcium (Ca) and magnesium (Mg) containing minerals to form thermodynamically stable and environmentally benign carbonate compounds, an example of which can be seen in equation 51 [178-182].



Research has shown that the aqueous reaction between CO₂ and the Ca/Mg bearing mineral is faster than the gas-solid reaction seen in equation 1; this is referred to as ex-situ aqueous mineral carbonation[182]. Naturally occurring calcium/magnesium rich minerals such as olivine, serpentine, brucite, forsterite, anorthite, wollastonite, and basaltic glass have been shown to sequester CO₂ via aqueous mineral carbonation[183]. However, disadvantages associated with aqueous mineral carbonation using natural minerals include:

- Pretreatment of the feed stock

- Elevated operating temperatures and pressures

Natural minerals need to be mined and then crushed for ex-situ aqueous mineral carbonation. It is estimated that the pretreatment of naturally occurring minerals would add 10 US\$/ton CO₂ stored to the overall cost of the mineral carbonation, currently estimated at 54 US\$/ton CO₂[184, 185]. The cost of pretreatment could be reduced by supplementing naturally occurring minerals with industrial waste materials when available. Vast quantities of waste material already exist with properties necessary for mineral carbonation that would not require pretreatment. Such wastes include cement kiln dust, waste cement, asbestos tailings, nickel tailings, red mud, coal fly ash, oil shale ash, and alkaline paper mill waste[185-191]. Coal fly ash is a particularly promising waste material as it is abundant, produced at large CO₂ point sources (coal combustion power plants), cheap, in powdered form, and high in calcium content. Although promising, research published on the carbonation of fly ash is scant and the overall potential of fly ash for CO₂ sequestration from coal burning power plants is not reported.

Aqueous mineral carbonation experiments using coal fly ash, conducted by Montez-Hernandez and colleagues (2009), were carried out in a pure CO₂ atmosphere of 10 bar and a temperature of 30 °C. After a reaction time of 18 hours they found that the fly ash could store 0.026 kg CO₂ / kg fly ash. Uliasz-Bochenczyk and colleagues (2009) conducted similar experiments in a pure CO₂ atmosphere of 10 bar and ambient temperature. After a 24 hour reaction time they were able to store 0.0785 kg CO₂ / kg fly ash. The use of a pure CO₂ atmosphere, as seen with the aforementioned studies, implies that CO₂ must first be removed from the combustion gas stream via a costly capture stage. This coupled with the long reaction times are drawbacks that render fly ash carbonation impractical. Because of these drawbacks, a combined approach to CO₂ capture and storage is studied in the present work to improve the aqueous mineral carbonation of coal fly ash. The aim

of this process is to simultaneously capture and sequester the CO₂ in one step. The process herein enhances ex-situ aqueous mineral carbonation of fly ash at ambient conditions by the addition of sodium carbonate (Na₂CO₃) to the aqueous environment. The addition of Na₂CO₃ enhances the carbonation kinetics and increases the capacity of the solution to capture CO₂.

The focus of this paper is to examine if a single stage CO₂ capture and storage process would be feasible using a chemically enhanced aqueous environment. For the present study, a 16% CO₂/84% air gas mixture was bubbled through a carbonate solution with varying masses of coal fly ash. Objectives of the study include the following:

- Determine the absorption rate of CO₂ into the various carbonate/fly ash mixtures,
- Determine the CO₂ storage capacity of the system in g CO₂ / g fly ash, and
- Determine the mass of emitted CO₂ that could be sequestered on a daily basis with the proposed process assuming an average size coal burning power plant (500 megawatt).

Materials and Methods

Materials used in the present study include:

- **Sodium Carbonate (Na₂CO₃):** Na₂CO₃ was used in the studies to buffer the absorbed CO₂. The Na₂CO₃ was granular, anhydrous, ACS reagent grade purchased from Sigma Aldrich with a purity of greater than or equal to 99.5% Na₂CO₃.
- **Distilled H₂O:** Distilled H₂O was mixed with the Na₂CO₃ to create the carbonate solvent.

- ***Basin Electric Power Cooperative (BEPC) Lignite Fly Ash:*** A 25 gallon drum of lignite fly ash was received from the Basin Electric Power Cooperative. The sample was split into 1.5 – 2 kg samples and sealed in air tight bags to limit exposure to CO₂.
- ***Gases:*** Industrial grade CO₂ and compressed air were used to create the contaminated gas mixture. The gas mixture was roughly 16% CO₂ and balance air.
- ***Gas Diffuser:*** A medium porosity, ASTM standard gas diffuser was purchased for bubbling the gas mixture through the absorbent. The pore diameter of the gas diffuser ranges from 10 – 15 microns

Combined CO₂ Capture and Storage Experimental Set-Up

The experimental set up for the combined CO₂ capture and storage experiments can be seen in Figure 30.

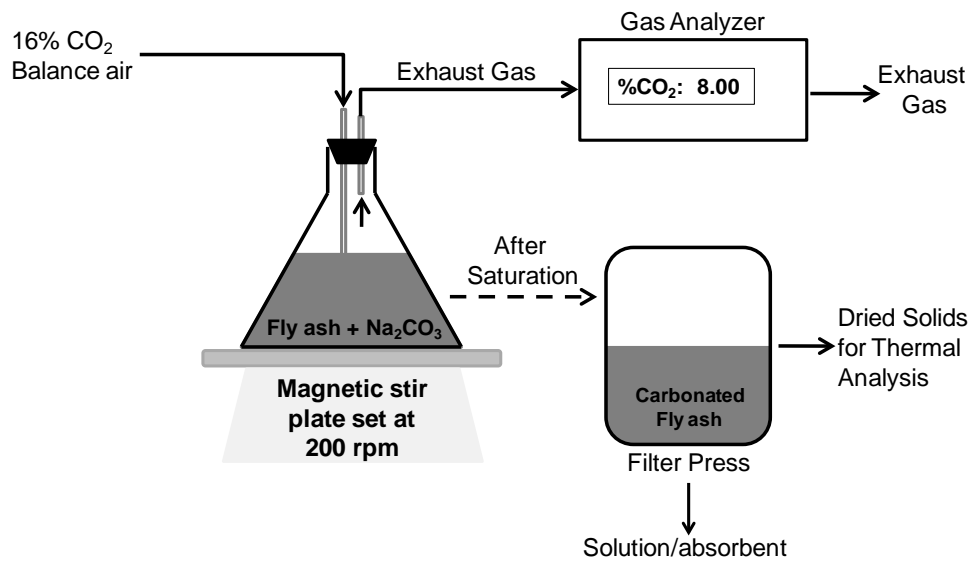


Figure 30: Experimental layout for carbonation experiments. 1 liter Erlenmeyer flask containing the carbonation mixture

The gas composition was set by the volumetric flowrates of CO_2 and air and confirmed by the gas analyzer reading. The gases were then uniformly mixed and bubbled into a 1000 ml Erlenmeyer flask containing 800 grams of distilled H_2O , varying concentrations of Na_2CO_3 (0 and 20 grams/liter), and varying weights of fly ash (0, 20, 40, 80, 160 grams). The Na_2CO_3 concentration (20 g/L) was optimized for CO_2 absorption from previous research[152]. During trials, the mixture was stirred on a magnetic stir plate at 200 rpm to fluidize the fly ash for sufficient contact with the CO_2 . The fly ash and Na_2CO_3 solution were in contact for less than 30 seconds prior to contact with CO_2 . The gas not absorbed by the mixture was exhausted through a flow meter and CAI 600 series infrared gas analyzer to obtain the % CO_2 in the exhaust gas stream. The CO_2 absorption rate was taken as the difference between the CO_2 fed and CO_2 exhausted during this process. The combined CO_2 capture and storage experiments were repeated in triplicate to ensure the accuracy of the data.

Absorption experiments were conducted until the CO₂ concentrations in the feed and exhaust gas streams were equal. This point was termed the “saturation point” and it defines the CO₂ capture/sequestration capacity of the system. After saturation of the mixture, the solids were filtered and dried for 12 hours in a drying oven at a temperature of 105 °C. Dried solids were analyzed for carbonate content using a thermo gravimetric analyzer and X-ray diffraction. The morphology of the solids was analyzed using a scanning electron microscope.

Fly Ash Characterization

The coal fly ash used in this study was received from the Basin Electric Power Cooperative (BEPC) located in Beulah, North Dakota. The fly ash sample was received in a sealed 25 gallon drum. The sample was appropriately split and stored in air tight bags to minimize exposure to atmospheric CO₂. Samples of fly ash were used as received for experiments. The fly ash sample was characterized on site using X-ray diffraction (XRD), thermal gravimetric analysis (TGA), atomic absorption (AA), scanning electron microscopy (SEM), and a particle size analyzer.

X-Ray Diffraction

X-ray diffraction was performed to examine the crystal structure of the fly ash material. The XRD was operated at 45 kV and 35 mA with monochromated Cu K α radiation ($\lambda=1.5406 \text{ \AA}$) at a scan speed of 1.8 sec/step and a step size of 0.02°.

XRD analysis of the raw fly ash material identified calcium sulfate hemihydrate (CaSO₄•0.5H₂O), calcium hydroxide (Ca(OH)₂), calcite (CaCO₃), and silica (SiO₂) as being present in the material. The XRD also showed a broad diffraction peak from 15 to 40 degrees. A broad diffraction peak is characteristic of amorphous solids, which tend to be highly reactive[192].

Thermo Gravimetric Analysis

A thermo gravimetric analysis carried out on the raw fly ash was able to verify the presence of calcium sulfate hemihydrate, calcium hydroxide, and calcite seen with the XRD analysis. From the TGA analysis it was also determined that the raw fly ash sample contained 1.25% CaCO_3 . The TGA procedure used is as follows: all samples were heated in an air atmosphere at an air flow rate of 5 L/min. The sample was first heated from room temperature to 105 °C at a ramp rate of 4 °C per minute and held until completely dry. The sample was then heated from 105 °C to 1000 °C at a ramp rate of 6 °C per minute and held until constancy at 1000 °C.

Atomic Absorption Analysis

Atomic absorption analysis was carried out to determine the amount of calcium present in the raw fly ash sample following ASTM standards D1971-02 (Standard Practices for Digestion of Water Samples for Determination of Metals by Flame Atomic Absorption, Graphite Furnace Atomic Absorption, Plasma Emission Spectroscopy, or Plasma Mass Spectrometry) and D511-09 (Standard Test Methods for Calcium and Magnesium In Water). It was determined that the fly ash sample contained 14.94 % $\text{Ca} \pm 0.26$ %.

Scanning Electron Microscopy Analysis

Scanning electron microscopy was used to examine the morphology of the particles before and after mineral carbonation. From the SEM analysis it was found that the raw fly ash sample had a spherical morphology with minimal surface precipitates.

Particle Size Analysis

Particle size analysis was carried out using a Microtrac SRA particle size analyzer to determine the size distribution present in the fly ash sample. From the particle size analysis it was determined that the 80% passing size of the sample was $36.85 \mu\text{m} \pm 2.05 \mu\text{m}$.

Results and Discussion

Carbon dioxide absorption experiments were carried out to determine the absorption rate of CO_2 into the mixture and to determine the CO_2 capacity of the mixture. All experiments were repeated in triplicate.

Carbon Dioxide Absorption Experiments

The results of the CO_2 absorption experiments can be seen in Figure 31 plotted as the cumulative moles of CO_2 absorbed with respect to time. These curves will herein be termed “saturation curves.” From the saturation curves it is possible to determine the amount of CO_2 absorbed by the solution and the steady state absorption rate of CO_2 into the mixture. The absorption capacity of the mixture/solution was defined as the point when the mixture/solution was no longer absorbing CO_2 , or the curves plateau. The distilled water curve has been carried out to 12 minutes for visual purposes. The CO_2 absorption capacity is on Figure 31 as the last data point on each curve or the beginning of the plateau.

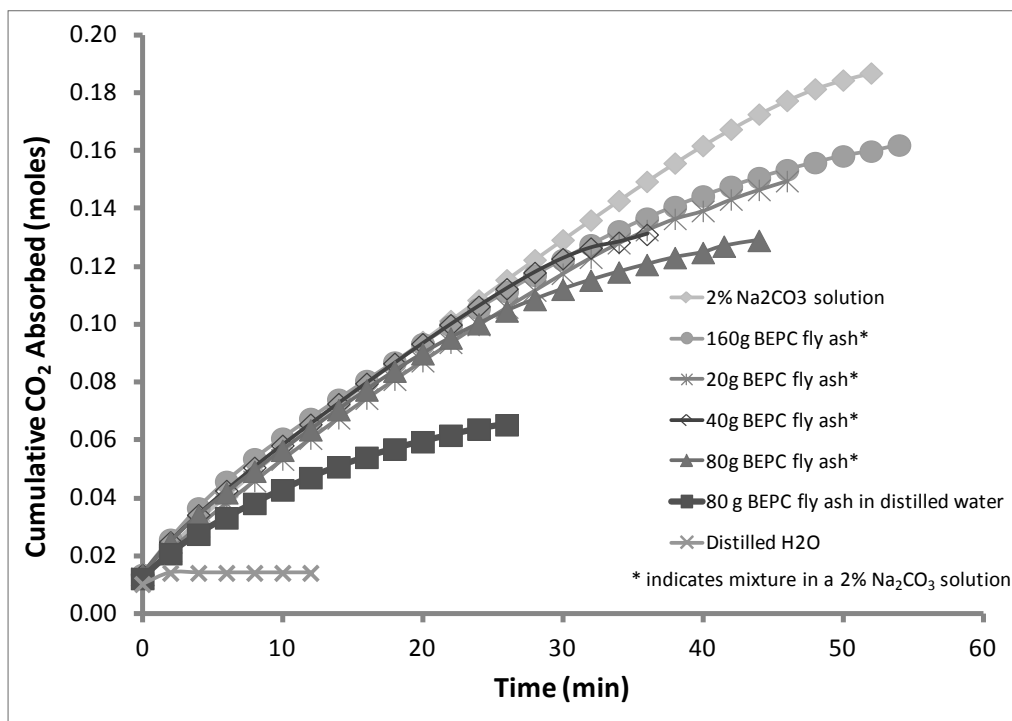


Figure 31: Carbon dioxide absorption in various Na₂CO₃/fly ash mixtures. Constant CO₂ feed rate of 7.42×10^{-3} mol/min CO₂. P = 1 atm, T = 25 °C

Distilled water alone was able to capture 0.014 moles of CO₂, while the 2% Na₂CO₃/distilled water solution was able to capture 0.184 moles of CO₂ before reaching saturation. The addition of Na₂CO₃ increased the amount of CO₂ captured by 1,200%. This means a larger quantity of aqueous CO₂ will be available for contact with the fly ash in solution. Increased CO₂ absorption is seen because the Na₂CO₃ in solution acts to buffer the carbonic acid being formed from the reaction of CO₂ with H₂O[118]. Initially, the solution is at a high pH and consists mostly of carbonate ions. As CO₂ is bubbled through the solution, the hydrogen ions (H⁺) formed from the ionization of carbonic acid consumes the carbonate ions (CO₃²⁻) producing bicarbonate ions (HCO₃⁻). Over time, as the carbonate ions are consumed the pH of the solution decreases until it becomes neutral and can no longer buffer

the formation of H⁺ ions. At this point the solution can no longer capture CO₂. The overall reaction of CO₂ with a Na₂CO₃ solution can be seen in equation 52.



The saturation curves containing fly ash revealed a decrease in CO₂ absorption capacity of the solution for each fly ash/Na₂CO₃ mixture compared to just Na₂CO₃ in solution. It is hypothesized that the reduction in CO₂ capacity is due to carbonate ions being consumed by the calcium ions from the fly ash, thus reducing the buffering capacity of the solution. However, from the figure it is clear that either, a) a considerable amount of the carbonate ions are not being consumed or b) the basicity of the fly ash is contributing to the CO₂ absorption potential of the mixture. If a considerable amount of carbonate ions were being consumed the saturation curves would behave similarly to the saturation curve for 80 g fly ash in distilled water. It should be noted that the fly ash material exhibited alkaline properties; when 80 g was added to distilled water the pH increased to 12.03.

Figure 31 also shows that the addition of fly ash to the Na₂CO₃ solution did not significantly hinder the CO₂ absorption rate. However, the addition of Na₂CO₃ to the fly ash mixtures significantly increased the absorption rate. Comparison between the absorption rates for 80 g fly ash in solution with no Na₂CO₃ and 80 g fly ash with Na₂CO₃ show that the addition of Na₂CO₃ increased the absorption rate by as much as 155%.

In summary, the addition of Na₂CO₃ to the fly ash mixture increased the CO₂ absorption capacity of the solution and the CO₂ absorption rate. The increased CO₂ absorption capacity and rate means the fly ash is being exposed to a larger volume of aqueous CO₂ when Na₂CO₃ is present compared to a traditional aqueous mineral carbonation mixture of fly ash and water.

Mineral Carbonation Analysis

The reacted fly ash samples were analyzed for the formation of calcium carbonate by XRD, for visual confirmation of calcium carbonate precipitation by SEM, and for the amount of CO₂ stored in the sample by TGA. Figure 32 is an example of a XRD plot comparing the crystal structure of an un-carbonated and carbonated fly ash sample.

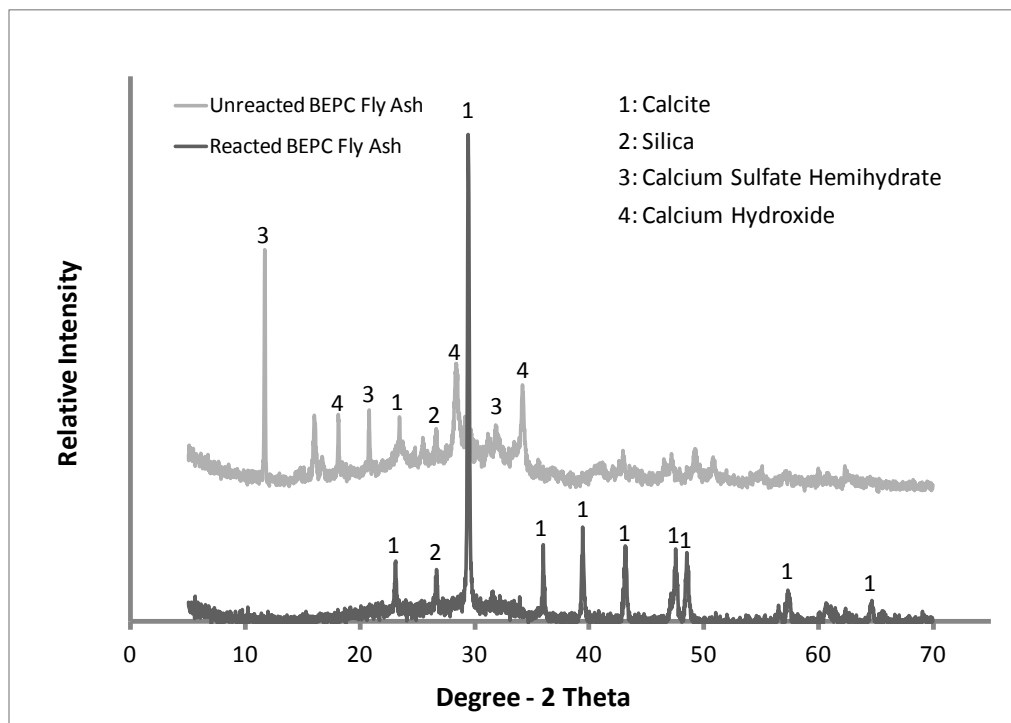
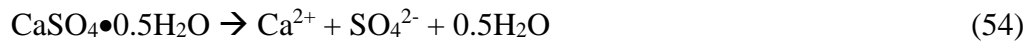


Figure 32: XRD comparison of the BEPC fly ash before and after reaction with CO₂. Calcite is the dominant mineral present in the reacted fly ash. Calcium sulfate hemihydrate and calcium hydroxide are no longer present in the reacted waste.

From Figure 32 it is evident that calcium carbonate, in the form of calcite, was formed during the combined CO₂ capture and storage experiments. No form of magnesium carbonate was found in the carbonated fly ash samples. Magnesium carbonates will typically form under elevated temperatures and pressures [193-195] which are not encountered in our system. From Figure 32 it can also be seen that the reacted fly ash sample no longer contains the minerals calcium sulfate hemihydrate and calcium hydroxide. It is believed that these two mineral compounds are dissolving into solution and contributing calcium ions to the formation of calcite. The dissolution of calcium hydroxide and calcium sulfate hemihydrate can be seen in equations 53 and 54.



The participation of calcium sulfate hemihydrate is unique in that it suggests the possibility that waste gypsum (CaSO₄•2H₂O) could be used for the sequestration of CO₂. To the author's knowledge, studies are not reported in literature that examines the storage potential of gypsum. To confirm the XRD results, fly ash particles were observed under SEM. From the SEM analysis rhomboidal structures were found to be precipitated on the surface of the carbonated fly ash particles. Rhomboidal structures are characteristic of calcite crystallization[196]. An EDS analysis performed on the surface of a carbonated fly ash sphere and a rhomboidal structure found that the sphere contained mostly silica and that the rhomboidal structure was largely calcium, carbon, and oxygen; all elements that comprise calcite. The SEM analysis was able to confirm the XRD analysis and provide insight into the precipitation mechanism of calcite.

Fly Ash Storage Capacity

To determine the experimental CO₂ storage capacity of the fly ash, the thermal decomposition of the calcite formed during carbonation of the fly ash was studied. Literature states that calcite will undergo thermal decomposition from 600 °C to 800 °C[197]. As calcite thermally decomposes it releases gaseous CO₂, as seen in equation 55.



Thus, any weight loss between 600 °C – 800 °C is CO₂ that has been sequestered by the fly ash in the form of calcite. The CO₂ present in the unreacted fly ash sample was subtracted from the value of CO₂ in the reacted fly ash sample to assure that only CO₂ sequestered during the experiments was accounted for. The theoretical amount of CO₂ that could be stored in the fly ash was determined using equations 55 and 56 and the % Ca determined during characterization.



It was determined that the BEPC fly ash has a theoretical CO₂ storage capacity of 0.164 kg CO₂ / kg fly ash. Table 9 gives the experimental CO₂ storage capacity of the reacted fly ash material at varying masses of BEPC fly ash in solution.

| Table 9: Carbon dioxide storage capacity of fly ash during ex-situ mineral carbonation studies with varying liquid to solid ratios. Theoretical storage capacity of fly ash is 0.164 kg CO₂ / kg ash. T = 25 °C P = 1 atm. | | |
|--|--------------------------------|---|
| Na₂CO₃ in Solution (g) | Fly Ash in Solution (g) | Experimental Storage Capacity (kg CO₂ / kg ash) |
| 0 | 80 | 0.012 |
| 16.33 | 20 | 0.093 |
| 16.33 | 40 | 0.099 |
| 16.33 | 80 | 0.067 |
| 16.33 | 160 | 0.048 |

The addition of Na₂CO₃ to solution significantly improved the sequestration of CO₂ via the fly ash. As shown in Figure 31, the addition of Na₂CO₃ allows for more CO₂ to be captured by the solution, thus increasing the amount of CO₂ that comes into contact with the fly ash. Results found that the mixture with 40 g fly ash and 16.33 g Na₂CO₃ had the highest CO₂ storage capacity at 0.099 kg CO₂ / kg ash after roughly 36 minutes. This value is higher than the aforementioned literature values. The equivalent liquid to solid ratio is 20:1 (800 g H₂O:40 g fly ash).

Although the storage capacity of the fly ash was determined to be higher than the aforementioned values in literature, there still needs to be a realistic perspective about the amount of CO₂ which could be sequestered by the fly ash on a daily basis. Assuming a 500 MW coal (90% Carbon and 10% ash[24]) burning power plant emits roughly 12,200 metric tons CO₂ per day[5], almost 3,700 metric tons of coal would need to be combusted to produce that quantity of CO₂. This would result in roughly 370 metric tons of ash per day. Using the optimal results from the

experimental studies (0.099 metric tons CO₂ / metric ton ash) means it would be possible to sequester roughly 36 metric tons of CO₂ per day. This would result in about 0.3% of the total CO₂ emitted per day from a 500 MW coal burning power plant being sequestered via aqueous mineral carbonation by fly ash. Even if the maximum sequestration potential of the fly ash could be achieved it would still result in only 0.5% of the total CO₂ emitted on a daily basis being sequestered. Although the sequestration of CO₂ via mineral carbonation by fly ash is possible, not nearly enough ash is produced on a daily basis to have a significant impact on mitigating CO₂ emissions from coal burning power plants.

Conclusions

From the results obtained it can be concluded that the addition of Na₂CO₃ to solution enhanced the CO₂ absorption capacity of the solution. The amount of CO₂ in solution was increased from 0.014 moles in distilled water to 0.184 moles with the addition of Na₂CO₃ to distilled water. The addition of Na₂CO₃ also had a significant impact on the storage capacity of the fly ash. Without Na₂CO₃ in solution, the storage capacity of the fly ash was 0.012 kg CO₂ / kg ash. When Na₂CO₃ was added to solution the storage capacity of the solution increased to as much as 0.099 kg CO₂ / kg ash. Although the storage capacity of the fly ash was an improvement over literature values, the impact for CO₂ sequestration is negligible. It was determined that the amount of fly ash produced per day from a fossil fuel burning power plant would have the potential to sequester roughly 0.3% of the total CO₂ emitted per day using the present approach. If the max sequestration capacity were achieved the fly ash would still only be able to sequester roughly 0.5% of the total CO₂ emitted on a daily basis.

Acknowledgements

The authors would like to acknowledge the Department of Education, the National Science Foundation, and the ASISC for support of this work.

Chapter 8: A Novel Approach to Carbon Capture and Storage

Abstract

The approach to carbon capture and storage (CCS) presented herein is different from the conventional idea of CCS. The novel approach uses a 2% w/w sodium carbonate solution to capture CO₂ from post combustion flue gas streams, avoiding the hazards associated with amine solutions used in conventional CCS. The CO₂ loaded solution is then reacted with an alkaline industrial waste material, at ambient conditions, to regenerate the carbonate solution and permanently store the CO₂ in the form of an added value carbonate mineral. Conventional CCS makes use of a costly thermal regeneration stage and the underground storage of supercritical CO₂. The objective of the present study was to prove the feasibility of the unique storage stage for proposed approach to CCS. Three coal combustion fly ash materials were chosen as the alkaline industrial waste materials for CO₂ storage and regeneration the absorbent. The goal was to utilize a significant fraction of the fly ash for CO₂ storage while regenerating the absorbent. Studies found that after a five day reaction time 75% utilization of the waste material for CO₂ storage could be achieved, while regenerating the absorbent. The regenerated absorbent exhibited a nearly identical CO₂ absorption capacity and CO₂ absorption rate as a fresh Na₂CO₃ solution.

Introduction

Carbon dioxide capture and storage (CCS) technologies are widely considered to possess the most potential as a near term option for reducing anthropogenic CO₂ emissions from sources such as fossil fuel burning power plants [1, 2]. The implementation of CCS would mitigate environmental risks associated with emitting CO₂ to the atmosphere while allowing for the continued use of fossil fuels until alternative energy technologies mature. However, CCS is sometimes thought of as just an “insurance” policy for reducing CO₂ emissions because of the high operating cost [3]. At the current state of technological development, one cost estimate predicts a carbon price/tax of \$60-65 per metric ton of CO₂ before installation of a CCS system would be economical [4]. To add perspective to that value, on average, a 500 MW fossil fuel burning power plant emits 8,000 metric tons of CO₂ per day [5, 6].

Herein, the authors propose a novel approach to CCS using carbonate solutions as the absorbent for post combustion capture of CO₂ and alkaline industrial waste materials for the permanent storage of CO₂ and regeneration of the absorbent. The novel aspect of the proposed approach is that thermal regeneration is not used to regenerate the absorbent, as is the case with the commercially available technology, amine absorption systems [7-9]. In the current approach, the CO₂ loaded solution will be reacted with an industrial waste material, at ambient conditions, to permanently store the captured CO₂ in the form of a carbonate mineral while simultaneously regenerating the carbonate solution.

Background

In commercially available CCS technology, the CO₂ contaminated gas stream is fed to an absorption column where the CO₂ is absorbed from the gas stream by an amine solution. A CO₂ depleted exhaust gas stream leaves out the top of the

absorption column and a CO₂ loaded solution exits out the bottom. The CO₂ loaded solution is then sent to a stripping column where the solution is heated (between 100-200 °C) to desorb high purity CO₂ and regenerate the amine solution [2, 10-12]. The high purity CO₂ is then compressed to a supercritical state (11-14 MPa [13]) and transported, typically via pipeline, for storage in an underground reservoir.

This process has several disadvantages associated with it. The most common amine used for absorption is monoethanolamine (MEA). MEA is highly hazardous, highly volatile, corrosive, degrades in the presence of oxygen and other flue gas impurities (NO_x and SO_x), and it is costly (\$1.25/kg [14]). The regeneration stage requires heating large volumes of absorbent anywhere from 100-200 °C and compression of the high purity CO₂ to a supercritical state for transportation. [10-12]

The proposed approach to CCS is different from the conventional approach to CCS described above. A block diagram of the proposed approach to CCS can be seen in Figure 33.

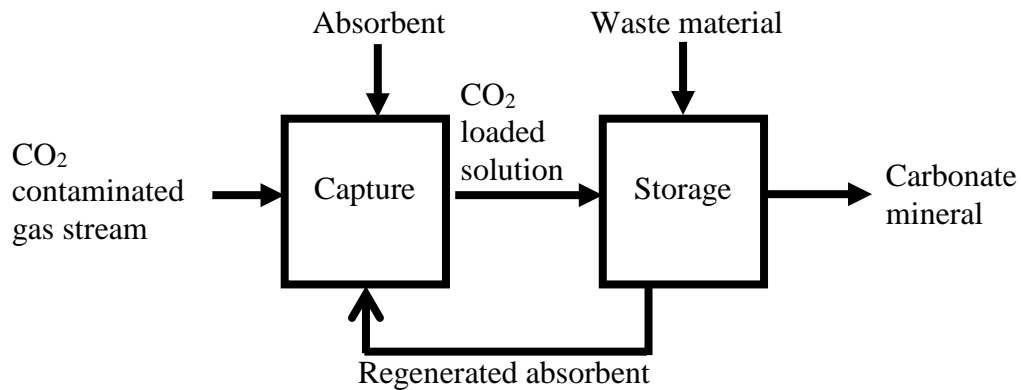


Figure 33: Flow diagram for the proposed carbon dioxide capture and storage process. The proposed process aims to eliminate the need for thermal regeneration of the absorbent

In the proposed approach to CCS, the capture stage is similar to the aforementioned amine capture stage except a Na_2CO_3 solution is used instead of an amine solution. After CO_2 capture, the CO_2 loaded solution is fed to a stirred tank reactor where it is reacted with an alkaline industrial waste material, at ambient conditions, to regenerate the absorbent and to permanently store the CO_2 as an added value carbonate mineral. After reaction, the carbonate mineral is filtered from the solution forming a regenerated absorbent that can be reused to capture more CO_2 .

The proposed CCS system has many advantages over the commercially available technology. The carbonate based solution is considered non-hazardous, has a low volatility, is non-fouling, has a low equipment corrosion rate, low raw material costs (\$0.11/kg [15]), and the possibility for use as a multi pollutant capture system (NO_x , SO_x , and CO_2 removal) [16]. Operating costs of the system are likely to be lower than that of the amine system due to operation at ambient conditions and no need for gas compression. The theory behind the proposed approach to CCS will be discussed in more detail.

Carbon Dioxide Capture

Capture of CO_2 by carbonate solutions is an acid-base reaction, seen in Eqns. (57)-(59). First, the gaseous CO_2 is preferentially absorbed from the gas stream into the carbonate solution becoming aqueous CO_2 , Eq. (57).



Once in the aqueous form CO_2 will hydrolyze to bicarbonate, carbonate (CO_3^{2-}), and hydrogen (H^+) ions depending upon pH, seen in Eqs. (58) and (59). At a pH above 10.5 carbonate ions will dominate in solution (Eq. (59)), below 10.5 bicarbonate ions will dominate (Eq. (58)). A carbonate solution will initially have a pH greater than 11.00 and consist predominantly of CO_3^{2-} ions. [142]



As CO₂ is absorbed the solution pH steadily decreases. In CO₂ absorption into carbonate solutions, the CO₃²⁻ ions added to solution buffer the hydrogen ions formed when CO₂ hydrolyzes. This leads to gaseous CO₂ being captured in the form of bicarbonate ions, the reverse of Eq. (59). This occurs until the pH of the solution becomes neutral and can no longer buffer the H⁺ ions. When pH neutralizes, the solvent can no longer capture CO₂. The bicarbonate solution (or CO₂ loaded solution) is then reacted with the industrial waste material for permanent storage of the captured CO₂ and regeneration of the solution.

Carbon Dioxide Storage

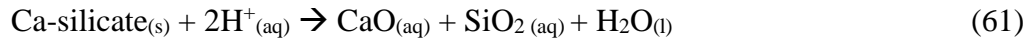
Accelerated CO₂ storage is carried out utilizing the fundamentals of mineral carbonation. The basic concept behind mineral carbonation is that of natural rock weathering. In weathering, gaseous CO₂ reacts chiefly with solid calcium and magnesium containing minerals to form thermodynamically stable and environmentally benign carbonate compounds, Eq. (60) [178-182].



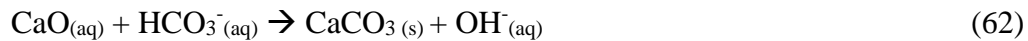
The gas-solid reaction seen in Eq. (60) takes place over hundreds to thousands of years, much too slow for use on an industrial scale. Thus, aqueous mineral carbonation has been used to substantially increase the rate of carbonation [182].

The mechanism for aqueous mineral carbonation of a calcium silicate mineral (Ca-silicate) in a bicarbonate solution can be seen in Eqs. (61) and (62) [182]. In the

first stage of carbonation, Eq. (61), the calcium ions needed for carbonation are leached from the silicate mineral. At this stage a low pH is desirable to promote the leaching of calcium ions from the solid material to the bulk solution.



The hydrogen ions present in solution after CO₂ absorption accelerate the leaching of the calcium ions from the silicate. The reaction between the Ca-silicate and H⁺ ions produces calcium oxide (CaO), silica (SiO₂), and water (H₂O). In the second stage of carbonation, Eq. (62), the CaO produced in the first stage will react with the bicarbonate ions in solution (the captured CO₂).



Upon reaction of the calcium oxide with the bicarbonate ions solid calcium carbonate (CaCO₃) and hydroxide (OH⁻) ions are formed. The capture CO₂ is effectively stored in the form of calcium carbonate and the buffering capacity of the solution is recovered through the formation of hydroxide ions. [182]

Possible feedstock for the storage stage include naturally occurring minerals such as wollastonite, or industrial waste materials such as cement kiln dust, waste cement, asbestos tailings, nickel tailings, red mud, coal fly ash, oil shale ash, and alkaline paper mill waste [185-191]. Wollastonite has been thoroughly studied as a carbonation feedstock [194, 198]. Although successful to a degree, the use of naturally occurring minerals for permanent CO₂ storage can be costly. Minerals must be mined, crushed, and pretreated to make them more reactive before use. Many industrial wastes are easily accessible (stored on site), already in the powdered form, and highly reactive owing to their amorphous structure [185]. For this reason, the use of industrial waste materials as a carbonation feedstock has

gained attention. This article will focus on coal fly ash as a mineral carbonation feedstock. Coal fly ash is a promising waste material as it is produced at large CO₂ point sources (coal combustion power plants), cheap, in powdered form, and high in calcium content.

The goal of the present work was to study the feasibility of the proposed CCS system. The initial capture stage of this system has already been explored in detail in previous work [148, 167, 199]. The article is divided into two sections. The first section of the article examines the storage stage of the system. Storage of the captured CO₂ was carried out via aqueous mineral carbonation with three coal combustion fly ash materials. The objectives of the first section are as follows:

- Examine the mineral carbonation kinetics with respect to the three fly ash materials,
- Determine what is controlling the rate of mineral carbonation in the materials, and
- Compare the experimental CO₂ storage capacity of the materials to the theoretical CO₂ storage capacity.

The second section examines the potential of the materials for regenerating the original absorbent. Regenerative potential is based on if the fly ash material can recoup the pH of the initial capture solution during the carbonation reaction while still storing a significant amount of CO₂.

- Determine if the fly ash materials can regenerate the original absorbent and, if so, determine a time frame for regeneration to occur, and
- Compare CO₂ absorption in a fresh carbonate solution to the regenerated solution created during storage.

Materials and Methods

Materials used in the present study include:

- **Sodium Carbonate (Na_2CO_3):** The Na_2CO_3 was granular, anhydrous, ACS reagent grade purchased from Sigma Aldrich with a purity of greater than or equal to 99.5% Na_2CO_3 .
- **Sodium bicarbonate ($NaHCO_3$):** $NaHCO_3$ was ACS reagent grade with a purity in the range of 99.7-100.3 %. Purchased from MACRON Chemicals.
- **Distilled H_2O :** Distilled H_2O was mixed with the Na_2CO_3 to create the carbonate solution.
- **Gases:** Industrial grade CO_2 and compressed air were used to create the contaminated gas mixture. The gas mixture was roughly 16% CO_2 and 84% air.
- **Gas Diffuser:** A medium porosity, ASTM standard gas diffuser was purchased for bubbling the gas mixture through the absorbent. Pore diameters of the gas diffuser range from 10 – 15 microns.

Mineral Carbonation Feedstock Characterization

Materials chosen as feedstock for mineral carbonation include three different coal fly ashes. The three fly ash materials were received from Basin Electric Power Cooperative (BEPC), Great River Energy (GRE), and Minnesota Power (MN Power). The fly ash samples split into 1.5 – 2 kg samples and sealed in air tight bags to limit exposure to atmospheric CO_2 during storage. All materials were used as received.

An in-depth characterization of the materials was performed utilizing:

- **Atomic absorption (AA):** Atomic absorption analysis was carried out to determine the amount of calcium present in the raw fly ash sample following ASTM standards D1971-02 (Standard Practices for Digestion of Water Samples for Determination of Metals by Flame Atomic Absorption, Graphite Furnace Atomic Absorption, Plasma Emission Spectroscopy, or Plasma Mass Spectrometry) and D511-09 (Standard Test Methods for Calcium and Magnesium In Water).
- **X-ray diffraction (XRD):** X-ray diffraction was performed to examine the mineralogy of the materials. The XRD was operated at 45 kV and 35 mA with monochromated Cu K α radiation ($\lambda=1.5406 \text{ \AA}$) at a scan speed of 1.8 sec/step and a step size of 0.02 $^\circ$.
- **Thermo gravimetric analysis (TGA):** A thermo gravimetric analysis carried out on the materials to determine if calcium carbonate was inherently present. All samples were heated in an air atmosphere at an air flow rate of 5 L/min. The samples were first heated from room temperature to 105 $^\circ\text{C}$ at a ramp rate of 4 $^\circ\text{C}$ per minute and held until completely dry. The sample was then heated from 105 $^\circ\text{C}$ to 1000 $^\circ\text{C}$ at a ramp rate of 6 $^\circ\text{C}$ per minute and held until constancy at 1000 $^\circ\text{C}$.
- **Particle size analysis:** Particle size analysis was carried out to determine the size distribution for each material. Particle size results are presented as the 80% passing size, P₈₀.

Table 10 is a summary of results obtained during characterization of the carbonation feedstock materials.

Table 10
Characterization summary for the carbonation feedstock materials used in the study

| Feedstock Material | % Calcium | Mineralogy | % CaCO₃ | Particle Size, P₈₀ (µm) |
|---------------------------|---------------------|--|---------------------------|---|
| BEPC fly ash | 14.94 (+/- 0.26) | Calcium sulfate hemi-hydrate, calcite, silica, calcium hydroxide | 1.5 | 36.85 (+/- 2.05) |
| GRE fly ash | 11.57 (+/- 0.34) | Amorphous material | 0 | 37.71 (+/- 0.33) |
| MN Power fly ash | 12.20 (+/- 0.90) | Quartz and amorphous material | 0 | 23.88 (+/- 0.23) |

Fly ash materials were received in the powdered form and used as received.

Calcium content of the fly ash materials varied from 11.57% for GRE to 14.94% for BEPC. No two fly ash materials tested shared the same mineralogy. The differences in mineralogy could lead to significantly different behavior during carbonation. For example, the soluble compounds present in BEPC fly ash, calcium sulfate hemihydrate ($\text{CaSO}_4 \cdot 0.5\text{H}_2\text{O}$) and calcium hydroxide ($\text{Ca}(\text{OH})_2$), may contribute easily accessible calcium ions for carbonation. Calcium carbonate, in the form of calcite, was only detected in the BEPC fly ash. The inherent value of calcite found was subtracted from the calculated value of calcium carbonate formed after the carbonation reaction. This was done so only calcium carbonate formed during the carbonation reaction was accounted for. The 80% passing size for the fly ash materials were all very similar, ranging from 23.88 μm for the MN Power fly ash to 37.71 μm for the GRE fly ash.

Carbon Dioxide Capture Experiments

The experimental set-up used for CO_2 capture experiments can be seen in Figure 34. The set-up is well suited for measuring the CO_2 absorption capacity and CO_2 absorption rate of the absorbent.

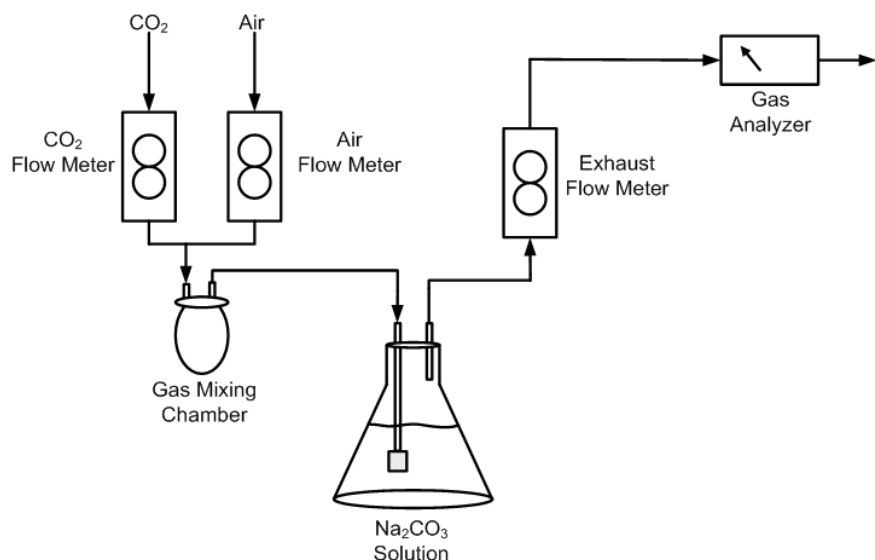


Figure 34: Experimental set-up for carbon dioxide capture experiments. Set-up allows for simple calculation of the CO₂ absorption capacity and CO₂ absorption rate of the solution. System is operated at ambient temperature and pressure.

The %CO₂ in the gas stream was controlled by using separate CO₂ and air flow meters to monitor the volumetric flow rates. The gas mixture was set to contain 16% CO₂. The gases were then sent to a gas mixing chamber to assure uniform composition of the gas entering the absorption flask. Once mixed, the gas was bubbled into a 1000 ml Erlenmeyer flask containing a 20 g/L Na₂CO₃ solution or the regenerated solution. Previous studies found that a 20 g/L Na₂CO₃ solution was ideal for the current system. The 20 g/L solution offered the best tradeoff between the CO₂ absorption rate and CO₂ capacity of the solution [148]. The gas not absorbed by the solution was emitted out of the flask to an exhaust gas flow meter to record the exit volumetric flow rate of the gas. After the flow meter, the gas was passed through a CAI 600 series infrared gas analyzer to obtain the %CO₂ in the exhaust gas stream. The CO₂ absorption rate was taken as the difference between the CO₂ fed and CO₂ exhausted during this process. Absorption experiments were conducted until the CO₂ concentrations in the feed and exhaust gas streams were equal. This point was termed the “saturation point” and it defines the CO₂ capture

capacity of the solution. CO₂ absorption rate measurements were repeated in triplicate to ensure the accuracy of the data.

Mineral Carbonation Experiments

The fly ash materials were reacted with the CO₂ saturated solution for reaction times of 5, 10, 15, and 20 minutes, and two weeks, in a sealed 500 ml beaker at a stir rate of 240 rpm. The pH of the solution was recorded before addition of the fly ash and after the carbonation reaction was stopped. After the desired reaction time was completed, the solids were filtered from solution, dried at 105 °C for 12 hours, and then analyzed for calcium carbonate content using the TGA procedure described above. In the case of the regeneration studies, the solution left over after filtration was immediately saturated with CO₂. The values for the CO₂ absorption rate and CO₂ absorption capacity of the solution were compared to the original solution. TGA analysis made it possible to determine the total calcium carbonate that was formed during the storage stage. From the value of calcium carbonate formed it was possible to determine the % calcium reacted over time and the CO₂ storage capacity of the fly ash materials. Literature states that calcite, the only form of calcium carbonate seen in the present study, will undergo thermal decomposition from 600 °C to 800 °C [197]. As calcite thermally decomposes it releases gaseous CO₂ and forms solid calcium oxide, as seen in Eq. (63).



Any weight loss between 600 °C – 800 °C is attributed to CO₂ that has been stored in the form of calcite. Thus, using Eq. (63) and the weight loss due to evolved CO₂, it is possible to back calculate the amount of calcium carbonate that was formed during carbonation. The inherent CO₂ present in the BEPC fly ash sample was subtracted from the value of CO₂ in the carbonated sample to assure that only CO₂ stored during the experiments was accounted for.

As a time saving measure, a sodium bicarbonate solution was created to mimic a CO₂ saturated Na₂CO₃ solution for the carbonation experiments at reaction times of 5, 10, 15, and 20 minutes. For the regeneration studies a fresh Na₂CO₃ solution was saturated with CO₂ and used as the aqueous media. This was so the absorption of CO₂ into the regenerated solution could be compared directly to CO₂ absorption in the original solution. The fly ash material was added to solution so that calcium would be the limiting reagent in the carbonation reaction, Eq. (62). This allowed for the possibility that 100% of the material could be carbonated. The total calcium present in the fly ash added to solution totaled 0.89 grams.

Results and Discussion

The results and discussion is broken down into three sections. The first two sections examine the storage of CO₂ via mineral carbonation with the fly ash materials. Of particular importance are the reaction kinetics and the CO₂ storage capacity of the materials. The third section studies the potential of the materials to regenerate the original carbonate solution.

Mineral Carbonation Kinetics

Figure 35 is a comparison of the reaction kinetics for the fly ash materials studied. Plotted is the % Ca reacted vs time for 5, 10, 15, and 20 minute reaction times. The slope of the curves gives a general idea to the rate of the carbonation reaction.

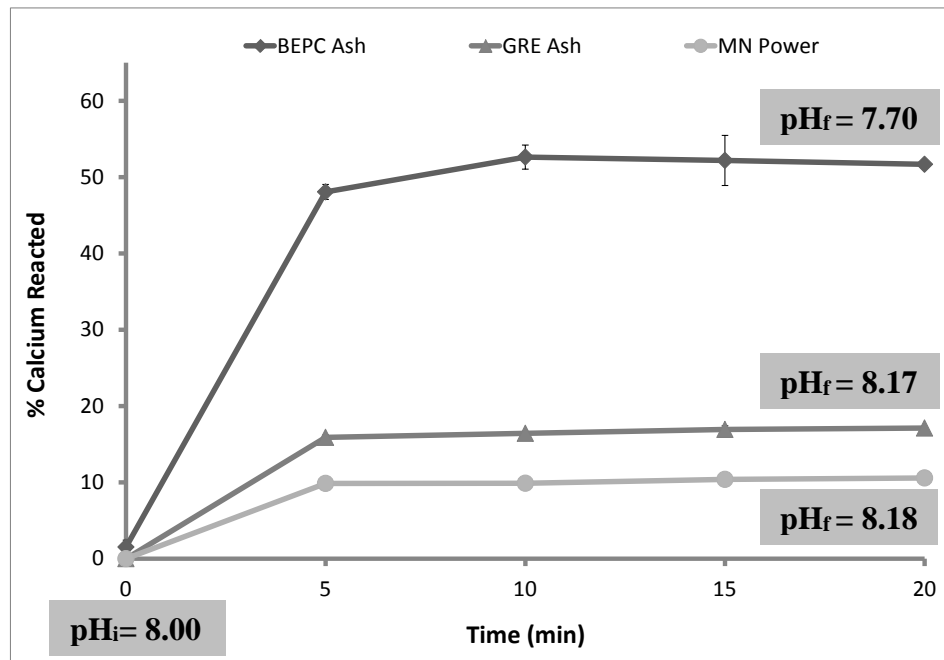


Figure 35: % Calcium reacted vs. time for the fly ash materials used as carbonation feedstock. BEPC fly ash exhibited the fastest initial reaction kinetics (0-5 min). Weight of fly ash added to solution equaled 0.89 grams of calcium.

After a reaction time of five minutes with the CO₂ loaded solution a significant difference in the reaction rate is seen between the BEPC fly ash with respect to the GRE and MN Power fly ash materials. This difference in rate could be attributed to the differences in mineralogy of the materials. Characterization revealed that the BEPC fly ash contained calcium hydroxide (solubility of 1.73 g/L at 20 °C) and calcium sulfate hemihydrate (slightly soluble in water). These soluble compounds provide easily accessible Ca²⁺ ions for carbonation of the dissolved CO₂. The dissociation of calcium sulfate hemihydrate (CaSO₄·0.5H₂O) will also produce an abundance of sulfate ions (SO₄²⁻) in solution. It is possible that the sulfate ions in solution could limit the CO₂ storage capacity of the fly ash. The effect of sulfate ions on the system will be discussed in more detail later in the article. Characterization of the GRE and MN Power fly ash materials did not reveal the presence of any soluble material. It's possible then that the initial reaction kinetics

are controlled largely by the diffusion of calcium ions from the fly ash particles to the bulk solution.

Figure 35 also shows that the carbonation reaction has two distinct reaction kinetic zones over the 20 minute reaction time. The first zone, from 0-5 minutes, corresponds to a fast initial reaction rate. The second zone, from 5-20 minutes, corresponds to a slow rise in the reaction rate for the GRE and MN Power fly ash and a slow decrease in the rate for the BEPC fly ash. It is important to understand what is controlling the reaction rate in both of these zones. Investigation found that the initial reaction rate was strongly dependent upon the percentage of soluble material present. The BEPC fly ash contained roughly 75% more soluble material than the MN Power fly ash and 50% more than the GRE fly ash. Neither the MN Power nor GRE fly ash contained any form of calcium sulfate or calcium hydroxide, which contributed to the high solubility of the BEPC fly ash.

For the GRE and MN Power fly ash, the second zone showed very slow rate of storage and may be controlled by the mass transfer rate of calcium ions from the solid fly ash particles to the bulk solution. Literature has shown that a pretreatment stage such as heat activation, surface activation (steam or chemical), or further crushing and grinding could be used to improve upon the mass transfer rate of calcium ions from the material to the bulk solution [180, 182, 183]. Pretreatment is not explored in the present work because any additional processing of the fly ash material would lead to an increased cost of mineral carbonation. Unlike the GRE and MN Power fly ash, the BEPC fly ash exhibited a slight decrease in the storage rate over the second zone. The decrease in rate may be caused by the decrease in solution pH over time, as seen in Figure 35 (the initial solution pH was 8.00 and the final solution pH was 7.70). The addition of BEPC fly ash to solution caused the pH to drop below eight after 20 minutes of reaction with the bicarbonate solution. Carbonate equilibrium states that as solution pH drops, bicarbonate ions will

become more favorable in solution than carbonate ions [142]. It's possible that the addition of a base, such as calcium hydroxide, could increase the carbonation rate. In the proposed approach to CCS, the role of the fly ash is to increase the solution pH to regenerate the absorbent. Thus, addition of a base to the solution was not examined.

Results from Figure 35 show that it is possible to react a significant amount of the fly ash with the dissolved CO₂ on a relatively short time scale.

Carbon Dioxide Storage Capacity

The storage capacity of a material can be defined as the mass of CO₂ stored, in the form of a carbonate mineral, per mass of material added to solution. The amount of CO₂ a material can store is important when considering the quantity of material needed to store a given mass of CO₂. Figure 36 is a comparison of the storage capacities for the fly ash materials tested after a 20 minute and two week reaction time with the CO₂ saturated carbonate solution. The figure compares experimental values to the calculated theoretical storage capacity based off the %Ca of the material obtained during characterization. The two week experiments were conducted to better understand the mechanisms behind carbonation for each fly ash. The pH of the solutions was also monitored to determine if any of the fly ash materials could regenerate the absorbent.

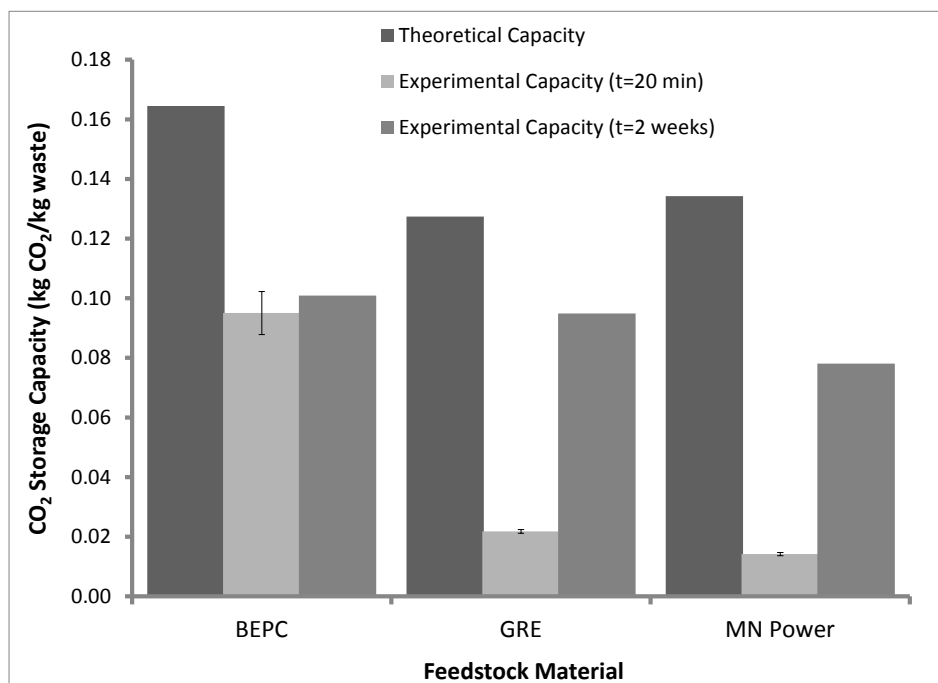


Figure 36: Carbon dioxide storage capacities for the fly ash materials after a 20 minute and two week reaction time with the CO₂ saturated solution. Weight of fly ash added to solution equaled 0.89 grams of calcium.

After a 20 minute reaction time the BEPC fly ash exhibited the highest CO₂ storage capacity (0.095 g CO₂/g waste) out of the three fly ash materials. The higher storage capacity of the BEPC fly ash can be attributed to the presence of the soluble minerals calcium sulfate hemihydrate and calcium hydroxide in the material. The GRE and MN Power fly ash materials exhibited significantly smaller CO₂ storage capacities after a reaction time of 20 minutes than BEPC fly ash. The mass transfer of the calcium ions from the fly ash particles is likely to be limiting the initial storage capacity of the GRE and MN Power fly ash materials. Results suggest that an ash similar in mineralogy to BEPC fly ash would be best for storage on short time scales (order of minutes), although, the reduction in the solution pH over the 20 minute reaction time is not promising for regeneration of the absorbent.

After two weeks, the CO₂ storage capacity of the MN Power and GRE ashes significantly increased. The longer reaction time allowed for the calcium ions to diffuse out of the fly ash particles and react with the solution. This supports the previous assumption that the kinetics of MN Power and GRE fly ash materials are limited by the mass transfer of calcium ions from the particles to the bulk solution. Unlike the GRE and MN Power fly ash, the BEPC fly ash showed a negligible change in capacity after the two week reaction time. The negligible increase in capacity could be because of two reasons; (1) the decrease in in solution pH is limiting the availability of carbonate ions in solution to drive the carbonation reaction or (2) all the calcium ions available for carbonation are being consumed within the first 20 minutes of the carbonation reaction. Further studies are needed to determine the true cause. Results show that ashes similar GRE and MN Power fly ash possess significant potential for CO₂ storage at longer reaction times (order of days) with potential for absorbent regeneration.

Regenerative Capabilities

For the present study, the fly ash material was said to possess regenerative potential if during the carbonation reaction the pH of the solution became greater than or equal to that of the initial carbonate solution (pH \geq 11). Solution pH measurements can be seen in Figure 37 for the 5-20 minute reaction times.

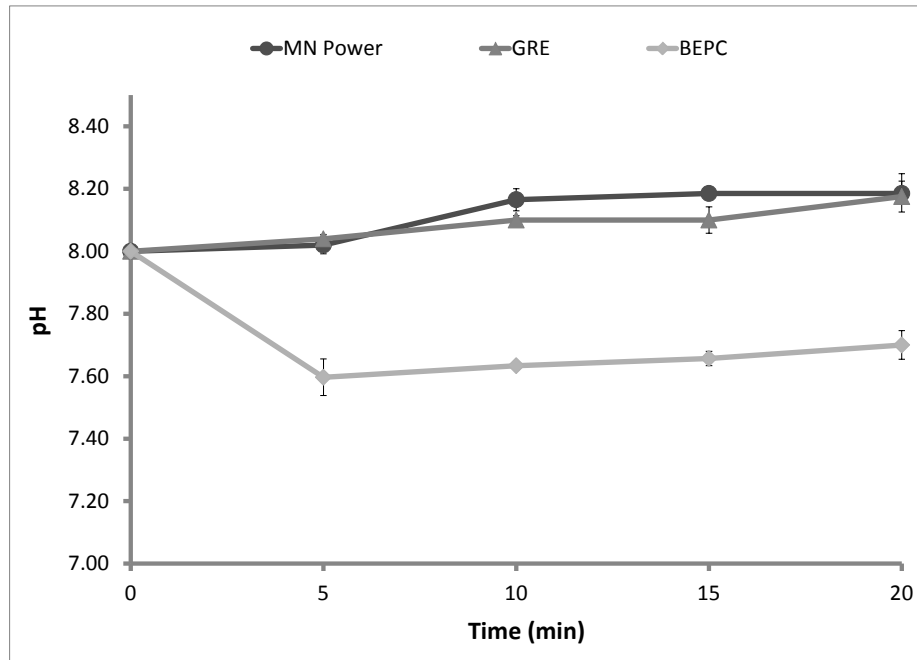


Figure 37: Solution pH during the carbonation reaction for different fly ash materials. BEPC fly ash appeared to form an acidic compound during the carbonation reaction, evident by the decrease in pH.

The BEPC fly ash caused a reduction in the pH of the solution during the carbonation reaction. This implies that during the carbonation reaction the BEPC fly ash was producing an acidic compound. It's possible that the sulfate ions produced during the dissolution of calcium sulfate hemihydrate (seen in Eq. (8)) could be reacting with the hydrogen ions in solution to form sulfuric acid (H_2SO_4), Eq. (64).



The GRE and MN Power fly ash slightly increased the pH of the solution after a reaction time of 20 minutes. This suggests that the GRE and MN Power fly ash

may possess the potential to recover the pH of the original solution at increased reaction times.

A summary of the results from the two week reaction time study using the three fly ashes can be seen in Table 11. For the two week reaction time studies, a 2:1 molar ratio of Ca:HCO₃⁻ ions was in solution to ensure enough calcium would be present for regeneration. Even at an increased reaction time, the BEPC fly ash only increased the solution pH to about 9.00. Although the BEPC fly ash sequestered CO₂ rapidly, the solvent could not be recovered. Thus, it appears that materials containing a form of calcium sulfate are not desirable for present approach to CCS. After a reaction time of two weeks, the GRE and MN Power fly ash increased the solution pH to 12.34 and 11.66. The increase in pH implies that the calcium is reacting with the bicarbonate solution to create hydroxide ions in solution over an extended period of time, as seen in Eq. (62). The two week studies suggest that the GRE or MN Power fly ash could possibly be used to regenerate the absorbent and permanently store the CO₂.

| Table 11 Results from mineral carbonation experiments carried out for two weeks | | | |
|--|--------------------------|----------------------------|--------------------------|
| Waste Material | % Calcium Reacted | Initial Solution pH | Final Solution pH |
| BEPC fly ash | 57.38 | 8.00 | 8.99 |
| GRE fly ash | 74.57 | 8.00 | 12.34 |
| MN Power fly ash | 58.16 | 8.00 | 11.66 |

Based upon the two week study, the GRE fly ash was chosen to further study regeneration of the original carbonate solution. The GRE fly ash was chosen because it was able to increase the solution pH the most over the two week reaction time and exhibited the highest % calcium reacted (74.57%). Further experimentation revealed that after a reaction time of five days the GRE fly ash was able to increase the solution pH to 12.00, indicating complete regeneration. To test if the solution was indeed regenerated, the solids were filtered out of solution and the remaining solution was saturated with CO₂. The results were compared to CO₂ absorption in a fresh Na₂CO₃ solution. Figure 38 is a comparison of the moles of CO₂ absorbed versus time between a fresh Na₂CO₃ solution and the regenerated solution.

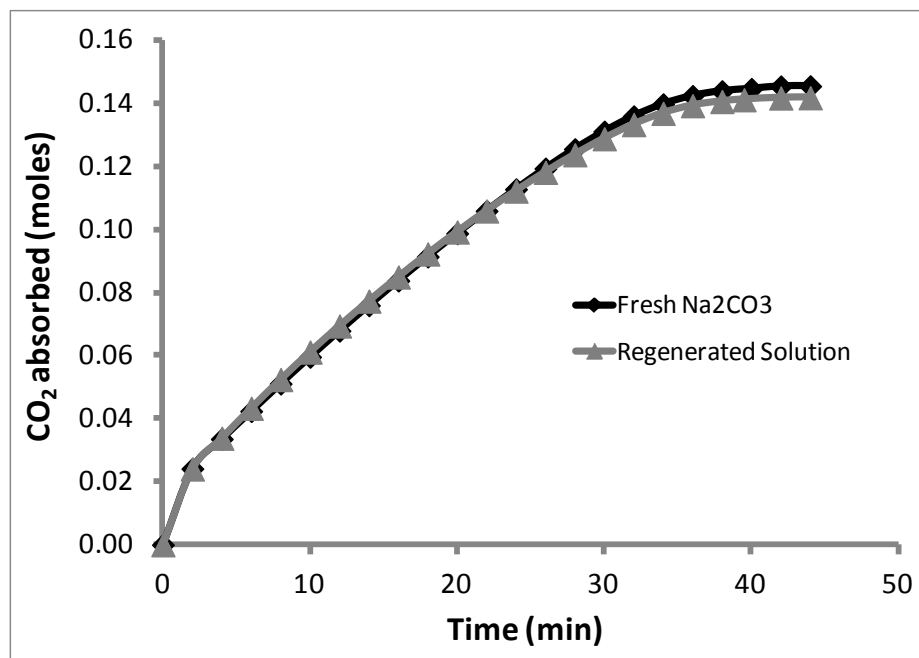


Figure 38: Carbon dioxide absorption results for the fresh Na₂CO₃ solution and regenerated solution. Absorption curves are almost identical, indicating the solution was able to be regenerated. Fresh Na₂CO₃ solution is 2% w/w.

In Figure 38, the last set of data points for each curve is the CO₂ absorption capacity of the solution (in moles) and the slope of the curves is the absorption rate (moles/minute). Results show that the regenerated solution had a similar CO₂ absorption capacity (roughly 0.14 moles of CO₂) and CO₂ absorption rate to the fresh Na₂CO₃ solution. Results from the CO₂ absorption experiments show that the regenerated solution was able to capture a similar quantity of CO₂ at a nearly identical rate as the original carbonate solution.

The present results have demonstrated the feasibility of using an alkaline industrial waste material to simultaneously regenerate a carbonate absorbent while permanently storing CO₂ as a value added carbonate mineral. Future analysis will be focused on determining the composition of the regenerated solution, methods to

improve upon the rate of carbonation, and performance of the regenerated solvent after several regeneration cycles.

Conclusions

The current work has demonstrated that the novel approach to CCS described herein is feasible. In the novel approach, CO₂ was captured from a gas stream using a 2% w/w carbonate solution. The CO₂ loaded solution was then reacted with an alkaline industrial waste material to regenerate the carbonate solution and permanently store the CO₂ in the form of a carbonate mineral. The current study focused largely on the storage/regeneration stage as CO₂ capture in Na₂CO₃ solutions has been thoroughly studied in previous work by the authors.

Due to the presence of the soluble compounds calcium sulfate hemihydrate and calcium hydroxide, the BEPC fly ash exhibited the fastest reaction kinetics (50% calcium reacted) and largest CO₂ storage capacity (0.095 g CO₂/g waste) between the fly ash materials after a 20 minute reaction time. However, on a longer time scale (14 days) the BEPC fly ash was unable to regenerate the original absorbent. It is believed that the sulfate ions formed during the dissociation of the calcium sulfate hemihydrate were reacting with free hydrogen ions in solution to form sulfuric acid. The formation of an acidic compound resulted in the BEPC fly ash being unable to regenerate the absorbent.

The GRE and MN Power fly ash materials showed little potential for regeneration of the absorbent and permanent storage of the CO₂ after a 20 minute reaction time with the CO₂ loaded solution. After a two week reaction time, however, both fly ash materials displayed a significant increase in CO₂ storage capacity and the potential for regeneration of the solution. After the two week reaction time the GRE ash was able to increase the solution pH to 12.34 and achieve 74% calcium reacted. The MN Power fly ash increased solution pH to 11.66 and achieved 58% calcium

reacted. The GRE fly ash was selected to further study the absorbent regeneration because of its ability to achieve a higher solution pH and % calcium reacted after the two week reaction time. Further studies found that after a five day reaction period the GRE fly ash was able to regenerate the absorbent (a solution pH of 12 was reached). Carbon dioxide absorption experiments, using the regenerated solution, showed no reduction in the CO₂ absorption capacity or absorption rate in comparison to the original Na₂CO₃ solution. Thus, it was concluded that regeneration of the original solution was possible using an alkaline industrial waste material, such as fly ash.

Chapter 9: Reference List

1. Metz, B., et al., *IPCC Special Report on Carbon Dioxide Capture and Storage*, 2005, Intergovernmental Panel on Climate Change: Cambridge, United Kingdom and New York. p. 107-171.
2. Yang, H., et al., *Progress in Carbon Dioxide Separation and Capture: A Review*. *Journal of Environmental Sciences*, 2008(20): p. 14-27.
3. Herzog, H.J. and E.M. Drake, *CARBON DIOXIDE RECOVERY AND DISPOSAL FROM LARGE ENERGY SYSTEMS*. *Annual Review of Energy and the Environment*, 1996. **21**: p. 145-166.
4. Herzog, H.J., *Scaling up carbon dioxide capture and storage: From megatons to gigatons*. *Energy Economics*, 2011. **33**(4): p. 597-604.
5. EPA, U.S. *Air Emissions*. 2007 [cited 2012 June 13]; Available from: <http://www.epa.gov/cleanenergy/energy-and-you/affect/air-emissions.html>.
6. EPA, U.S. *Clean Energy: Calculations and References*. 2012 [cited 2012 May 01]; Available from: <http://www.epa.gov/cleanenergy/energy-resources/refs.html>.
7. Fluor. *Fluor: Econamine FG PlusSM*. 2012 [cited 2012 March 28]; Available from: <http://www.fluor.com/econamine/Pages/default.aspx>.
8. Mitsubishi Heavy Industries, L. *KM CDR Process*. 2011 [cited 7/20/2011; MHI provides MHI offers high performance & reliable CO₂ recovery process called KM CDR Process.]. Available from: http://www.mhi.co.jp/en/products/detail/km-cdr_process.html.
9. Barchas, R. and R. Davis, *The Kerr-McGee/ABB Lummus Crest Technology for the Recovery of CO₂ from Stack Gases*. *Energy Conversion and Management*, 1992. **33**(5-8): p. 333 - 340
10. D'Alessandro, D.M., B. Smit, and J.R. Long, *Carbon Dioxide Capture: Prospects for New Materials*. *Angewandte Chemie International Edition*, 2010. **49**: p. 6058-6082.

11. Herzog, H. and D. Golomb, *Carbon Capture and Storage from Fossil Fuel Use*. Encyclopedia of Energy, 2004. **1**: p. 1-11.
12. Olajire, A.A., *CO₂ Capture and Separation Technologies for End-of-Pipe Applications - A Review*. Energy, 2010(35): p. 2610-2628.
13. Rubin, E.S., *CO₂ Capture and Transport*. Elements, 2008. **4**(5): p. 311-317.
14. Abanades, J.C., E.S. Rubin, and E.J. Anthony, *Sorbent Cost and Performance in CO₂ Capture Systems*. Industrial & Engineering Chemistry Research, 2004. **43**(13): p. 3462-3466.
15. Reddy, K., et al., *Instantaneous Capture and Mineralization of Flue Gas Carbon Dioxide: Pilot Scale Study*. Available from Nature Precedings <<http://dx.doi.org/10.1038/npre.2010.5404.1>>, 2010.
16. Knuutila, H., H.F. Svendsen, and M. Anttila, *CO₂ capture from coal-fired power plants based on sodium carbonate slurry; a systems feasibility and sensitivity study*. International Journal of Greenhouse Gas Control, 2009(3): p. 143-151.
17. Doman, L.E., et al., *International Energy Outlook 2010*, 2010, U.S. Energy Information Administration: Washington, D.C. p. 123-137.
18. Ciferno, J.P., et al., *Capturing Carbon from Existing Coal-Fired Power Plants*. Chemical Engineering Progress, 2009: p. 33-41.
19. DOE, *Report of the Interagency Task Force on Carbon Capture and Storage*, 2010, The U.S. Department of Energy and the Environmental Protection Agency.
20. Haszeldine, R.S., *Carbon Capture and Storage: How Green Can Black Be?* Science, 2009. **325**: p. 1647-1652.
21. Zero. *Stationary Point Sources of CO₂*. 2012 [cited November 29, 2012 November 29, 2012]; Available from: <http://www.zero.no/ccs/capture/sources-of-co2>.
22. Griswold, J., *Fuels, Combustion, and Furnaces*. Chemical Engineering Series, ed. McGraw-Hill1946, New York: McGraw-Hill Book Company, Inc.

23. Babcock and Wilcox, *Steam: Its Generation and Use*. 40th ed 1992, Barberton, Ohio: The Babcock and Wilcox Company.
24. Lowrie, R.L., *SME Mining Reference Handbook* 2002, Littleton, CO: Society for Mining, Metallurgy, and Exploration.
25. Feron, P.H.M. and C.A. Hendricks, *CO₂ Capture Process Principles and Costs*. Oil & Gas Science and Technology, 2005. **60**(3): p. 451-459.
26. Elwell, L.C. and W.S. Grant, *Technical Overview of Carbon Dioxide Capture Technologies for Coal Fired Power Plants*, 2005, MPR Associates, Inc.
27. Elwell, L.C. and W.S. Grant, *Technology options for capturing CO₂*. Power 2006. **149**(8): p. 60,62-65.
28. Pires, J.C.M., et al., *Recent Developments on Carbon Capture and Storage: An Overview*. Chemical Engineering Research and Design, 2011. **89**: p. 1446-1460.
29. Yeh, A.C. and H. Bai, *Comparison of ammonia and monoethanolamine solvents to reduce CO greenhouse gas emissions*. The Science of the Total Environment, 1999. **228**(2-3): p. 121-133.
30. Reddy, S., D. Johnson, and J. Gilmartin, *Fluor's Econamine FG PlusSM Technology for CO₂ Capture at Coal-Fired Power Plants*, in *Power Plant Air Pollutant Control "Mega" Symposium* 2008: Baltimore, MD.
31. Yeh, J.T., et al., *Semi-batch absorption and regeneration studies for CO₂ capture by aqueous ammonia*. Fuel Processing Technology, 2005. **86**(14-15).
32. Parker, L. and P. Folger, *Capturing CO₂ from Coal Fired Power Plants: Challenges for a Comprehensive Strategy*, 2010, Congressional Research Service.
33. Fluor, *Fluor's Econamine FG PlusSM Technology*, in *NETL Carbon Sequestration Conference* 2003.
34. Johnson, D.W., S. Reddy, and J.H. Brown. *Commercially Available CO₂ Capture Technology*. 2009 [cited 7/20/11; Available from:

http://www.powermag.com/coal/Commercially-Available-CO2-Capture-Technology_2064.html#tools.

35. Reddy, S., *Econamine FG PlusSM Technology for Post Combustion CO₂ Capture*, in *7th Annual Conference on Carbon Capture and Sequestration*2008: Pittsburgh, Pennsylvania.
36. Scherffius, J., *Fluor's Econamine FG PlusSM Technology for CO₂ Capture*, in *Carbon Constraint*2007.
37. Kishimoto, S., et al., *Current Status of MHI's CO₂ Recovery Technology and Optimization of CO₂ Recovery Plant with a PC Fired Power Plant*. *Energy Procedia*, 2009(1): p. 1091-1098.
38. Mimura, T., et al. *Recent Developments in Flue Gas CO₂ Recovery Technology*. in *Greenhouse Gas Control Technologies, Proceedings of the 6th International Conference on Greenhouse Gas Control Technologies (GHGT-6)*. 2003. Kyoto, Japan.
39. Mimura, T., et al., *RESEARCH AND DEVELOPMENT ON ENERGY SAVING TECHNOLOGY FOR FLUE GAS CARBON DIOXIDE RECOVERY AND STEAM SYSTEM IN POWER PLANT*. *Energy Conversion and Management*, 1995. **36**(6-9): p. 397-400.
40. Mimura, T., et al., *Development of Energy Saving Technology for Flue Gas Carbon Dioxide Recovery in Power Plant by Chemical Absorption Method and Steam System*. *Energy Conversion and Management*, 1997. **37**: p. S57-S62.
41. Resnik, K.P., J.T. Yeh, and H.W. Pennline, *Aqua ammonia process for simultaneous removal of CO₂, SO₂ and NO_x*. *International Journal of Environmental Technology and Management*, 2004. **4**(1/2).
42. Figueroa, J.D., et al., *Advances in CO₂ capture technology—The U.S. Department of Energy's Carbon Sequestration Program*. *International Journal of Greenhouse Gas Control*, 2008. **2**: p. 9-20.

43. Liu, J., et al., *Absorption of carbon dioxide in aqueous ammonia*. Energy Procedia, 2009(1): p. 933-940.
44. Yun, Z., et al., *Preliminary Study to Capture CO₂ in Flue Gas by Spraying Aqueous Ammonia to Produce NH₄HCO₃*, 2003, National Power Plant Combustion Engineering Technology Research Center: Shenyang, P.R. China.
45. Bai, H. and A.C. Yeh, *Removal of CO₂ Greenhouse Gas by Ammonia Scrubbing*. Industrial & Engineering Chemistry Research, 1997. **36**: p. 2490-2493.
46. Walsh, M.A., *Marsulex AS Technology Significantly Cuts Power Generation Costs*, in *Marsulex Environmental Technologies, LLC2000*.
47. Lunt, R.R. and J.D. Cunic, *Profiles in Flue Gas Desulfurization*2000, Hoboken, NJ, USA: John Wiley & Sons, Inc.
48. Schulte, W., *Flue Gas Cleaning with Ammonia Reduces SO₂ and NO_x Emissions*. Fuel and Energy Abstracts, 1997. **38**(4): p. 266.
49. He, Q., et al. *Study on Carbon Dioxide Removal from Flue Gas by Absorption of Aqueous Ammonia*. in *Third Annual Conference on Carbon Capture and Sequestration*. 2004.
50. Huang, H.P., et al., *Dual Alkali Approaches for the Capture and Separation of CO₂*. Energy and Fuels, 2001. **15**: p. 263-268.
51. Comstock, C.S. and B.F. Dodge, *Rate of carbon Dioxide Absorption by Carbonate Solutions in a Packed Tower*. Industrial & Engineering Chemistry, 1937. **29**(5): p. 520-529.
52. Howe, H.E., *Manufacture of Carbon Dioxide*. Industrial & Engineering Chemistry, 1928. **20**(10): p. 1091-1094.
53. Knuutila, H., O. Juliussen, and H.F. Svendsen, *Kinetics of the reaction of Carbon Dioxide with Aqueous Sodium and Potassium Carbonate Solutions*. Chemical Engineering Science, 2010(65): p. 6077-6088.

54. Wappel, D., et al., *The effect of SO₂ on CO₂ absorption in an aqueous potassium carbonate solvent*. Energy Procedia, 2009(1): p. 125-131.
55. Cullinane, J.T. and G.T. Rochelle, *Carbon dioxide absorption with aqueous potassium carbonate promoted by piperazine*. Chemical Engineering Science, 2004. **59**(17): p. 3619-3630.
56. Mahajani, V.V. and P.V. Danckwerts, *The stripping of CO₂ from amine-promoted potash solutions at 100°C*. Chemical Engineering Science, 1983. **38**(2): p. 321-327.
57. Sharma, M.M. and P.V. Danckwerts, *Fast reactions of CO₂ in alkaline solutions— (a) Carbonate buffers with arsenite, formaldehyde and hypochlorite as catalysts (b) Aqueous monoisopropanolamine (1-amino-2-propanol) solutions*. Chemical Engineering Science, 1963. **18**(12): p. 729-735.
58. Tseng, P.C., W.S. Ho, and D.W. Savage, *Carbon dioxide absorption into promoted carbonate solutions*. AIChE Journal, 1988. **34**(6): p. 922-931.
59. Yang, Q., et al., *CH₄ storage and CO₂ capture in highly porous zirconium oxide based metal-organic frameworks*. Chemical Communications, 2012(48): p. 9831-9833.
60. Ho, M.T., G.W. Allinson, and D.E. Wiley, *Reducing the Cost of CO₂ Capture from Flue Gases Using Pressure Swing Adsorption*. Industrial & Engineering Chemistry Research, 2008. **47**(14): p. 4883-4890.
61. Drage, T.C., et al., *Comparison of pre and post-combustion CO₂ adsorbent technologies*, in *8th International Conference on Greenhouse Gas Control Technologies 2006*.
62. Choi, S., J.H. Drese, and C.W. Jones, *Adsorbent Materials for Carbon Dioxide Capture from Large Anthropogenic Point Sources*. ChemSusChem, 2009. **2**(9): p. 796-854.

63. Lee, K.B., et al., *Reversible Chemisorbents for Carbon Dioxide and Their Potential Applications*. Industrial & Engineering Chemistry Research, 2008. **47**(21): p. 8048-8062.
64. Bertsch, L. and H.W. Habgood, *An Infrared Spectroscopy Study of the Adsorption of Water and Carbon Dioxide by Linde Molecular Sieve X¹*. Journal of Physical Chemistry, 1963. **67**(8): p. 1621-1628.
65. Ward, J.W. and H.W. Habgood, *The Infrared Spectra of Carbon Dioxide Adsorbed on Zeolite X*. Journal of Physical Chemistry, 1966. **70**(4): p. 1178-1182.
66. Sayaria, A., Y. Belmabkhout, and R. Serna-Guerrero, *Flue gas treatment via CO₂ adsorption*. Chemical Engineering Journal, 2011. **171**(3): p. 760-774.
67. Rege, S.U. and R.T. Yang, *A novel FTIR method for studying mixed gas adsorption at low concentrations: H₂O and CO₂ on NaX zeolite and γ -alumina*. Chemical Engineering Science, 2001. **56**(12): p. 3781-3796.
68. Hernández-Huesca, R., L. Díaz, and G. Aguilar-Armenta, *Adsorption equilibria and kinetics of CO₂, CH₄ and N₂ in natural zeolites*. Separation and Purification Technology, 1999. **15**(2): p. 163-173.
69. Sircar, S., T.C. Golden, and M.B. Rao, *Activated carbon for gas separation and storage*. Carbon, 1996. **34**(1): p. 1-12.
70. Davini, P., *Flue gas treatment by activated carbon obtained from oil-fired fly ash*. Carbon, 2002. **40**(11): p. 1973-1979.
71. Bae, Y.S. and C.H. Lee, *Sorption kinetics of eight gases on a carbon molecular sieve at elevated pressure*. Carbon, 2005. **43**(1): p. 95-107.
72. Zhou, L., et al., *Synthesis of ordered mesoporous carbon molecular sieve and its adsorption capacity for H₂, N₂, O₂, CH₄ and CO₂*. Chemical Physics Letters, 2005. **413**(1-3): p. 6-9.
73. Kishimoto, Y. and K. Hata, *Behaviors of single CO₂ molecule on pentagon at carbon nanotube tip observed by field emission microscopy*. Surface and Interface Analysis, 2008. **40**(13): p. 1669-1672.

74. Siriwardane, R.V., et al., *Adsorption of CO₂ on Molecular Sieves and Activated Carbon*. Energy and Fuels, 2001. **15**(2): p. 279-284.
75. Kikkinides, E.S., R.T. Yang, and S.H. Cho, *Concentration and recovery of carbon dioxide from flue gas by pressure swing adsorption*. Industrial & Engineering Chemistry Research, 1993. **32**(11): p. 2714-2720.
76. Yue, M.B., et al., *Promoting the CO₂ adsorption in the amine-containing SBA-15 by hydroxyl group*. Microporous and Mesoporous Materials, 2008. **114**(1-3): p. 74-81.
77. Yue, M.B., et al., *CO₂ Capture by As-Prepared SBA-15 with an Occluded Organic Template*. Advanced Functional Materials, 2006. **16**(13): p. 1717-1722.
78. Yue, M.B., et al., *Efficient CO₂ Capturer Derived from As-Synthesized MCM-41 Modified with Amine*. Chemistry - A European Journal, 2008. **14**(11): p. 3442-3451.
79. Hafizovic, J., et al., *The Inconsistency in Adsorption Properties and Powder XRD Data of MOF-5 Is Rationalized by Framework Interpenetration and the Presence of Organic and Inorganic Species in the Nanocavities*. Journal of the American Chemical Society, 2007. **129**: p. 3612-3620.
80. Rosi, N.L., et al., *Hydrogen Storage in Microporous Metal-Organic Frameworks*. Science, 2003. **300**: p. 1127.
81. Yaghi, O.M., et al., *Selective Guest Binding by Tailored Channels in a 3-D Porous Zinc(II)-Benzenetricarboxylate Network*. Journal of the American Chemical Society, 1997. **119**: p. 2861-2868.
82. Seo, J.S., et al., *A homochiral metal - organic porous material for enantioselective separation and catalysis*. Nature, 2000. **404**: p. 982.
83. Eddaoudi, M., et al., *Systematic Design of Pore Size and Functionality in Isorecticular MOFs and Their Application in Methane Storage*. Science, 2002. **295**: p. 469.

84. Huang, L., et al., *Synthesis, morphology control, and properties of porous metal–organic coordination polymers*. *Microporous and Mesoporous Materials*, 2003. **58**: p. 105-114.
85. Arstad, B., et al., *Amine functionalised metal organic frameworks (MOFs) as adsorbents for carbon dioxide*. *Adsorption*, 2008. **14**(6): p. 755-762.
86. Millward, A.R. and O.M. Yaghi, *Metal-Organic Frameworks with Exceptionally High Capacity for Storage of Carbon Dioxide at Room Temperature*. *Journal of the American Chemical Society*, 2005. **127**(51): p. 17998-17999.
87. Himeno, S., T. Komatsu, and S. Fujita, *High-Pressure Adsorption Equilibria of Methane and Carbon Dioxide on Several Activated Carbons*. *Journal of Chemical and Engineering Data*, 2005. **50**(2): p. 369-376.
88. Cavenati, S., C.A. Grande, and A.E. Rodrigues, *Adsorption Equilibrium of Methane, Carbon Dioxide, and Nitrogen on Zeolite 13X at High Pressures*. *Journal of Chemical and Engineering Data*, 2004. **49**(4): p. 1095-1101.
89. Li, H., et al., *Design and synthesis of exceptionally stable and highly porous metal organic framework*. *Nature*, 1999. **42**: p. 276-279.
90. Chae, H.K., et al., *A route to high surface area, porosity and inclusion of large molecules in crystals*. *Nature*, 2004(427): p. 523-527.
91. Khoo, H.H. and R.B.H. Tan, *Life Cycle Investigation of CO₂ Recovery and Sequestration*. *Environmental Science and Technology*, 2006(40): p. 4016-4024.
92. Scholes, C.A., S.E. Kentish, and G.W. Stevens, *Carbon Dioxide Separation through Polymeric Membrane Systems for Flue Gas Applications*. *Recent Patents on Chemical Engineering*, 2008(1): p. 52-66.
93. Treybal, R.E., *Mass-Transfer Operations*. *Chemical Engineering Series* 1955, New York: McGraw-Hill Book Company, Inc.

94. Powell, C.E. and G.G. Qiao, *Polymeric CO₂/N₂ gas separation membranes for the capture of carbon dioxide from power plant flue gases*. Journal of Membrane Science, 2006. **279**(1-2): p. 1-49.
95. Scholes, C.A., S.E. Kentish, and G.W. Stevens, *Effects of Minor Components in Carbon Dioxide Capture Using Polymeric Gas Separation Membranes*. Separation and Purification Reviews, 2009(38): p. 1-44.
96. Stern, S.A., et al., *Structure/permeability relationships of polyimide membranes. Applications to the separation of gas mixtures*. Journal of Polymer Science, 1989. **27**(9): p. 1887-1909.
97. Lin, H. and B.D. Freeman, *Gas solubility, diffusivity and permeability in poly(ethylene oxide)*. Journal of Membrane Science, 2004. **239**(1): p. 105-117.
98. Stern, S.A., *Polymers for gas separations: the next decade*. Journal of Membrane Science, 1994. **94**(1): p. 1-65.
99. Illing, G., et al., *Preparation and characterisation of polyaniline based membranes for gas separation*. Journal of Membrane Science, 2001. **184**(1): p. 69-78.
100. Xu, Z.-K., et al., *Novel poly(arylene ether) as membranes for gas separation*. Journal of Membrane Science, 2002. **205**(1-2): p. 23-31.
101. Pixton, M.R. and D.R. Paul, *Gas transport properties of polyarylates part I: Connector and pendant group effects*. Journal of Polymer Science, 1995. **33**(7): p. 1135-1149.
102. Aguilar-Vega, M. and D.R. Paul, *Gas transport properties of polyphenylene ethers*. Journal of Polymer Science, 1993. **31**(11): p. 1577-1589.
103. Favre, E. and H.F. Svendsen, *Membrane contactors for intensified post-combustion carbon dioxide capture by gas-liquid absorption processes*. Journal of Membrane Science, 2012. **407-408**: p. 1-7.
104. Klaassen, R., P.H.M. Feron, and A.E. Jensen, *Membrane Contactors in Industrial Applications*. Chemical Engineering Research and Design, 2005. **83**(3): p. 234-246.

105. Feron, P.H.M. and A.E. Jansen, *CO₂ separation with polyolefin membrane contactors and dedicated absorption liquids: performances and prospects*. Separation and Purification Technology, 2002. **27**(3): p. 231-242.
106. Bounaceur, R., et al., *Membrane processes for post-combustion carbon dioxide capture: A parametric study*. Energy, 2006(31): p. 2556-2570.
107. Favre, E., *Carbon dioxide recovery from post-combustion processes: Can gas permeation membranes compete with absorption?* Journal of Membrane Science, 2007(294): p. 50-59.
108. Zhao, L., et al., *A parametric study of CO₂/N₂ gas separation membrane processes for post-combustion capture*. Journal of Materials Research Society, 2008. **325**(1): p. 284-294.
109. Brunetti, A., et al., *Membrane technologies for CO₂ separation*. Journal of Membrane Science, 2010(359): p. 115-125.
110. Merkel, T.C., et al., *Power plant post-combustion carbon dioxide capture: An opportunity for membranes*. Journal of Membrane Science, 2010(359): p. 126-139.
111. Tuiniera, M.J., et al., *Cryogenic CO₂ capture using dynamically operated packed beds*. Chemical Engineering Science, 2010(65): p. 114-119.
112. Clodic, D. and M. Younes, *A NEW METHOD FOR CO₂ CAPTURE: FROSTING CO₂ AT ATMOSPHERIC PRESSURE*, in *Sixth International Conference on Greenhouse Gas Control Technologies, GHGT62002*: Kyoto. p. 155-160.
113. Clodic, D., et al. *CO₂ capture by anti-sublimation: Thermo-economic process evaluation*. in *Fourth Annual Conference on Carbon Capture and Sequestration*. 2005. Alexandria, USA.
114. Tuiniera, M.J., M.v.S. Annaland, and J.A.M. Kuipers, *A novel process for cryogenic CO₂ capture using dynamically operated packed beds—An experimental and numerical study*. International Journal of Greenhouse Gas Control, 2011(5): p. 694-701.

115. Blomen, E., C. Hendriks, and F. Neele, *Capture Technologies: Improvements and Promising Developments*. Energy Procedia, 2009. **1**: p. 1505-1512.
116. Hochgesand, G., *Rectisol and Purisol*. European and Japanese Chemical Industries Symposium, 1970. **62**(7): p. 37-43.
117. Gibbins, J. and H. Chalmers, *Carbon Capture and Storage*. Energy Policy, 2008. **36**: p. 4317-4322.
118. Quinn, E. and C. Jones, *Carbon Dioxide* 1936, New York: Reinhold Publishing Corporation.
119. Johnson, J.E. and A.C.J. Homme, *Selexol solvent process reduces lean, high-CO₂ natural gas treating costs*. Energy Progress, 1984. **4**(4): p. 241-248.
120. Ebenezer, S.A. and J.S. Gudmundsson, *REMOVAL OF CARBON DIOXIDE FROM NATURAL GAS FOR LNG PRODUCTION*, 2005, Institute of Petroleum Technology: Norwegian University of Science and Technology.
121. Padurean, A., C.-C. Cormos, and P.-S. Agachi, *Pre-combustion carbon dioxide capture by gas-liquid absorption for Integrated Gasification Combined Cycle power plants*. International Journal of Greenhouse Gas Control, 2012. **7**: p. 1-11.
122. Weiss, H., *Rectisol wash for purification of partial oxidation gases*. Gas Separation & Purification, 1988. **2**(4): p. 171-176.
123. Kanniche, M., et al., *Pre-combustion, post-combustion and oxy-combustion in thermal power plant for CO₂ capture*. Applied Thermal Engineering, 2010. **30**: p. 53-62.
124. Buhre, B.J.P., et al., *Oxy-fuel combustion technology for coal-fired power generation*. Progress in Energy and Combustion Science, 2005. **31**: p. 283-307.
125. Moullec, Y.L., *Assessment of carbon capture thermodynamic limitation on coal-fired power plant efficiency*. International Journal of Greenhouse Gas Control, 2012. **7**: p. 192-201.

126. Darling, S., et al., *Oxy-combustion: a sound CCS solution built from pilot operation*, in *Powergen International* 2010: Orlando, Florida, USA.
127. Wall, T., R. Stanger, and Y. Liu, *Gas cleaning challenges for coal-fired oxy-fuel technology with carbon capture and storage*. *Fuel*, 2011. **In Press**.
128. Klugera, F., et al., *CO₂ Capture System – Confirmation of Oxy-Combustion Promises Through Pilot Operation*. *Energy Procedia*, 2011. **4**: p. 917-924.
129. Wall, T., R. Stanger, and S. Santos, *Demonstrations of coal-fired oxy-fuel technology for carbon capture and storage and issues with commercial deployment*. *International Journal of Greenhouse Gas Control*, 2011. **5S**: p. S5-S15.
130. Richter, H.J. and K.F. Knoche, *Reversibility of Combustion Processes, Efficiency and Costing - Second Law Analysis of Processes* 1983: American Chemical Society.
131. Ishida, M. and H. Jin, *A new advanced power-generation system using chemical-looping combustion*. *Energy*, 1994. **19**(4): p. 415-422.
132. Adanez, J., et al., *Selection of Oxygen Carriers for Chemical-Looping Combustion*. *Energy and Fuels*, 2004. **18**(2): p. 371-377.
133. Lyngfelt, A., B. Leckner, and T. Mattisson, *A fluidized-bed combustion process with inherent CO₂ separation; application of chemical-looping combustion*. *Chemical Engineering Science*, 2001. **56**(10): p. 3101-3113.
134. Cuadrat, A., et al., *Prompt considerations on the design of Chemical-Looping Combustion of coal from experimental tests*. *Fuel*, 2012. **97**: p. 219-232.
135. Adanez, J., et al., *Progress in Chemical-Looping Combustion and Reforming technologies*. *Progress in Energy and Combustion Science*, 2012. **38**(2): p. 215-282.
136. Hossain, M.M. and H.I.d. Lasa, *Chemical-looping combustion (CLC) for inherent CO₂ separations—a review*. *Chemical Engineering Science*, 2008. **63**(18): p. 4433-4451.

137. Cao, Y. and W.-P. Pan, *Investigation of Chemical Looping Combustion by Solid Fuels. 1. Process Analysis*. Energy and Fuels, 2006. **20**(5): p. 1836-1844.
138. Moghtaderi, B., *Review of the Recent Chemical Looping Process Developments for Novel Energy and Fuel Applications*. Energy and Fuels, 2012(26): p. 15-40.
139. Mattisson, T., M. Johansson, and A. Lyngfelt, *The use of NiO as an oxygen carrier in chemical-looping combustion*. Fuel, 2006. **85**(5-6): p. 736-747.
140. Jerndal, E., T. Mattisson, and A. Lyngfelt, *Thermal Analysis of Chemical-Looping Combustion*. Chemical Engineering Research and Design, 2006. **84**(9): p. 795-806.
141. Hockstad, L. and B. Cook, *Inventory of U.S. Greenhouse Gas Emissions and Sinks: 1990 - 2008*, U.S. EPA, Editor 2010: Pennsylvania. p. ES-3.
142. Butler, J.N., *Carbon Dioxide Equilibria and Their Applications* 1991, Chelsea, MI: Lewis Publishers, Inc.
143. Corti, A., *Thermoeconomic evaluation of CO₂ alkali absorption system applied to semi-closed gas turbine combined cycle*. Energy, 2004. **29**(3): p. 415-426.
144. Hikita, H. and Y. Konish, *The Absorption of SO₂ into Aqueous Na₂CO₃ Solutions Accompanied by the Desorption of CO₂*. The Chemical Engineering Journal, 1983. **27**: p. 167-176.
145. Sander, R., *Compilation of Henry's Law Constants for Inorganic and Organic Species of Potential Importance in Environmental Chemistry*, 1999, Max-Planck Institute of Chemistry: Mainz, Germany. p. 57.
146. Bandyopadhyay, A., *Amine versus ammonia absorption of CO₂ as a measure of reducing GHG emission: a critical analysis*. Clean Technologies and Environmental Policy, 2011. **13**(2): p. 269-294.

147. Fogash, K., *Flue Gas Purification Utilizing SO_x/NO_x Reactions During Compression of CO₂ Derived from Oxyfuel Combustion*, 2009, National Energy Technology Laboratory/Air Products and Chemicals.
148. Spigarelli, B.P., *An Approach to Carbon Dioxide Capture and Storage at Ambient Conditions*, in *Chemical Engineering* 2012, Michigan Technological University: Houghton, MI.
149. Rupert, J.P., H.P.H. Jr., and C.A. Wulff, *The Solution Thermochemistry of Polyvalent Electrolytes. IV. Sodium Carbonate, Sodium Bicarbonate, and Trona*. *Journal of Physical Chemistry*, 1965. **69**(9): p. 3059 - 3062.
150. Ciferno, J., et al., *DOE/NETL Advanced Carbon Dioxide Capture R&D Program: Technology Update*, 2010, National Energy Technology Laboratory (NETL).
151. Abramoff, M.D., P.J. Magalhaes, and S.J. Ram, *Image Processing with ImageJ*. Biophotonics International, 2004. **11**(7): p. 36-42.
152. Spigarelli, B. and S.K. Kawatra, *An Approach to Carbon Dioxide Capture and Storage at Ambient Conditions: Laboratory Studies*, 2012, Michigan Technological University: Houghton, MI.
153. Danckwerts, P.V., *Gas-Liquid Reactions* 1970, New York: McGraw-Hill Book Company.
154. Motarjemi, M. and G.J. Jameson, *Mass Transfer from Very Small Bubbles - The Optimum Bubble Size for Aeration*. *Chemical Engineering Science*, 1978. **33**: p. 1415-1423.
155. Vazquez, G., G. Antorrena, and J.M. Navaza, *Influence of Surfactant Concentration and Chain Length on the Absorption of CO₂ by Aqueous Surfactant Solutions in the Presence and Absence of Induced Marangoni Effect*. *Industrial & Engineering Chemistry Research*, 2000(39): p. 1088-1094.

156. Vazquez, G., et al., *Application of the Danckwerts Method in a Bubble Column Effects of Surfactants on Mass Transfer Coefficient and Interfacial Area*. Chemical Engineering Journal, 2000. **78**: p. 13-19.
157. Vasconcelos, J.M.T., S.P. Orvalho, and S.a.S. Alves, *Gas-Liquid Mass Transfer to Single Bubbles: Effect of Surface Contamination*. AIChE Journal, 2002. **48**(6): p. 1145-1154.
158. Akita, K. and F. Yoshida, *Bubble Size, Interfacial Area, and Liquid-Phase Mass Transfer Coefficient in Bubble Columns*. Industrial & Engineering Chemistry Process Design and Development, 1974. **13**(1): p. 84-91.
159. Clift, R., J.R. Grace, and M.E. Weber, *Bubbles, Drops, and Particles* 1978, New York: Academic Press.
160. Hikita, H., et al., *Gas Hold-up in Bubble Columns*. The Chemical Engineering Journal, 1980. **20**: p. 59-67.
161. Fuerstenau, D.W., *Froth Flotation: 50th Anniversary Volume* 1962, New York: The American Institute of Mining, Metallurgical, and Petroleum Engineers, Inc.
162. Harte, C.R., E.M. Baker, and H.H. Purcell, *Absorption of Carbon Dioxide in Sodium Carbonate - Bicarbonate Solutions*. Industrial & Engineering Chemistry, 1933. **25**(5): p. 528-531.
163. García-Abuín, A., et al., *Effect of surfactant nature upon absorption in a bubble column*. Chemical Engineering Science, 2010. **65**(15): p. 4484-4490.
164. McCabe, W.L., J.C. Smith, and P. Harriot, *Unit Operations of Chemical Engineering*. 7th ed 2005, New York: McGraw-Hill.
165. Painmanakul, P., et al., *Effect of surfactants on liquid-side mass transfer coefficients*. Chemical Engineering Science, 2005. **60**(22): p. 6480-6491.
166. Vasconcelos, J.M.T., et al., *Effect of contaminants on mass transfer coefficients in bubble column and airlift contactors*. Chemical Engineering Science, 2003. **58**(8): p. 1431-1440.

167. Spigarelli, B., P. Hagadone, and S.K. Kawatra, *Increased Carbon Dioxide Absorption Rates in Carbonate Solutions by Surfactant Addition*. Minerals and Metallurgical Processing, 2013(In Press).
168. Akita, K. and F. Yoshida, *Gas Holdup and Volumetric Mass Transfer Coefficient in Bubble Columns*. Industrial & Engineering Chemistry Process Design and Development, 1973. **12**(1).
169. Lockett, M.J. and R.D. Kirkpatrick, *Ideal Bubbly Flow and Actual Flow on Bubble Columns*. Transactions of the Institution of Chemical Engineers, 1975. **53**: p. 267-273.
170. Hughmark, G.A., *Holdup and Mass Transfer in Bubble Columns*. Industrial & Engineering Chemistry Process Design and Development, 1967. **6**(2): p. 218-220.
171. Joshi, J.B., et al., *Gas Hold-Up Structure in Bubble Column Reactors*. PINSA, 1998. **64 A**(4): p. 441-597.
172. Dudley, J., *Mass Transfer in Bubble Columns: A Comparison of Correlations*. Water Research, 1995. **29**(4): p. 1129-1138.
173. Sardeing, R., P. Painmanakul, and G. Hébrard, *Effect of surfactants on liquid-side mass transfer coefficients in gas-liquid systems: A first step to modeling*. Chemical Engineering Science, 2006. **61**(19): p. 6249-6260.
174. ASTM, *Standard Test Methods for Interfacial Tension of Oil Against Water by the Ring Method*, 2004, ASTM International: West Conshohocken, PA.
175. ASTM, *Standard Test Methods for Surface and Interfacial Tension of Solutions of Surface Active Agents*, 2011, ASTM International: West Conshohocken, PA.
176. Grau, R.A., J.S. Laskowski, and K. Heiskanen, *Effect of Frothers on Bubble Size*. International Journal of Mineral Processing, 2005. **76**: p. 225-233.
177. Pugh, R.J., *The Physics and Chemistry of Frothers*, in *Froth Flotation: A Century of Innovation*, M.C. Fuerstenau, G. Jameson, and R.-H. Yoon,

- Editors. 2007, Society for Mining, Metallurgy, and Exploration, Inc.: Littleton, Colorado. p. 259 - 283.
178. Seifritz, W., *CO₂ Disposal by Means of Silicates*. Nature, 1990. **345**(6275): p. 486.
179. Lackner, K.S., et al., *Carbon Dioxide Disposal in Carbonate Minerals*. Energy, 1995. **20**(11): p. 1153-1170.
180. Sipila, J., S. Teir, and R. Zevenhoven, *Carbon Dioxide Sequestration by Mineral Carbonation*, 2008, Abo Akademi University Turku, Finland.
181. Lackner, K.S., *Carbonate Chemistry for Sequestering Fossil Carbon*, 2002, Columbia University: New York.
182. Huijgen, W.J.J. and R.N.J. Comans, *Carbon Dioxide Sequestration by Mineral Carbonation*, 2004, Energy Research Centre of the Netherlands: Petten, The Netherlands.
183. Oelkers, E.H., S.R. Gislason, and J. Matter, *Mineral Carbonation of CO₂ Elements*, 2008. **4**(5): p. 333-337.
184. Gerdemann, S.J., et al., *Ex Situ Aqueous Mineral Carbonation*. Environmental Science and Technology, 2007. **41**(7): p. 2587-2593.
185. Bobicki, E.R., et al., *Carbon capture and storage using alkaline industrial wastes*. Progress in Energy and Combustion Science, 2012. **38**(2): p. 302-320.
186. Bonenfant, D., et al., *CO₂ Sequestration by Aqueous Red Mud Carbonation at Ambient Pressure and Temperature*. Industrial & Engineering Chemistry Research, 2008. **47**(20): p. 7617-7622.
187. Huntzinger, D.N., et al., *Carbon Dioxide Sequestration in Cement Kiln Dust through Mineral Carbonation*. Environmental Science and Technology, 2009. **43**(6): p. 1986-1992.
188. Montes-Hernandez, G., et al., *Mineral Sequestration of CO₂ by Aqueous Carbonation of Coal Combustion Fly-Ash*. Journal of Hazardous Materials, 2009. **161**(2-3): p. 1347-1354.

189. Soong, Y., et al., *CO₂ Sequestration with Brine Solution and Fly Ashes*. Energy Conversion and Management, 2006. **47**(13-14): p. 1676-1685.
190. Uliasz-Bocheńczyk, A. and R. Pomykała, *Mineral sequestration of CO₂ with the use of cement waste*. Energy Procedia, 2011. **4**: p. 2855 - 2860.
191. Uliasz-Bocheńczyk, A., et al., *Estimation of CO₂ sequestration potential via mineral carbonation in fly ash from lignite combustion in Poland*. Energy Procedia, 2009. **1**(1): p. 4873-4879.
192. Zallen, R., *The Physics of Amorphous Solids* 1983, New York: John Wiley & Sons.
193. Back, M., et al., *Reactivity of Alkaline Fly Ashes Towards CO₂ in Water*. Environmental Science and Technology, 2008. **42**(12): p. 4520-4526.
194. Huijgen, W.J.J. and R.N.J. Comans, *Mineral CO₂ Sequestration by Carbonation of Industrial Residues*, 2005, Energy Research Centre of the Netherlands.
195. Zhao, L., et al., *Aqueous Carbonation of Natural Brucite: Relevance to CO₂ Sequestration*. Environmental Science and Technology, 2010. **44**(1): p. 406-411.
196. Cornelius S. Hurlbut, J., *The Manual of Mineralogy*. 19th ed 1977, New York: John Wiley & Sons.
197. Duval, C., *Inorganic Thermogravimetric Analysis*. Second ed 1963, New York: Elsevier Publishing Company.
198. Huijgen, W.J.J., G.-J. Witkamp, and R.N.J. Comans, *Mechanisms of Aqueous Wollastonite Carbonation as a possible CO₂ Sequestration Process*. Chemical Engineering Science, 2006. **61**: p. 4242 - 4251.
199. Spigarelli, B.P., *Equilibrium Analysis of Carbon Dioxide Absorption in Alkali Solutions*. Minerals & Metallurgical Processing, 2012. **29**(2): p. 131-132.